CHAPTER I

INTRODUCTION

A modified version of this chapter is published under the title "Building an asymmetric brain: Development of the zebrafish epithalamus" in *Seminars in Cell and Developmental Biology*, November 25, 2008 (Snelson and Gamse, 2008).

Abstract

The human brain exhibits notable asymmetries. Little is known about the development of these symmetry deviations; however we are beginning to understand them by employing the lateralized zebrafish epithalamus as a model. The zebrafish epithalamus consists of the pineal and parapineal organs and paired habenular nuclei located bilateral to the pineal complex. While the zebrafish pineal and parapineal organs arise from a common population of cells, parapineal cells undergo a separate program that allows them to migrate left of the pineal anlage. Studying the processes that lead to brain laterality in zebrafish will allow a better understanding of how human brain laterality is established.

Nervous System Asymmetry

Nervous system asymmetry is a conserved feature across phyla, from the relatively simple olfactory nerves of the nematode nervous system to the highly specialized human brain (Hobert et al., 2002; Toga and Thompson, 2003).

Several aspects of brain asymmetry, including asymmetry within epithalamic structures, are conserved throughout the vertebrate lineage, leading to questions regarding how these lateralities arise and speculation about their evolutionary origins. Other lateralized features may be even more ancient; early chordates were thought to rest on one side of their bodies, causing left-right (L/R) differences in sensory input (Cooke, 2004). Until recently it was thought that gross morphological differences between the left and right hemispheres of the brain were a uniquely human trait (Cantalupo and Hopkins, 2001; Sherman and Spear, 1982). Recent investigation into the behavior of humans and chickens, however, suggests that functional lateralization of the brain may have its roots in an ancient common ancestor as both chickens and humans use the right side of their brain to understand spatial relations (Vallortigara et al., 1999). Indeed, language lateralities within the brain of human subjects is thought to be derived from an ancient system established in early primates (Corballis, 2003) and reviewed in (Halpern et al., 2005).

Interest in brain lateralization dates back to Hippocrates who observed speech and language difficulties in patients suffering from traumatic brain injuries to one side of the head (McManus, 2002). In the mid-nineteenth century, Broca and Wernicke independently noted that tumors and strokes on the left side of the brain severely impaired patients' ability to speak (Toga and Thompson, 2003). While dissection pointed out gross anatomical asymmetries, rigorous scientific investigation began in earnest when Geschwind and Levitsky (Geschwind and Levitsky, 1968) reopened a long dormant area of study by carefully assessing the

size of the left and right planum temporale of the human brain. They conclusively demonstrated significant size differences between these two bilateral structures with the left planum temporale appreciably larger than the right.

Recent interest in the development of brain asymmetry has been sparked because defects in such symmetry have been implicated in various diseases, many of which affect a large number of individuals. For instance, greater symmetry between the left and right planum temporale of young patients has been correlated with an increase in both reading disorders and dyslexia (Eckert and Leonard, 2004; Habib and Robichon, 2004). Individuals can also be struck later in life by diseases such as Alzheimer's disease, which progresses asymmetrically (Toga and Thompson, 2003). Asymmetry is also currently a topic of debate in susceptibility to schizophrenia (Green et al., 2004); reduced planar asymmetry in the planum temporale has been correlated with auditory hallucinations (Green et al., 2004; Lennox et al., 1999).

In order for scientists to begin to understand the cellular and molecular processes that give rise to brain asymmetries, a tractable system for genetic and embryological studies is necessary. A fruitful venue for such studies is the dorsal diencephalon (or epithalamus) of the zebrafish, *Danio rerio* (Figure 1). The diencephalon of all vertebrates arises from a portion of the prosencephalon of the developing neural tube. The rudimentary diencephalon gives rise to the retina, epithalamus, thalamus, and hypothalamus in the adult brain (Purves et al., 2001). The epithalamus of both the human and zebrafish consists of the pineal complex and adjacent habenular nuclei. Additionally, the zebrafish pineal complex

contains a left sided accessory called the parapineal organ. Though the mammalian brain does exhibit other lateralities, the diencephalon itself does not appear to be asymmetric. The lack of lateralized diencephalic structures in mammals and their presence in fish suggests that mammals may have evolved away from a need for these structures (Concha and Wilson, 2001). Nevertheless, by using the simpler, genetically tractable zebrafish epithalamus as a model for the development of asymmetric brain structures, we may begin to understand how basic developmental processes influence overall brain morphology.

High fecundity, rapid development outside of the mother, available mutant lines, and transgenic tools make the zebrafish particularly well suited to development studies (Driever et al., 1994). The zebrafish parapineal organ, in particular, can be used to assay various basic processes common to development of all vertebrate brains (ie. neuron specification, proliferation, and migration). For instance, pineal and parapineal cells develop from a seemingly uniform population of cells but undergo separate programs of proliferation, specification, and differentiation that ultimately give rise to mature structures with different functions (Snelson et al., 2008a; Snelson et al., 2008b). Parapineal cells exhibit an ability to migrate to a characteristic position on the left side of the brain, while pineal cells do not migrate. By understanding the processes that give rise to laterality in the zebrafish epithalamus, we may begin to understand the complex developmental processes in the human brain that lead to gross anatomical differences with respect to the L/R axis, and when altered, to various

developmental defects.

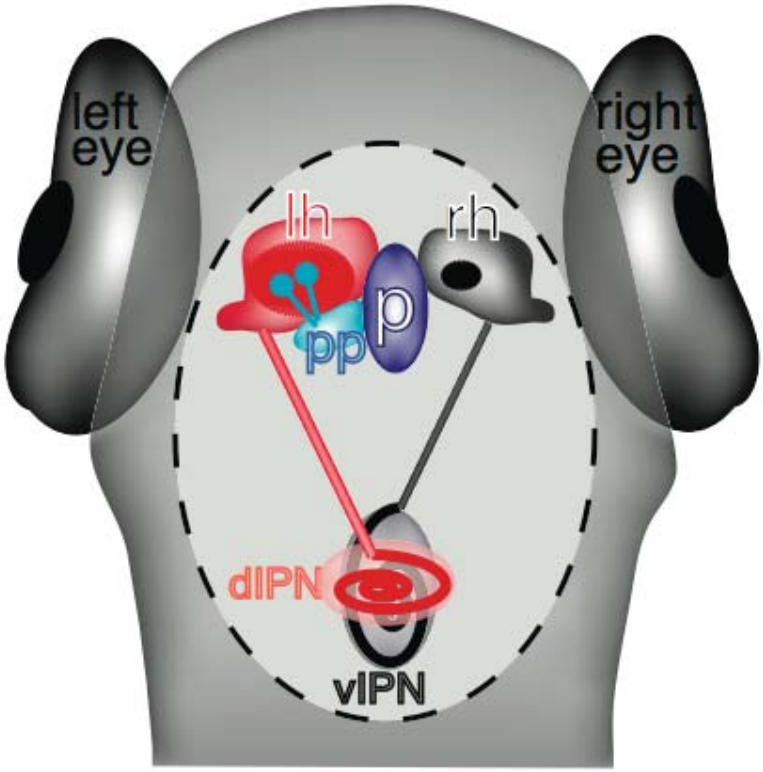

Figure 1.
Schematic of a 4 dpf larval zebrafish epithalamus, viewed from the dorsal aspect. The pineal organ (p) is located in the midline; the parapineal (pp) is located to its left. The left (lh, red) and right (rh, black) habenulae are located on either side of the pineal complex. The region of dense neuropil in the left habenula (red oval) is larger than in the right habenula (black oval). The left habenula primarily sends axonal projections (red) to the dorsal interpeduncular nucleus (dIPN) while the right habenula sends projections (black) to the ventral IPN (vIPN).

Anatomical asymmetry of the zebrafish epithalamus

The medially-placed pineal organ is a bulbous structure that forms at the end of a stalk attached to the dorsal habenular surface. The parapineal organ arises as an outcropping of cells from the anterior region of the pineal complex anlage, which becomes morphologically distinct from the pineal organ between 28 and 31 hours post fertilization (hpf). The parapineal organ then migrates leftward in 95% of individuals (Concha et al., 2000; Gamse et al., 2002). As the pineal organ begins to develop the afferent nerves that will eventually form its stalk, the parapineal organ completes its migration and begins to extend afferent processes that coalesce into the parapineal tract. This tract then joins and courses with the habenular commissure (axons that connect the left and right habenulae) before splitting into smaller tracts that extend to the left medial habenular ganglion (Yanez and Anadon, 1996). The habenular nuclei, in turn, extend long axon tracts, called the fasiculi retroflexus (FR), to a midbrain structure termed the interpeduncular nucleus (IPN). The left FR preferentially innervates the dorsal IPN, while the right FR primarily innervates the ventral IPN, thereby converting L/R laterality to dorsal/ventral differences (Aizawa et al., 2005; Gamse et al., 2005).

Besides location of the parapineal to the left side of the pineal organ, other gross asymmetries are also apparent in the zebrafish epithalamus. For example, the base of the stalk upon which the pineal organ is situated is slightly biased to the left in wild-type embryos (Liang et al., 2000). Additionally, the habenular nuclei also display gross anatomical differences; the left habenula is 20%

greater, volumetrically, than the right habenular nucleus. Antibody labeling with anti-acetylated tubulin, which labels neuropil, also shows a region of dense neuropil associated with the left habenula and a reduced volume of neuropil associated with the right habenula (Concha et al., 2000; Gamse et al., 2003).

Consistent with differences in anatomical features, the habenulae also differ in expression of several asymmetrically expressed genes. The gene *leftover* (*lov*) contains a Potassium Channel Tetramerization Domain (KCTD) also found in voltage gated potassium channels. Lov is expressed throughout the left habenular nucleus, but only in a small caudal section of the right habenula (Gamse et al., 2003). Other KCTD-containing genes, *right on* (*ron*) and *dexter* (*dex*) are asymmetrically expressed, but with the opposite pattern; they are more broadly expressed in the right habenular nucleus than the left (Gamse et al., 2005). While differential expression of KCTDs may define functional subdomains of the habenular nuclei, the molecular role of KCTD proteins in habenular neurons has not yet been established. Additionally, a glycoprotein required for central axon guidance Contactin2 (Cntn2/Tag1) (Liu and Halloran, 2005) is expressed in a larger region in the right habenula than the left (Carl et al., 2007). Furthermore, the axon guidance molecule Neuropilin 1a (Nrp1a) is more abundant in the left habenular nucleus, and depletion of its axon guidance cue Semaphorin 3d (Sema3d) causes disruption of projections to the dorsal IPN (Kuan et al., 2007) suggesting a molecular mechanism for differences in left versus right habenular axon targeting.

Epithalamic Asymmetry is a conserved feature of many vertebrates

Asymmetry of the pineal complex (epiphysis) of teleosts is also shared with several other vertebrates. The most primitive of vertebrates, the lamprey (*Petromyzon marinus*), and other members of this family, have a pineal complex organization similar to the zebrafish (Concha et al., 2000). One striking difference however, is that the pineal and parapineal organs (termed parapineal ganglion in lampreys) emanate from two separate stalks. Further, the parapineal ganglion of lampreys more closely resembles the left habenula neurochemically (Yanez et al., 1999) and ultrastructurally (Meiniel and Collin, 1971). Additionally, the anciently derived coelacanth (*Latimeria chalumnae*) has both a pineal and parapineal organ. Coelacanths and teleost fish have a common ancestry that diverged during the Mesozoic period. The coelacanth parapineal organ develops from an anlage similar to that of the zebrafish parapineal organ, but differs in that it contains more specialized photoreceptive, supportive, and nerve cells. The coelacanth parapineal organ is not lateralized, but separates from the pineal anlage to occupy an anterior region where it remains in open communication with the pineal organ (Hafeez and Merhige, 1977). Some reptiles also retain a parapineal homolog called the parietal eye. The parietal eye remains the least devolved of all epiphyseal structures, and contains a cornea, lens, and retina with photoreceptive cells, and has been shown to be fully functional in response to light stimulation (Solessio and Engbretson, 1993; Solessio and Engbretson, 1999).

Compared to the parapineal, volumetric asymmetry of the habenular nuclei is much more conserved throughout different phyla. With notable exceptions, the left habenula of most cartilaginous fishes is much larger than the right habenula (for a more detailed evolutionary comparison see (Concha and Wilson, 2001)). Left habenular asymmetry is also found in modern frogs (Anura), and newts and salamanders (Urodela). The left habenula of these vertebrates is highly specialized consisting of a medial and lateral subnucleus, with the right habenula consisting of only one nucleus. In frogs, the left habenula shows seasonal and sex differences, likely reflecting a response to hormonal inputs involved in the timing of seasonal reproduction (Concha and Wilson, 2001). Along these same lines, detailed studies of the habenulae of the frog *Rana esculenta* have shown a sex-linked asymmetry in the size of the medial subnucleus of the left habenula. This asymmetry is more pronounced in female frogs during the springtime, the frogs' mating season, and is probably directly related to secretion of reproductive hormones (Kemali et al., 1990). Chickens also display similar asymmetries but with the opposite sex and directional bias; males have a much larger right medial habenula while females appear to have symmetrical habenulae. Though postulated, no data indicating a seasonal sex-dependent size difference in chickens exist (Gurusinghe and Ehrlich, 1985). In mammals, there are subtle volumetric differences in the size of the habenulae, but the side on which the larger habenulae is found is not conserved among even the closest of evolutionarily divergent species (i.e. albino rat (Zilles et al., 1976) and mouse (Wree et al., 1981)). Taken together, these phylogenetic surveys

suggest that habenular asymmetry is somehow linked to proper function, though the direction of these asymmetries appears not to be critical for correct function.

Function of the Epithalamus

The pineal gland in zebrafish serves two functions: first as a photoreceptive organ, gathering environmental light/dark information, and second as a neuroendocrine organ, secreting melatonin in response to night-time conditions. The mammalian pineal organ has evolved away from the need to gather light information, and its sole function is to secret melatonin in response to environmental conditions. In mammals, light information is instead gathered from the retina, which then relays information to the pineal gland via the suprachiasmatic nucleus, which is the main circadian pacemaker responsible for daily light/dark fluctuations and seasonal variations.

The mammalian habenulae receive input from the basal ganglia and limbic system and relays it to the midbrain where it signals the release of dopamine and serotonin (Christoph et al., 1986; Herkenham and Nauta, 1977; Park, 1987). The habenulae have been implicated in control of circadian behavior, motor control, sexual and maternal behavior, secretion of hormones, and aversive learning, among other functions (Herkenham and Nauta, 1977).

Development of the Epithalamus

Development of the zebrafish epithalamus has been studied by fate-mapping of early embryos with photoactivatable dyes in combination with *in situ* hybridization of markers expressed in the diencephalon. Such lineage tracing has shown that the forebrain, midbrain, and hindbrain precursors are specified by 50% epiboly (Kimmel et al., 1990; Woo and Fraser, 1995; Woo et al., 1995), the stage during which the embryo begins to develop three separate germ layers. The presumptive diencephalon covers a region starting near the animal pole and extending towards the vegetal pole in a rough arrowhead shape that partially overlaps with the telencephalic region (Kozlowski et al., 1997). Gene expression profiling by *in situ* hybridization shows that the diencephalic tissues express discrete regional markers by bud stage (10 hpf, completion of epiboly). Ectopic cell transplants and ablations of those tissues further demonstrated that those regions are indeed specified by bud stage (Staudt and Houart, 2007). An early marker of the presumptive epiphysis, the homeobox transcription factor *floating head* (*flh*), is expressed in two small discrete regions on the lateral edges of the neural plate (Masai et al., 1997; Staudt and Houart, 2007). The activity of *flh* is important for initiating pineal neurogenesis, and its expression within the CNS is controlled by both rostralizing and caudalizing factors (Masai et al., 1997).

Careful control of the Wnt signaling pathway is required for the proper formation of the zebrafish forebrain, including the diencephalon. The *masterblind* (*mbl*; *axin1*) mutation causes an over-activation of Wnt signaling resulting in rostralized embryos missing both eyes and telencephalic structures. In the

absence of *axin1*, pineal neurogenesis is grossly increased, expanding into the telencephalon (Heisenberg et al., 2001; Masai et al., 1997). *flh* expression marking the presumptive pineal tissue is confined dorso-ventrally by a gradient of bone morphogenetic gene (BMP) activity. In the *bmp2b* mutation *swirl*, *flh* expression is expanded ventrally (Barth et al., 2005), suggesting that a very fine gradient of BMP proteins along the dorsal-ventral axis and Wnt activity in the forebrain is required for the specification of pineal complex precursors.

Proceeding through development, the neural plate bends to form the neural keel, and then fuses to form the neural rod before developing into the neural tube (Gilbert, 2006). These two regions of *flh* expression meet in the dorsal region as a roughly rectangular group of cells at approximately 6 somites (s) during the formation of the neural keel (Karlstrom and Kane, 1996). By 24 hpf, this region has coalesced into a flat, circular area of cells highly expressing *flh* that defines the pineal complex anlage (Masai et al., 1997), which ultimately gives rise to both the pineal and parapineal organs.

As the pineal organ matures, the parapineal emerges as a separate group of cells and migrates to its characteristic position on the left side of the pineal organ. Since its discovery by Charles Hill in the late nineteenth century (Hill, 1891), growing interest has focused on the development and placement of the parapineal organ with respect to the left-right axis as a model for vertebrate brain asymmetry. In most teleost fish, the parapineal organ arises from a pineal complex anlage as a cluster of migratory cells that buds from the anterior region of the anlage to occupy a position ventral, rostral and lateral to the pineal organ.

Analysis of *flh* mutants has revealed some details of pineal versus parapineal development. During its development, the zebrafish pineal organ requires *flh* activity for its proper formation. In *flh* mutants, pineal neurogenesis begins as in wild type embryos but abruptly halts around 16 to18 hpf, resulting in a much smaller epiphyseal vesicle (Masai et al., 1997). In contrast, parapineal neurogenesis is not affected, and *flh* mutants develop the same number of parapineal cells as their wild-type siblings (Gamse et al., 2002). This indicates that the pineal and parapineal lineages are already undergoing different genetic programs by the time pineal neurogenesis has stalled in *flh* mutants. BrdU labeling of pineal and parapineal precursor cells in wild-type embryos show a peak of proliferation of both cell types at 18 hpf, and in wild-type pineal cells, a second peak of proliferation around 24 hpf. In *flh* mutants, however the second peak of pineal neurogenesis does not occur. BrdU incorporation studies in parapineal cells of *flh* mutants is unaffected, providing further evidence for separate programs for pineal and parapineal development (Snelson et al., 2008a).

The function of the parapineal organ is largely unknown. It expresses the melatonin biosynthetic enzyme *arylalkamine N-acetyltransferase*, (*aanat2*) (Gamse et al., 2002; Gothilf et al., 1999) and innervates the left habenular nucleus (Concha and Wilson, 2001). Fish in which a directed laser is used to selectively destroy the emerging parapineal organ are able to survive to adulthood (JTG, unpublished observation), even though the parapineal cells do not regenerate. In addition, parapineal ablation affects the molecular

development of the habenular nuclei (see below). Behavioral assays performed on adult zebrafish with reversed parapineal laterality have shown that their motor responses are largely indistinguishable from normally lateralized siblings (Facchin et al., 2008). Though the direction of asymmetry appears to not affect motor behavior, similar assays performed on adult zebrafish in which the parapineal has been ablated may provide some insight to the functional role of the parapineal organ.

Nodal signaling dictates the direction of brain asymmetry in zebrafish

How is seemingly identical tissue on the left and right sides influenced to consistently assign the placement of asymmetric organs such that every individual within a population of fish develops with identical laterality? Breaking of symmetry along the left-right axis in zebrafish is thought to be due to the activity of Kupffer's vesicle (KV), a structure that contains ciliated cells thought to be equivalent to ciliated cells within the mouse embryonic node. This structure forms just as gastrulation is completed (Cooper and D'Amico, 1996). Microscopic inspection of cilia within KV reveals a stereotypic pattern of leftward beating which influences calcium signaling and Nodal gene expression in the left lateral plate mesoderm (LLPM) (Sarmah, et al., 2005). Zebrafish with defective ciliary beating or KV formation result in randomized placement of visceral organs (Amack et al., 2007; Essner et al., 2005; Kramer-Zucker et al., 2005; Sarmah et al., 2007). A detailed review of the establishment of L/R asymmetry for many different model organisms can be found in (Raya and Belmonte, 2006).

The *nodal* genes *cyclops* (*cyc*) and *southpaw* (*spaw*), as well as the Nodal antagonist *lefty-1* (*lft-1*) and the downstream effector gene of Nodal signaling *pitx2* (*pitx2a*) are transiently expressed in the LLPM, following symmetry breaking by KV, and are responsible for the asymmetric placement of visceral organs (Hamada et al., 2002; Wright and Halpern, 2002). The discovery that these same genes, with the important exception of *spaw*, were also briefly expressed in tissue fated to become the left epithalamus was the first molecular indication of how L/R asymmetry may be established in the brain (Long et al., 2003).

Although *spaw* is not expressed in the presumptive left epithalamus, knockdown of its function by morpholino injection causes randomization of parapineal placement (Long et al., 2003). Currently, little is known about how signals from the LLPM are transduced to the presumptive left epithalamus. One clue comes from the transcription factors Six3b and Six7. These genes are bilaterally expressed in the early neuroectoderm including the epithalamus (Inbal et al., 2007). In Six3b/Six7 mutant/morphants, *nodal* gene expression is bilaterally expanded in the epithalamus, but unaffected in the LLPM (Inbal et al., 2007). These data suggest that Six genes repress Nodal expression in the epithalamus and this repression is relieved either directly or indirectly by Spaw; identification of Six3b/7 effector genes or transcriptional targets should shed light on the pathway.

Abrogation of Nodal signaling in the epithalamus (by mutation/knockdown of *oep*, a cofactor required for Nodal signaling (Zhang et al., 1998), or of *cyc* or *spaw*) influences placement of the pineal organ stalk with respect to the L/R axis.

In wild-type embryos, stalk placement is subtly biased ot the left, but in rescued oep mutants, placement of the stalk can be found anywhere along the L/R axis (Halpern et al., 2003; Liang et al., 2000). Expression of the Nodal genes in the epithalamus also influences the placement of the parapineal organ. In rescued *oep* or other Nodal mutants or morphants, placement of the parapineal organ is randomized along the L/R axis, but other aspects of parapineal organ development are unaffected (Concha et al., 2000; Gamse et al., 2002).

Mutations affecting formation of the notochord such as *no tail* (*ntl*), or physical ablation of the midline, result in bilateral Nodal signaling in the epithalamus (Bisgrove et al., 2000; Concha et al., 2000; Liang et al., 2000). Similar to absence of Nodal signaling, placement of the parapineal is randomized, indicating that unilateral Nodal signaling acts as a cue for parapineal placement; when Nodal signaling is either bilateral or absent, placement is stochastic.

Specification and migration of the parapineal organ

The cells that will eventually coalesce into the parapineal organ not only need to be properly specified and determined, they must also migrate properly to occupy their final position within the epithalamic region, to the left of the pineal organ. Parapineal cells are morphologically indistinguishable from pineal cells until about 28 hpf (Figure 2 A-D) when they become visible as an outcropping of cells from the larger pineal complex anlage (Gamse et al., 2003). Time-lapse imaging of the pineal complex anlage from 24 hpf using a *foxd3:gfp* transgenic

line (which labels both pineal and parapineal cells (Gilmour et al., 2002) shows that one to two parapineal cells become visible around 31 hpf. Between 31 and 46 hpf, a group of *foxd3*:*gfp* expressing cells migrates away from the pineal complex (Snelson et al., 2008b). Migration slows around 48 hpf when the cluster of GFP+ cells begin to extend long processes that coalesce into the parapineal tract between 48 and 72 hpf (Figure 2 G, H and unpublished observations). To date, the events that occur prior to the emergence of the parapineal organ in wild-type embryos are unknown, though parapineal cells likely migrate from a location within the pineal complex anlage before becoming morphologically distinguishable. Studies of the *masterblind* (*mbl*; *axin1*) mutation reveal that migration of the parapineal organ is initially delayed, however by 4 dpf, the parapineal organ has completed its migration in 90% of embryos (Carl et al., 2007) indicating that Wnt signaling is a critical component of proper timing of migration. Currently, there are no known molecular markers of parapineal cells before *gfi-1* expression begins at 48 hpf, though *flh* expression is downregulated in the parapineal organ as migration begins. Identification of earlier parapineal specific markers along with time-lapse analysis of parapineal cell migration will allow for the description of early parapineal cell behavior.

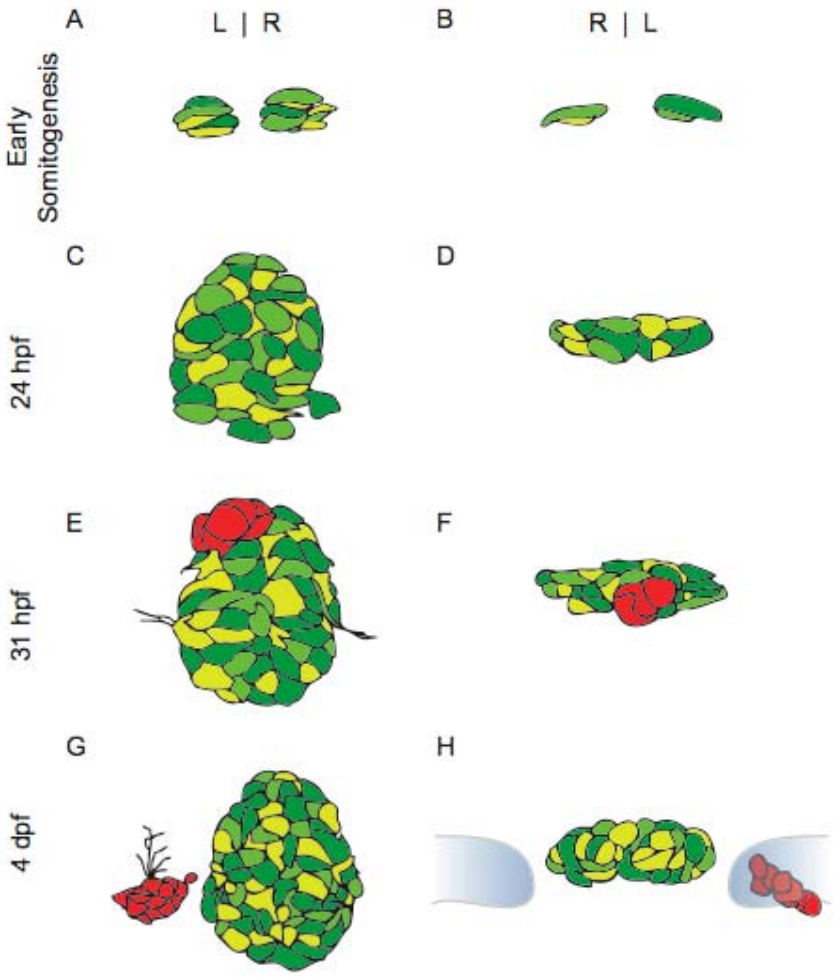

Figure 2:
Schematic drawings of pineal complex development from somitogenesis through embryogenesis. Drawings are based on expression of the *foxd3*:*gfp* transgenic line. Different shades of green indicate varying levels of transgene expression within the pineal organ. (A) Dorsal and (B) frontal views of the pineal complex during early somitogenesis. (C) and (D) The pineal complex at 24 hpf prior to the emergence of the parapineal. (E) and (F)The parapineal (red) forms as a group of cells in the anterior region of the pineal complex and is beginning to undergo the morphological changes that will result in two separate organs. (G) Dorsal view of a 4 dpf wild type embryo. The parapineal (red) has completed its migration. (H) A frontal view of the 4 dpf pineal complex. The habenulae are depicted in blue and outlined in grey. The parapineal (red) is located adjacent to the left habenula.

Fate mapping experiments performed just prior to migration of parapineal cells reveal a bilateral origin within the anterior portion of the pineal complex anlage. Parapineal cells located to the right of the midline migrate leftward and cross the midline of the brain to join the parapineal organ (Concha et al., 2003). However very little is known about the spatial origin of parapineal cells relative to pineal cells before 24 hpf, raising the question of how both the pineal and parapineal lineages diverge from within a seemingly homogenous population of cells that express *foxd3:gfp* in the epithalamus.

The molecular events that differentiate parapineal cells from pineal cells also largely remain to be determined. A clue comes from the *from beyond* mutant (*fby*; *tbx2b*), which shows a reduction in the total number of parapineal cells, demonstrating a requirement for *tbx2b* in the specification of parapineal cells, while leaving the pineal organ largely intact (Snelson et al., 2008b). Time-lapse imaging of *fby* mutants shows that some cells in the pineal complex are able to extend processes similar to parapineal cells in WT siblings, but are unable to initiate the leftward migration of the cell soma. Experiments in which the total number of parapineal cells was reduced by laser ablation to mimic the number found in *fby* mutants show that migration is not dependent on the total number of cells, but is likely to depend on genes that are activated or repressed by *tbx2b* (Snelson et al., 2008b). Currently, the transcriptional targets of *tbx2b* within the pineal complex anlage are unknown. Identification and careful characterization of such targets, for instance genes involved in neuronal

migration or extracellular matrix formation, will help elucidate the role that *tbx2b* plays in parapineal cell migration.

Laterality of the parapineal organ and habenular nuclei is coordinated in zebrafish

Two hypotheses have been proposed to explain how sidedness of the parapineal and the habenular nuclei are coordinated. One hypothesis suggests that Nodal signaling acts on parapineal cells to bias their migration to the left. Subsequently, the parapineal organ communicates with the left habenula to set the direction of habenular laterality. In support of this theory, expression of *lov* begins by 40 hpf in the habenular nuclei, following the migration of the parapineal organ away from the pineal anlage. The strongest evidence comes from experiments in which the parapineal is laser ablated at 28 to 32 hpf and results in nearly symmetric expression of the normally asymmetrically expressed habenular genes *lov* and *ron* (Gamse et al., 2003; Snelson et al., 2008b). A second hypothesis suggests that Nodal signaling in the diencephalon biases the asymmetric development of the habenular nuclei, which in turn influences the parapineal to undergo migration to the left side. Supporting this idea, components of the Nodal signaling pathway are expressed not only in left-sided pineal and parapineal precursor cells, but also in the left ventral epithalamus, which includes left habenula precursor cells. Ablation of these cells leads to randomization of parapineal placement (Concha et al., 2003). These hypotheses are not mutually exclusive; it is likely that a complete explanation of epithalamic laterality will incorporate aspects of both models.

Conserved habenulo-interpeduncular projections are dependent on the presence of the parapineal organ

Placement of the parapineal organ not only influences the molecular characteristics of the habenular nuclei, but also dictates how those habenulae connect to their midbrain target, the interpeduncular nucleus (IPN). Immunostaining of larval and adult wild-type zebrafish show that Lov staining is primarily found in habenular axons innervating the dorsal IPN(with a few axons contributing to the ventral IPN), while right habenular projections that express Ron exclusively target the ventral domain of the IPN. Parapineal ablation studies in wild-type fish demonstrate that in the absence of the parapineal organ, projections from the left habenula mimic those of the right habenula, suggesting that the parapineal organ is necessary to establish asymmetry in epithalamic output as well (Gamse et al., 2003). A similar phenotype is seen in *fby* embryos, in which the parapineal organ is genetically ablated (Snelson et al., 2008b). Asymmetric neurogenesis and gene expression in the habenular nuclei is also influenced by the Notch signaling pathway (Aizawa et al., 2007). In *mindbomb* (*mib*) mutants, which are defective in a ubiquitin ligase required for the internalization of the Notch ligand, Delta, *lov* expression is symmetric, suggesting that Notch plays a role in the asymmetric development of the habenular nuclei. This role is distinct from that of the parapineal organ, which develops normally in *mib* mutants(Caleb Doll, personal communication).

Discussion

Although much is known about the molecular pathways that lead to the development of visceral organ asymmetry, we are just beginning to understand the molecular processes that lead to the development of brain laterality. The studies discussed in this review have shed light on how brain asymmetry is established. However, several significant questions remain unanswered. One of the more important questions is whether Nodal signaling directs brain laterality in organisms other than zebrafish. Although there is no left or right bias of Nodal signaling known so far in mouse brains (Hamada et al., 2001), studies in chick show that Nodal signaling controls both the expression of the Nodal antagonist *cerberus* (*cer*) in the head mesenchyme and the direction of head turning (Zhu et al., 1999). Though Nodal expression in chick is not specifically correlated with brain laterality, light exposure to the right or left eye of pre-hatched chicks, which is affected by the direction of head turning biased by *cer* expression, can influence how these animals perform during tests of lateralized behaviors as adults (Deng and Rogers, 2002). This suggests that Nodal signaling may indirectly influence brain asymmetry.

One of the most striking findings from Concha et. al. (2003) is that wild-type parapineal cells arise from both sides of the pineal complex anlage and right sided parapineal cells cross the midline to occupy a position within the migrating parapineal organ. This is particularly intriguing because it has been postulated that the notochord, located in the midline, serves as a chemical or physical barrier that prevents bilateral Nodal signaling by expressing the Nodal antagonist

lefty, preventing left-sided Nodal molecules from diffusing to the right. One explanation for why parapineal cells that arise on the right are capable of leftward migration is that they are uniquely able to respond to a signal from a leader cell, located on the left side, that initiates migration. Alternatively, parapineal cells only initiate leftward migration after *lefty* expression ceases in the notochord, thus allowing them to respond to a secondary, as yet unidentified, left-sided signal.

A single cell resolution fate map of the epithalamus will help us understand events that lead to the separation of the pineal and parapineal organs from a uniform primordium. For instance, when do pineal and parapineal precursors become distinct cell lineages? Are parapineal cells specified in the anterior region of the pineal complex anlage or do they originate elsewhere and coalesce in the anterior prior to leftward migration?

Understanding developmental processes like asymmetric migration of cells, communication between different tissues, and specification of different populations from a single lineage will help us identify the common themes that establish brain laterality in all vertebrates. In this way, the simple epithalamus of the zebrafish could give us insight into the vastly more complex hemispheres of the human brain.

CHAPTER II

Tbx2b IS REQUIRED FOR THE DEVELOPMENT OF THE PARAPINEAL ORGAN

This paper is published under the same title in *Development*, May 2008; 135(9): 1693-702.

Abstract

Structural differences between the left and right sides of the brain exist throughout the vertebrate lineage. By studying the zebrafish pineal complex, which exhibits notable asymmetries, both the genes and the cell movements that result in left-right differences can be characterized. The pineal complex consists of the midline pineal organ and left-sided parapineal organ. The parapineal is responsible for instructing the asymmetric architecture of the bilateral habenulae, the brain nuclei that flank the pineal complex. Using in vivo time-lapse confocal microscopy, we find that the cells that form the parapineal organ migrate as a cluster of cells from the pineal complex anlage to the left side of the brain. In a screen for mutations that disrupted brain laterality, we identified a nonsense mutation in the *t-box2b* (*tbx2b)* gene, which encodes a transcription factor expressed in the pineal complex anlage. The *tbx2b* mutant makes fewer parapineal cells, and they remain as individuals near the midline rather than migrating leftward as a group. The reduced number and incorrect placement of

parapineal cells result in symmetric development of the adjacent habenular nuclei. We conclude that *tbx2b* functions to specify the correct number of parapineal cells and regulate their asymmetric migration.

Introduction

The formation of an organ requires specification of multiple cell types within a primordium, followed by appropriate morphogenetic movements that shape the mature organ. In the case of asymmetrically shaped and positioned organs, morphogenesis must also be regulated along the left-right (L-R) axis. The zebrafish presents a unique opportunity to study the formation of an asymmetric region in the brain, namely the pineal complex, which is found in the dorsal diencephalon (epithalamus). The pineal complex includes the melatonin secreting pineal organ and the left-sided parapineal organ (Borg et al., 1983; Butler and Hodos, 1996) In adult fish, the pineal organ is attached to the brain via a stalk, which emerges just to the left of the midline (Liang et al., 2000). The parapineal organ is situated within the brain to the left of the pineal stalk (Gamse et al., 2002). Adjacent to the pineal complex are the bilateral habenular nuclei (habenulae). Along with the medial forebrain bundle, the habenulae and their efferent connections are a principal pathway connecting the limbic forebrain with the midbrain. Habenular axons travel via the fasciculi retroflexus (FR) to the interpeduncular nucleus (IPN) of the midbrain; this habenulo-interpeduncular connection is highly conserved throughout the vertebrate lineage (Sutherland, 1982). In teleosts including zebrafish, axons from the left versus right habenula

innervate different dorsoventral regions of the IPN, in contrast to other vertebrates, where the two habenulae exhibit similar connections to the IPN (Kuan et al., 2007).

In zebrafish, the asymmetric location of the parapineal organ imposes laterality on the flanking habenulae, which exhibit L-R differences in their neuropil density (Concha et al., 2000), size and expression of genes such as *leftover (lov)* (Gamse et al., 2003). In mutants in which the parapineal is on the right side of the brain, structural and gene expression differences in the habenulae are also L-R reversed (Concha et al., 2000; Gamse et al., 2003). Selective destruction of the parapineal by laser ablation reveals its instructive role on the left habenula. In the absence of the parapineal, both habenulae develop with equivalent size, patterns of gene expression, and neuropil density characteristic of the right habenula (Concha et al., 2003; Gamse et al., 2003). This abnormal development of the habenulae also affects efferent projections to the IPN. In wild-type (WT) embryos, the left habenular neurons project to both the dorsal and ventral regions of the IPN (Aizawa et al., 2005; Gamse et al., 2005). However, in parapineal-ablated larvae, left habenular neurons no longer project dorsally, but instead innervate the ventral IPN, characteristic of right habenular neurons (Gamse et al., 2005). Therefore, the development of the parapineal is important for asymmetry of the dorsal diencephalon as well as the formation of diencephalic connectivity to other brain regions.

The parapineal organ is morphologically distinguishable between 28 to 32 hours post-fertilization (hpf) as a cluster of cells adjacent to the anterior left edge

of the pineal anlage (Concha et al., 2003; Gamse et al., 2003). Studies of fixed samples suggest that over the course of the next three days, the parapineal becomes located more posteriorly and ventrally relative to the pineal organ (Gamse et al., 2002). A single parapineal organ is detected in 95% of WT zebrafish larvae on the left side of the brain, and only very rarely (<0.3%) are bilateral or no parapineal organs observed (Concha et al., 2000; Gamse et al., 2003). Precursors of the parapineal and pineal organ are thought to derive from a common pool of cells, as shown by lineage labeling of the pineal complex anlage at 22-24 hpf (Concha et al., 2003). The genes that regulate how parapineal cells are specified from this precursor pool, and that are responsible for their ultimate left-sided localization, are unknown.

To identify genes involved in asymmetric development of the epithalamus, we performed a genetic screen for mutations that disrupt L-R differences of *lov* expression in the habenulae. Here, we report the isolation and characterization of the *from beyond (fby)* mutation that produces homozygous embryos with reduced *lov* expression in the left habenula. We identify *fby* as a lesion in the *t-box2b (tbx2b)* gene that disrupts parapineal development. Time-lapse analysis reveals details of the morphogenetic process, showing that parapineal cells migrate leftward away from the pineal complex anlage as a cluster. In contrast, the parapineal cells of *fby* mutants are fewer in number and are scattered near the midline of the brain. We propose that *tbx2b* assigns cells to the parapineal lineage and regulates their asymmetric migration.

Materials and Methods

Zebrafish

Zebrafish were raised at 28.5°C on a 14/10 hour light/dark cycle and staged according to hours (h) or days (d) post fertilization. The wild-type AB strain (Walker, 1999) and WIK strain (Rauch et al., 1997); the transgenic lines Tg(*foxd3:*GFP)^{fkg17} and Tg(*foxd3:*GFP)$^{fkg3\ (Gilmour\ et\ al.,\ 2002)}$, the N-ethyl N-nitrosourea (ENU)-induced mutations *knypek*^{m119} and *trilobite*^{m747} (Solnica-Krezel et al., 1996), and *fby*^{c144} were used.

Mutagenesis and screening

ENU mutagenesis was performed by placing male zebrafish in 3 mM ENU for three one hour treatments with 48 hours between treatments. F1 fish were generated by crossing ENU mutagenized males to AB females. F2 fish were generated by intercrossing F1 males and females. F3 larvae were generated from F2 intercrosses and at 4 dpf were fixed for in situ hybridization with the *lov* probe. Putative mutations showing reversed or bilaterally symmetric expression of *lov* in the habenular nuclei were re-identified in F2 heterozygotes and lines established though outcrosses to AB fish.

Cloning of fby

Heterozygous fish (AB background) carrying the *fby*^{c144}mutation were crossed with wild-type WIK fish. F2 mutant larvae were used for meiotic mapping with simple sequence length polymorphism (SSLP) markers, as previously described (Bahary et al., 2004). For identification of the lesion in the *tbx2b* gene, cDNA was prepared using Superscript II reverse transcriptase (Invitrogen) from mRNA isolated from 4 day old AB and *fby* mutant larvae using Trizol reagent (Invitrogen). For sequencing, cDNA was amplified using primers that flanked the *tbx2b* open reading frame and *Pfu* DNA polymerase, and subcloned into the pCRII-Topo vector (Invitrogen). Clones were sequenced with an ABI 3730xl sequencer and sequence data was analyzed with Sequencher software.

Genotyping fby mutants

To genotype larvae, DNA was extracted by boiling for 10 minutes in 25µL of Embryo Lysis Buffer (Bahary et al., 2004). Proteinase K was added to a final concentration of 0.5mg/mL and samples were incubated at 55°C for two hours, then boiled for 10 minutes to deactivate the Proteinase K. The *fby* mutation introduces a *Mse*I restriction site at bp 134 of exon 3. Primers flanking this site were used to amplify genomic DNA (Forward primer: 5' TGTGACGAGCACTAATGTCTTCCTC 3'; Reverse primer: 5' GCAAAAAGCATCGCAGAACG 3'). The PCR product was digested with the restriction endonuclease *Mse*I (NEB) at 37°C for 1hr, then run on a 3% agarose gel.

Morpholino injections

Antisense morpholino (MO) sequences for *tbx2b* were derived from the translation initiation site and the splice donor site of the 3rd exon as described (*Tbx2b*-ATG and *Tbx2b*-SP, Gross and Dowling, 2005). The MO stock solution (10 mg/ml) was diluted to 6 ng/nl in dH_2O, and embryos (1-2 cell stage) were pressure injected with approximately 1 nl to deliver 6 ng of MO per embryo. Embryos from the transgenic line Tg(*foxd3*:*gfp*)^{fkg17} were used so that the location of the parapineal could be readily assessed by fluorescence in live larvae at 3 to 4 dpf.

RNA in situ hybridization

Whole-mount RNA in situ hybridization was performed as described previously (Gamse et al., 2003), using reagents from Roche Applied Bioscience. RNA probes were labeled using fluorescein-UTP or digoxygenin-UTP. To synthesize antisense RNA probes, pBS-*otx5* (Gamse et al., 2002), *znot* (*flh) (Talbot et al., 1995)*, pBS II SK-*znr1(cyc)* (Sampath et al., 1998), and pBK-CMV-*leftover* (Gamse et al., 2003) were linearized with *Eco*RI and transcribed with T7 RNA polymerase; pCRII-*tbx2b*, *zPitx2* (Tsukui et al., 1999) and pBK-CMV-*right on* (Gamse et al., 2005)with *Bam*HI and T7 RNA polymerase; pCRII-*dexter* (Gamse et al., 2005) with *Xho*I and SP6 RNA polymerase; pBSSK II – *ATV (lft1)* (Thisse and Thisse, 1999)with *Not*I and T7 RNA polymerase; pBSK+ *southpaw* (Long et al., 2003)with *Spe*I and T7 polymerase, pGEM-*frz7a* (El-Messaoudi and

Renucci, 2001)with *Apa*I and SP6 polymerase, *Wnt11* (Makita et al., 1998) with *Hind*III and T3 polymerase, and pBS-*gfi1* (Dufourcq et al., 2004) with *Sac*II and T3 RNA polymerase. Embryos were incubated at 70°C with probe and hybridization solution containing 50% formamide (or 60% for *cyc*). Hybridized probes were detected using alkaline phosphatase-conjugated antibodies and visualized by 4-nitro blue tetrazolium (NBT) and 5-bromo-4-chloro-3-indolyl-phosphate (BCIP) staining for single labeling, or NBT/BCIP followed by iodonitrotetrazolium (INT) and BCIP staining for double labeling. For sagittal sections, larvae were embedded in OCT (Sakura) and sectioned on a Leica cryostat. All in situ data was collected on a Leica DM6000B microscope with a 5x or 20x objective.

Immunofluorescence

For whole-mount immunohistochemistry with rabbit or mouse-derived antibodies, 4 dpf larvae were fixed overnight in 4% paraformaldehyde and stored at –20°C in methanol. Samples were permeabilized by treatment with 10 µg/ml Proteinase K (Roche Applied Bioscience), refixed in 4% paraformaldehyde, and blocked in PBS with 0.1%TritonX-100, 10% sheep serum, 1% DMSO, and 1% BSA (PBSTrS). For antibody labeling, rabbit anti-Lov or rabbit anti-Ron (1:500; (Gamse et al., 2005), rabbit anti-GFP (1:1000, Torrey Pines Biolabs), mouse anti-opsin (1:500, (Adamus et al., 1991) or mouse anti-Zpr-1 (1:250, Zebrafish International Resource Center, Eugene, Oregon) were used. Larvae were incubated overnight in primary antibody diluted in PBSTrS. Primary antibody was

detected using goat-anti-rabbit or goat-anti-mouse secondary antibodies conjugated to the Alexa 568 or Alexa 488 fluorophores (1:350, Molecular Probes).

To simultaneously detect Lov and Ron, chicken anti-Lov polyclonal antibody was generated. A bacterially expressed C-terminal fragment of Lov was generated and purified as described previously ((Gamse et al., 2005)), injected into hens, and total IgY was isolated from egg yolks (Aves Labs). For Lov/Ron double labeling, larvae were fixed in 100% Prefer fixative (Anatech) overnight and stored in PBS + 0.1% Tween-20 for up to 2 weeks. Samples were permeabilized, refixed, and blocked as above, then incubated overnight with chicken-anti-Lov (1:500 dilution of total IgY) and rabbit-anti-Ron antibody (1:500) simultaneously in PBSTrS, and primary antibodies detected with goat-anti-chicken:Alexa 568 and goat-anti-rabbit:Alexa 488. (1:350, Molecular Probes). All immunofluorescence data were collected on a Zeiss/Perkin Elmer spinning disk confocal microscope with a 40x oil-immersion objective and analyzed with Volocity software (Improvision).

Time-lapse imaging

For time-lapse imaging, wild type or *fby* mutant embryos carrying the transgene (*foxd3*:*gfp*)^{fkg3} were either uninjected or injected with a 6 ng/nl solution of *tbx2b* splice MO. Embryos were mounted in a 0.8% solution of low melt agarose containing 0.003% PTU and anesthetized using 0.04% Tricaine. Images were collected on a Zeiss/Perkin Elmer spinning disk confocal

microscope with a 40x oil-immersion objective every 15 minutes from 24 hpf to 48 hpf, and analyzed using Volocity software (Improvision).

Cell ablation

Ablation of a subset of parapineal cells was performed using Tg(*flh*:GFP)^{c161} or Tg(*foxd3:gfp*)^{fkg3} 31 hpf embryos, mounted dorsal-side-up in 0.8% agarose in 35 mm Petri dishes. Parapineal cells were visualized by GFP fluorescence and approximately 5 cells were ablated by 5-10 pulses/cell from a 440 nm laser beam (Photonic Instruments) focused through a 40x water immersion objective mounted on a Leica DM6000B microscope. An equivalent number of cells contra-lateral to the parapineal were ablated in controls.

Results

The from beyond mutation abolishes habenular asymmetry

We screened 4 dpf larvae to identify ENU-induced mutations that altered expression of the K^+ channel tetramerization domain-related (KCTD) gene *leftover (lov)*. In the habenulae, *lov* is typically expressed at high levels and in a broader domain on the left (Gamse et al., 2003 and Figure 3A). The *from beyond (fby)* mutation reproducibly caused reduced expression of *lov* in the left habenula (Figure 3A, B). In WT larvae, the left habenula is larger and contains more neuropil than the right (Concha et al., 2000; Gamse et al., 2003), while in *fby* mutants, the size and neuropil content of the left habenula is similar to the right (data not shown). Intercrosses between carriers from the original F2 family revealed that *fby* segregates as a simple Mendelian recessive mutation (104/438, 24%).

fby mutant larvae developed with normal overall body morphology, formed swim bladders and fed on schedule, but most larvae died at approximately 2 weeks of age. Rarely, mutants survived to adulthood (4/101; 4%). A morphological phenotype of reduced otic vesicle size was also detected, with 30% of mutant larvae showing fused otoliths in one or both otic vesicles at 4 dpf, and 100% by 7 dpf (data not shown).

Reduced *lov* expression in the left habenula was associated with other alterations in the usual L-R asymmetric pattern of the habenulae. In WT larvae, a smaller area of the left habenula compared to the right expresses the KCTD

genes *right on (ron)* and *dexter (dex)* (Gamse et al., 2005 and Figure 3C, E). By contrast, the left habenula of *fby* mutant larvae had an expanded region of *ron*- and *dex*-expressing cells similar to the right habenula (Figure 3D, F).

In addition to asymmetric gene expression, the left and right habenulae differ in their axonal projections to the IPN (Aizawa et al., 2005; Gamse et al., 2005; Kuan et al., 2007). In WT larvae, Lov^{+} axons project to the dorsal and ventral regions of the IPN, whereas Ron^{+} axons project to the ventral IPN only (Gamse et al., 2005) and Figure 3G, I-K). In *fby* mutant larvae, the dorsal/ventral (D/V) pattern of L-R habenula projections was altered. Fewer Lov^{+} axons projected dorsally and more projected ventrally (Figure 3H, L), and an increased number of Ron^{+} axons were detected ventrally (Figure 3M, N). These data are consistent with left habenular efferents adopting a projection pattern characteristic of the right habenula.

Figure 3. The left and right habenulae developed more symmetrically in *from beyond* (*fby*) mutants. (A-F) are dorsal views of the epithalamus of 4 dpf larvae, G-N are lateral views of the brain. (A) In wild type (WT) larvae, the KCTD gene *leftover* (*lov*) was expressed in more cells of the left habenula than the right. (B) In *fby* mutant larvae, the number of lov-expressing cells in the left habenula was reduced relative to WT. (C, E) In WT the *lov*-related *right-on* (*ron*) and *dexter* (*dex*) genes were expressed in more cells of the right habenula than the left, but (D, F) in *fby* mutants, *ron* and *dex* habenular expression appeared symmetrical. Brackets indicate the regions where expression was expanded in mutants. (G) Diagram depicting projections from the habenular nuclei (Lh and Rh) via the fasciculi retroflexus (FR) to the IPN in WT and (H) *fby* mutant larvae at 4 dpf. Red and green areas indicate Lov and Ron immunoreactive neurons respectively, while yellow indicates colocalization of Lov and Ron; grey boxes indicate the area of the brain imaged in (I-N). (I) An antibody against Lov labeled habenular efferents that terminated in both the dorsal and ventral IPN, whereas (J) an antibody against Ron labeled axons terminating in the ventral IPN. (K) Overlay of (I) and (J). (L) In *fby* mutants, Lov labeling decreased in the dorsal IPN and increased in the ventral IPN, and (M) Ron labeling increased in the ventral IPN. (N) Overlay of (L) and (M). Brackets labeled “d” and “v” in (K) and (N) indicate dorsal and ventral regions of the IPN. Scale bars: 25 μm.

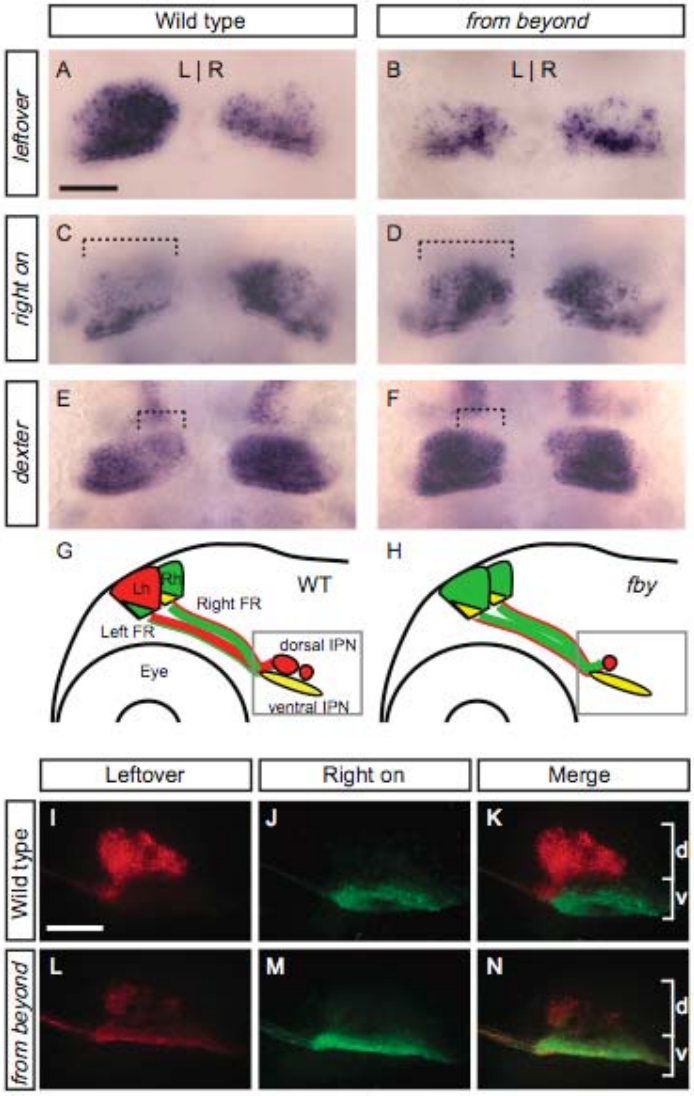
Wild type
from beyond
leftover
right on
dexter
A
L | R
B
L | R
C
D
E
F
G
WT
Lh
Rh
Right FR
Left FR
dorsal IPN
Eye
ventral IPN
H
fby
Leftover
Right on
Merge
Wild type
from beyond
I
J
K
L
M
N
d
v
d
v

The abnormal laterality in the brains of *fby* mutants prompted an examination of asymmetric Nodal signaling, a key early determinant of L-R axis formation (Shen, 2007). In WT embryos, two *nodal* genes, *southpaw (spaw)* and *cyclops (cyc)*, are expressed in the zebrafish left lateral plate mesoderm (LPM), as are the Nodal-induced genes *lefty1 (lft1)* and *pitx2* (Bisgrove et al., 2000; Concha et al., 2000; Liang et al., 2000; Long et al., 2003; Rebagliati et al., 1998a; Rebagliati et al., 1998b; Sampath et al., 1998) and refer to Figure 4A, B). *cyc, lft1,* and *pitx2* were also expressed in the left side of the epithalamus (Figure 4C-E). In *fby* mutants, expression of *spaw, cyc, lft1,* and *pitx2* was indistinguishable from WT siblings in both the left LPM and left epithalamus (Figure 4F-J). The right-sided position of the pancreas and rightward looping of the heart tube, which are influenced by Nodal signaling in the left lateral plate mesoderm (Yan et al., 1999), were also unaffected in *fby* mutants (data not shown).

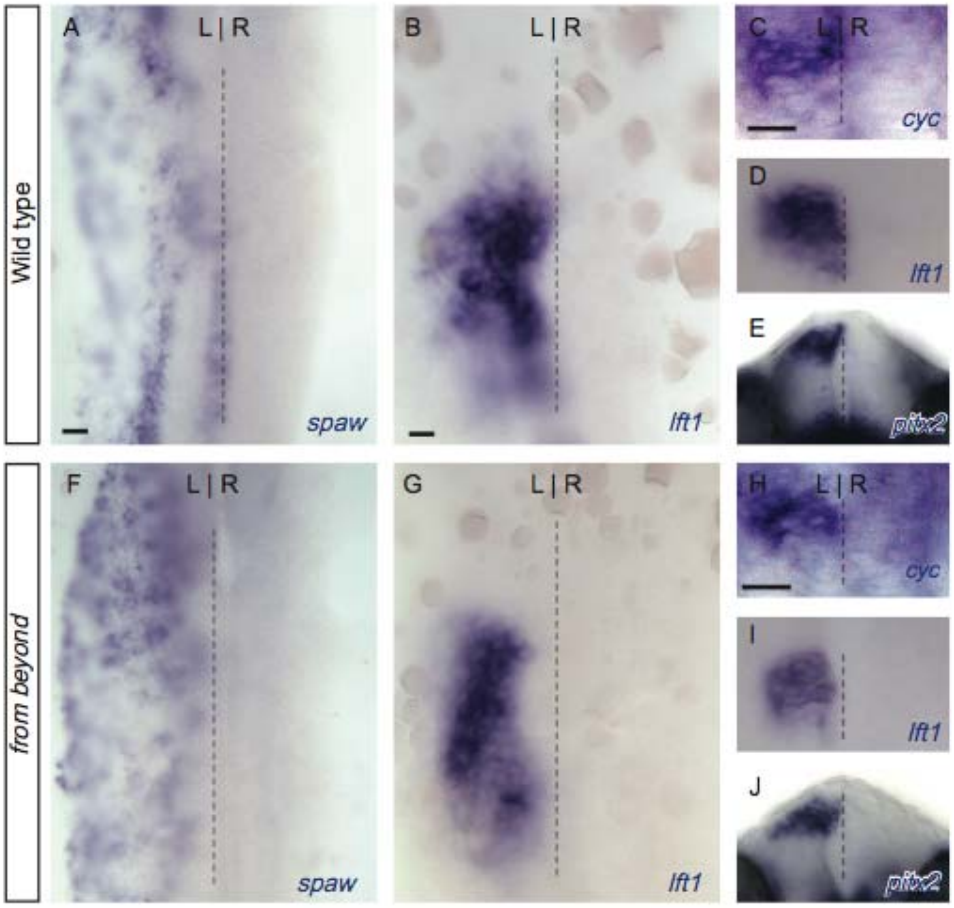

Figure 4. Asymmetric expression of Nodal pathway components was unaffected by the *fby* mutation. All images are 20 hpf embryos, focused on (A, B, F, G) the lateral plate mesoderm or (C-E, H-J) the dorsal diencephalon. All views are dorsal except for frontal views in E and J. Left sided expression of (A, F) the nodal-related genes *southpaw* (*spaw*) and (C, H) *cyclops* (*cyc*), (B, D, G, I) the nodal antagonist *lefty1* (*lft1*), and (E, J) the downstream nodal effector *pitx2* was observed in both wild type and *fby* mutant embryos during somitogenesis. Scale bars: 25 µm.

fby mutants have fewer and mispositioned parapineal cells

Previous studies have shown that the left-sided parapineal organ is required for the asymmetric identity of the habenulae, and therefore for L-R habenular neurons to adopt D/V differences in their projection to the IPN (Aizawa et al., 2005; Concha et al., 2003; Gamse et al., 2005; Gamse et al., 2003). To determine if the altered laterality of the habenulae in *fby* mutants was due to disrupted development of the parapineal, we examined pineal complex formation.

The pineal complex adopted an abnormal morphology in *fby* mutants. In 24 hpf WT larvae, the *otx5* gene is expressed throughout the pineal complex anlage (Gamse et al., 2002) and Figure 5A). By 34 hpf, the *otx5*-expressing parapineal is revealed as a morphologically distinct group of cells emerging from the left anterior border of the pineal complex anlage (Gamse et al., 2002) and Figure 5C). By 4 dpf, parapineal cells are found in a more posterior and ventral position adjacent to the left habenula (Concha et al., 2003; Gamse et al., 2003) and Fig. 5E, G). In *fby* mutants, the pineal complex anlage appeared similar to WT at 24 hpf (Figure 3B), but by 34 hpf, a distinct parapineal organ was not found (Figure 5D). At 4 dpf, individual *otx5*-expressing cells were ectopically located below the pineal organ (Figure 5F, H).

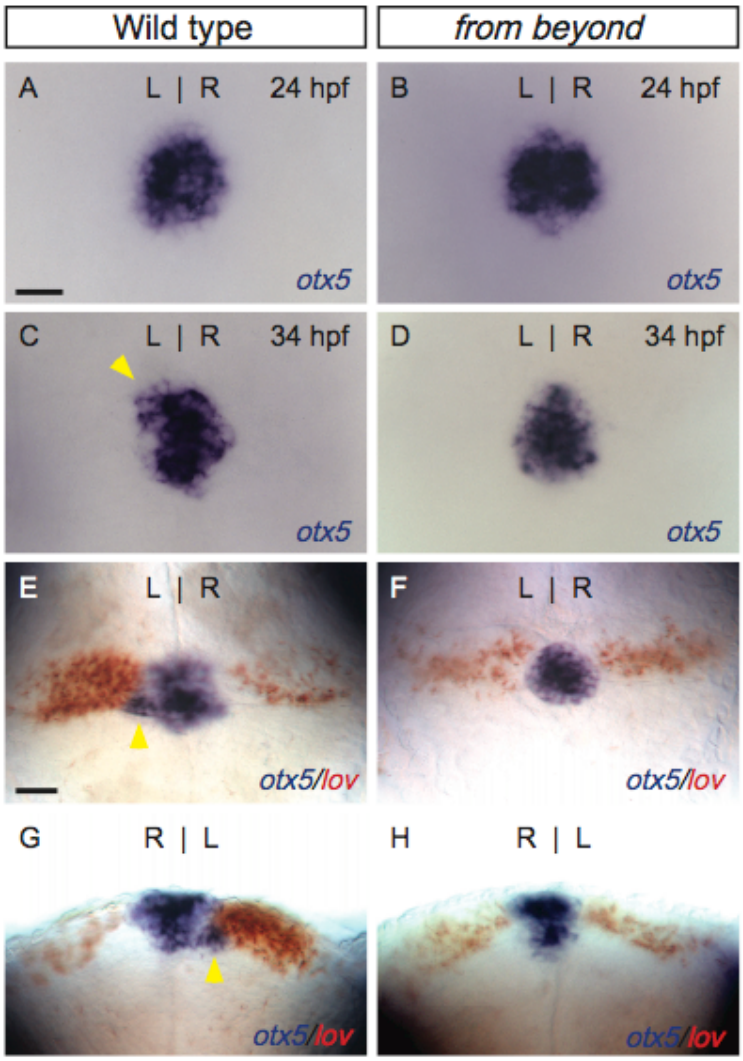

Figure 5. Disruption of parapineal formation in *fby* mutant larvae. (A-F) Dorsal or (G-H) frontal views of the epithalamus of (A, C, E, G) wild type and (B, D, F, H) *fby* mutant larvae. (A) In 24 hpf wild-type embryos, the pineal complex anlage was labeled with *otx5* (blue) and appeared similar to (B) *fby* mutants. (C) However, by 34 hpf, when a parapineal was apparent in WT embryos, (D) no parapineal organ developed in *fby* mutants. Arrowhead in C indicates the emerging parapineal organ. (E, G) By 4 dpf, WT larvae had a left-sided parapineal organ (arrowhead) and more cells expressed lov (red) in the left habenula. (F) In *fby* mutant larvae, no left-sided parapineal organ was apparent; rather, otx5-expressing cells were found below the pineal organ. (H) The number of *lov*-expressing cells in the left habenula was reduced compared to WT. Scale bar: 25 μm.

A number of molecular tools allow pineal and parapineal cells to be distinguished in WT larvae. The *growth factor independent-1 (gfi-1)* gene is selectively expressed at 48 hpf in a tight cluster of parapineal cells on the left side of the brain (10 +/- 1 cells, n=23; (Dufourcq et al., 2004) and refer to Figure 6A, C and Table 1) and are never detected in the pineal. We also examined pineal-specific markers, in the context of the transgenic line Tg*(foxd3:gfp)*^{fkg17} that labels both pineal and parapineal cells with GFP (Concha et al., 2003; Gilmour et al., 2002) and Figure 7). The entire pineal complex of WT larvae consisted of 60 +/- 10 GFP-positive cells (n=13, Table 1). Red-green cone cells labeled by the Zpr-1 antibody are found in the pineal but are absent from the parapineal (Figure 6E). Almost half of the GFP-positive pineal cells were identified in confocal sections as red-green cone cells (44%, n=13, Table 1). Rod cells in the dorsal midline of the pineal organ were labeled by the anti-rhodopsin antibody (Concha et al., 2000). Parapineal cells were negative for rhodopsin expression (Figure 6G, I and Table 1).

Table 1. Number of labeled cells present in the pineal complex of *fby* mutants

Gene/protein (cell types labeled)	**Genotype**	**Number of cells** [a]	**N**
GFP in Tg(*foxd3:gfp*)	WT	60 +/- 10	13
(pineal and parapineal cells except rod cells)	*fby*	61 +/- 17	12
Zpr-1 antibody	WT	21 +/- 6	13
(red-green double cone cells)	*fby*	24 +/- 6	12
Anti-Rhodopsin antibody	WT	41 +/- 2	4
(rod cells)	*fby*	37 +/- 2	6
gfi-1	WT	10 +/- 1	23
(parapineal cells)	*fby*	3 +/- 2 [b]	23

a. Average number of cells labeled per larvae at 4 dpf, plus or minus one standard deviation.
b. Significantly different from WT and *flh* by 2 tailed T-test, $p < 0.01$

In *fby* mutants, some ectopic cells located ventral to the pineal organ were labeled by *gfi-1* at 4 dpf (Figure 6B). However, there were far fewer *gfi-1* expressing cells in mutants than in WT larvae (Table 1), and these were scattered near the midline of the brain, rather than tightly clustered on the left as in WT (Figure 6D). Some of the ectopic cells in *fby* mutants sent out projections reminiscent of WT parapineal axonal projections to the left habenula (compare figure 6I with 6J). In mutants, projections from the ectopic cells did not appear to extend to either habenula, as assessed by GFP expression (Figure 6J and Figure 7). Other ectopically positioned cells expressed the pineal cone cell marker Zpr-1, but not rhodopsin (Figure 6F, H, J). These data indicate that the ectopic cell population consisted of a mixture of pineal and parapineal cells. The few parapineal cells that did develop in *fby* mutants failed to organize into a coherent structure.

Figure 6. Fewer and misplaced parapineal cells in *fby* mutants. (A-D, I, J) Dorsal or (E-H) frontal views of 4 dpf larvae. (A) In the epithalamus, expression of *gfi-1* was exclusive to parapineal cells of wild type larvae at 4 dpf, which formed a compact organ. (B) In *fby* mutants, fewer *gfi-1*-expressing cells developed than in WT, and they were found as individual cells in the middle of the brain. (C) The position of *gfi-1*-expressing cells from 10 individual WT or (D) *fby* larvae were represented by different colored dots for each sample. The vertical axis divides the left and right sides of the brain whereas the horizontal axis is the posterior border of the habenular nuclei. (E) Double immunofluorescent labeling of a WT larvae with foxd3:gfp (green) and the antibody Zpr-1 (red). Zpr-1 labeled red-green double cone cells, which were almost exclusively found in the pineal but not the parapineal (arrowhead). (F) In *fby* mutants, Zpr-1 labeled cells were found throughout the pineal complex including cells ventral to the pineal organ. (G, I) Double labeling of a WT larvae with *foxd3*:*gfp* (green) and anti-Rhodopsin antibody (red). Rhodopsin-expressing cells were near the dorsal midline of the pineal organ in WT as well as (H, J) *fby* mutant larvae. Scale bars: 25 μm.

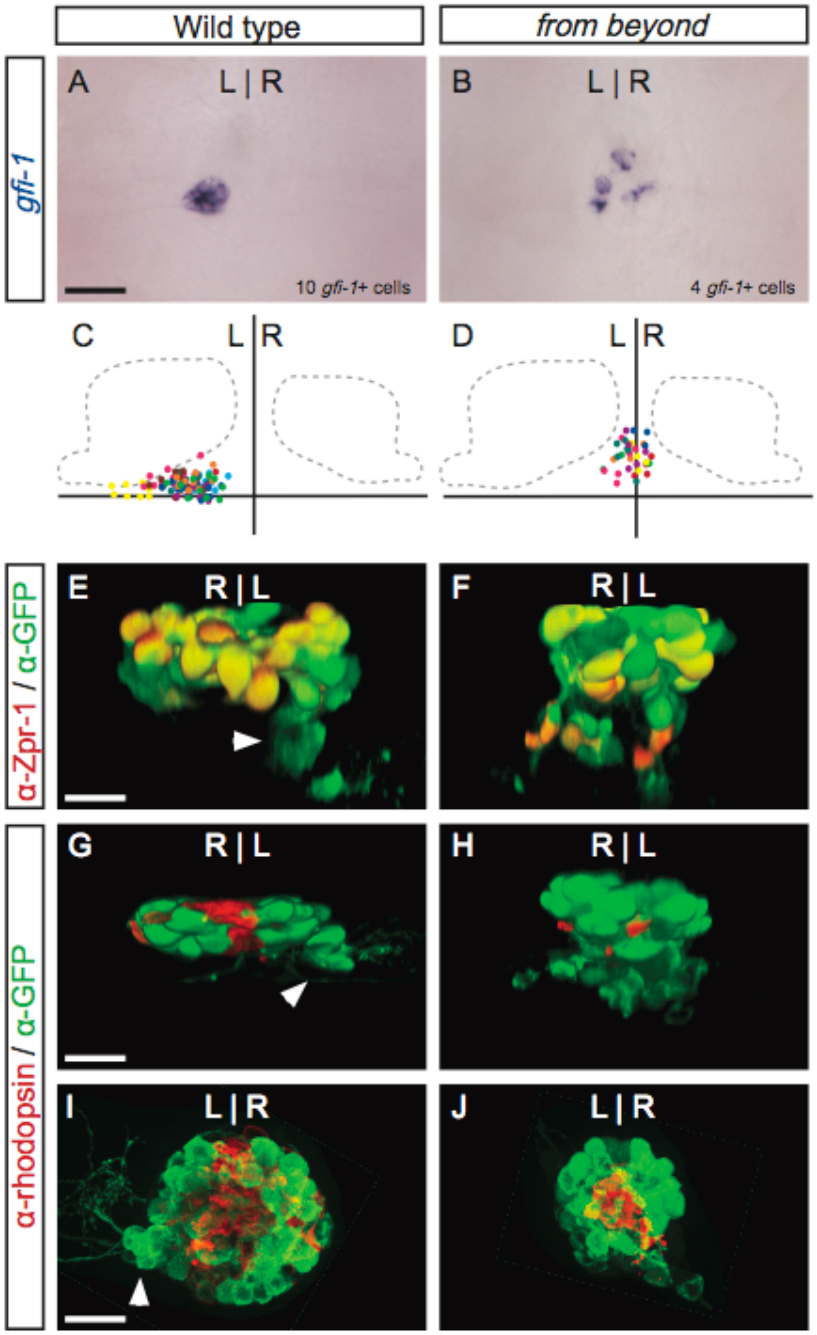
Wild type
from beyond
gfi-1
A
L | R
10 gfi-1+ cells
B
L | R
4 gfi-1+ cells
C
L R
D
L R
α-Zpr-1 / α-GFP
E
R | L
F
R | L
α-rhodopsin / α-GFP
G
R | L
H
R | L
I
L | R
J
L | R

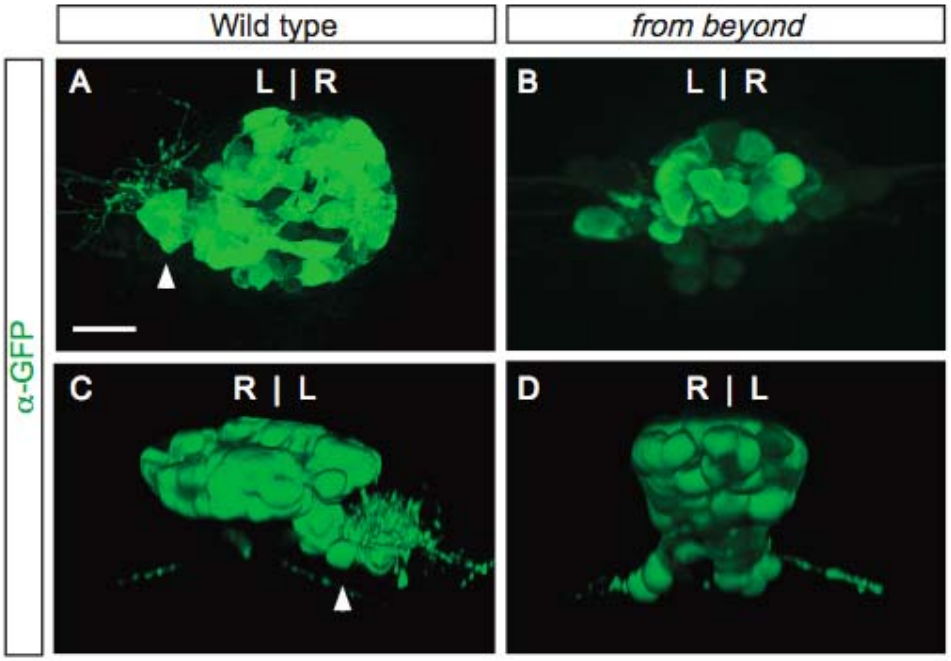

Figure 7. The *fby* mutation has ectopically placed GFP+ cells. (A,B) Dorsal and (C,D) frontal views of *foxd3:gfp* expression in the pineal complex of 4 dpf larvae. (A,C) In WT larvae, the parapineal organ (arrowhead) is a group of cells found to the left of and below the pineal organ. (B,D) In *fby* mutant larvae, the pineal complex is a single mass of cells without a discrete parapineal organ. Scale bar: 25 μm.

Migration of a group of cells, such as the lateral line primordium, requires polarization of the cell cluster (reviewed in (Ghysen and Dambly-Chaudiere, 2007). The failure of parapineal migration in *fby* mutants could therefore be a secondary consequence of specifying too few parapineal cells to form a polarized group. To test if parapineal migration and cohesion depends on cell number, ~5 cells were ablated at 31 hpf, prior to their movement away from the pineal complex anlage, leaving a number of cells comparable to *fby* mutants (Figure 8A-F). The placement of the remaining parapineal cells was assayed at 55 hpf, when they have moved leftward, as well as posteriorly and ventrally, and begin to express *gfi-1*. We find that the remaining parapineal cells form a coherent and correctly positioned, albeit smaller, parapineal organ, similar to controls (Figure 8 G-L).

Figure 8. Reduced numbers of WT parapineal cells are able to migrate. Dorsal views of the epithalamus in (A, B, D, E) 31 hpf embryos or (C, F, G-L) 55 hpf larvae. (A) Expression of *foxd3*:*gfp* labels parapineal precursor cells (yellow arrowhead) (B) which are subsequently ablated with laser pulses. (C) The remaining parapineal cells (average of 5 +/- 2 cells, n=18) migrate to the left side of the brain, as revealed by *foxd3*:*gfp* and (G) *gfi-1* expression. In (H) the position of *gfi-1* expressing cells in 10 larvae are overlaid, with different colors representing individual samples. (D, E, F) As a control, cells contralateral to the parapineal precurors were ablated (red arrowhead); (I, J) the number of parapineal cells (10 +/-1, n=8) and their migration is identical to (K, L) unablated controls (10 +/- 2 cells, n=10). Scale bars: 25 μm.

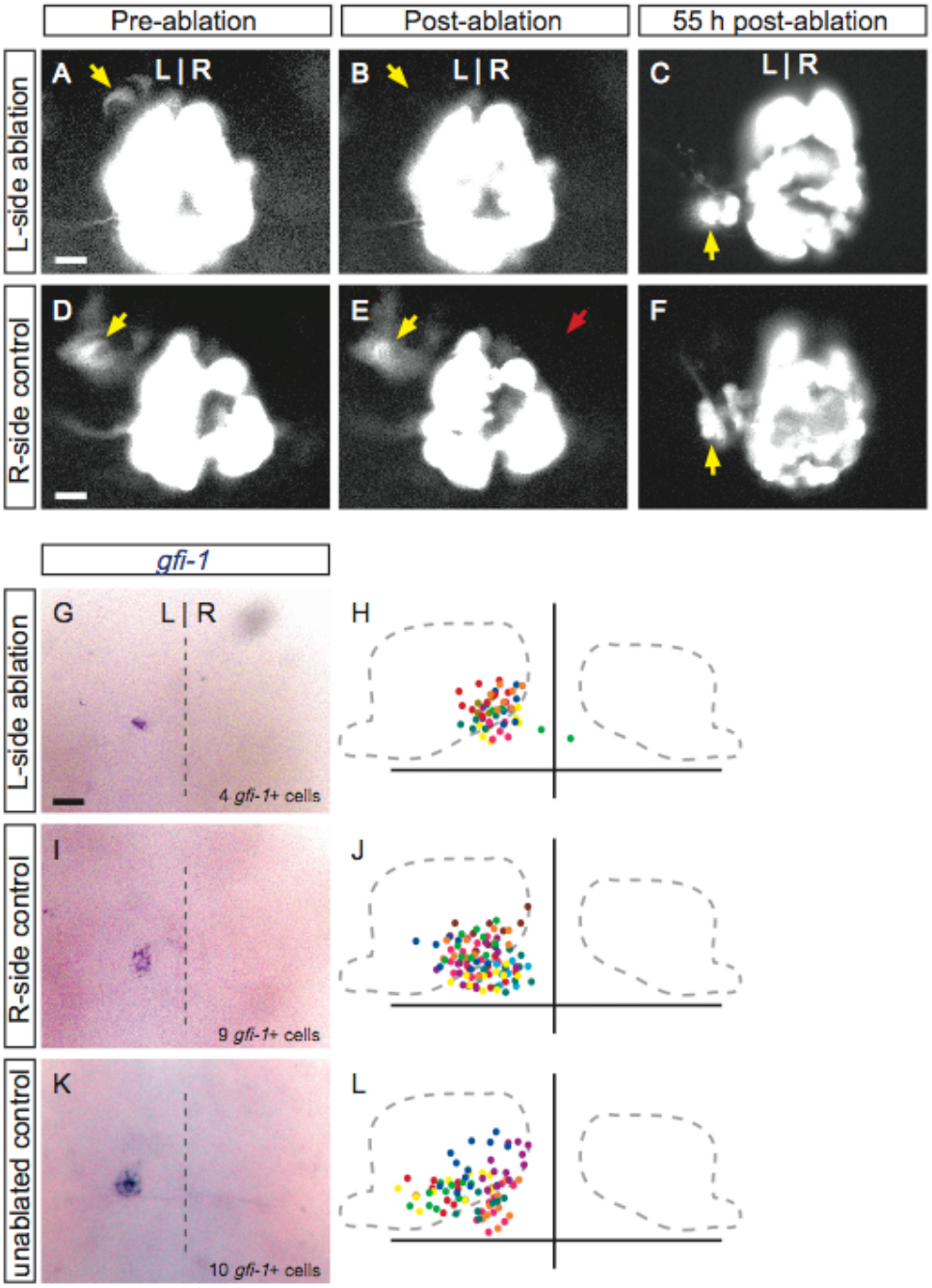
Pre-ablation
Post-ablation
55 h post-ablation
L-side ablation
R-side control
A
B
C
D
E
F
L | R
gfi-1
G
H
I
J
K
L
4 gfi-1+ cells
9 gfi-1+ cells
10 gfi-1+ cells
unablated control

The fby mutation introduces a premature stop codon in the tbx2b coding sequence

The *fby* mutation was mapped to a region of chromosome 15, approximately 100 kb telomeric to the SSLP marker z22430 (Figure 9A). Examination of the zebrafish genome sequence (Hubbard et al., 2006) revealed two genes, *tbx2b* and *tbx4*, in this region. The *tbx2b* gene was a likely candidate based on previous reports of expression in the pineal anlage (Dheen et al., 1999; Ruvinsky et al., 2000) and the observation that antisense morpholino (MO) treated embryos developed abnormal otic vesicles similar to those seen in *fby* mutants (Gross and Dowling, 2005). Sequencing of *tbx2b* cDNA from *fby* mutants at 4 dpf revealed a T to A transversion introducing a premature stop codon (Figure 9B). This lesion lies within the T-box sequence and is predicted to prevent translation of 9 of the 20 DNA-contacting residues (Sinha et al., 2000). Two different antisense morpholino oligonucleotides that blocked either *tbx2b* translation or removal of the third intron (Gross and Dowling, 2005) effectively phenocopied the *fby* mutation (Figure 9C, D). Microinjection of *tbx2b* morpholinos into *fby* mutants did not cause a further reduction in the number of *gfi-1*-expressing cells (data not shown), supporting that the *fby* mutation eliminates *tbx2b* function.

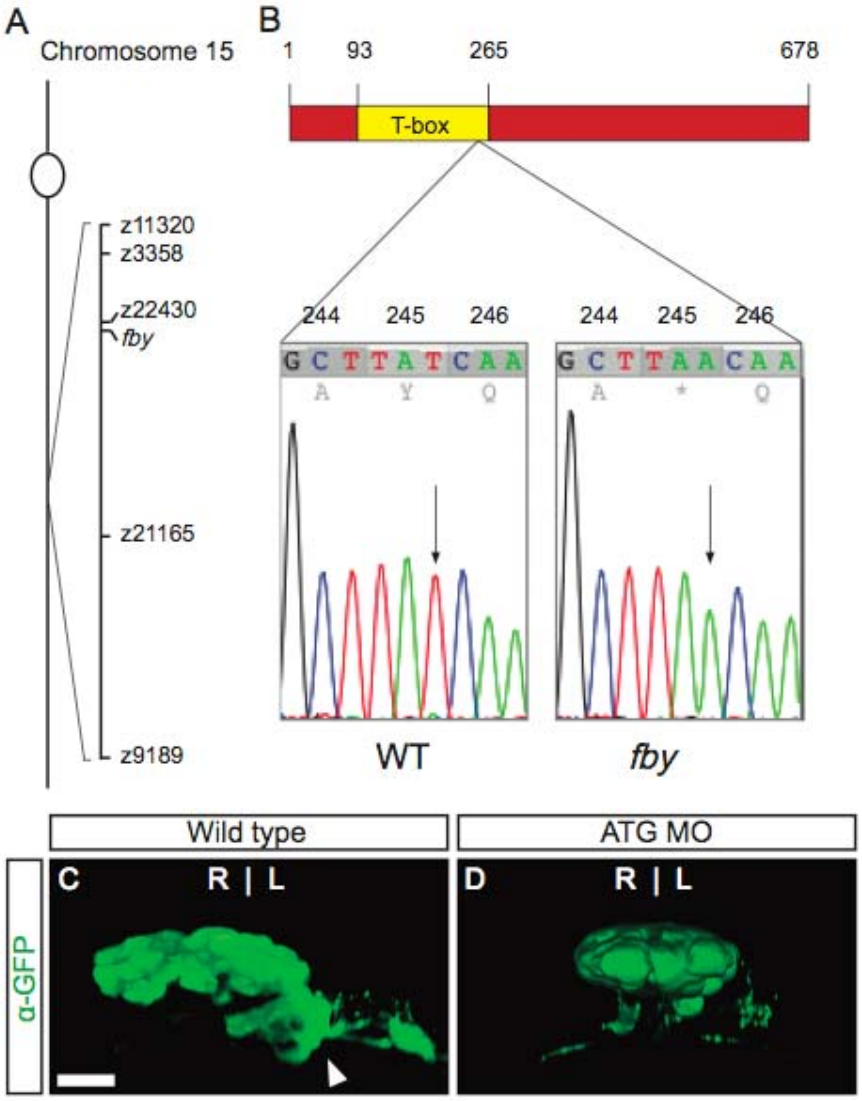

Figure 9. The *fby* mutation is a premature stop codon in the *tbx2b* gene. (C, D) are frontal views of 4 dpf larvae. (A) Diagram of chromosome 15, showing the location of the *fby* mutation relative to nearby SSLP markers. (B) In *fby*^{c144} mutants, the third position of codon 245 in the *tbx2b* gene was transverted from T to A, generating a stop codon within the T-box sequence. (C) Compared to uninjected *foxd3*:*gfp* controls, (D) injection of an antisense morpholino against the start codon of *tbx2b* (ATG MO) resulted in a similar phenotype to the *fby* mutation. Scale bar: 25 μm.

tbx2b is expressed early in the pineal complex anlage

Expression of *tbx2b* in the cells that give rise to the medially located pineal complex anlage was present at the 6 somite stage, in two clusters of cells at each lateral edge of the neural plate (Figure 10A). By the 10 somite stage, when the lateral edges of the neural plate meet to form the neural rod, a single dorsal midline domain of *tbx2b* expression was detected (Figure 10B and (Ruvinsky et al., 2000). At 24 hpf, expression of *tbx2b* was found in many cells of the pineal complex anlage, and was most intense in the midline (Cau and Wilson, 2003; Dheen et al., 1999; Ruvinsky et al., 2000)and Figure 10C). At 4 dpf, *tbx2b* expression was maintained in the parapineal organ and the pineal stalk (Figure 10D). In *fby* mutants, *tbx2b* RNA expression was still detected in the pineal complex anlage similar to wild type (Figure 10E,F) indicating that the *fby* mutation did not cause nonsense-mediated decay.

The *tbx2b* expression pattern resembled *flh*, a homeobox transcription factor also expressed in the pineal complex anlage (Masai et al., 1997), although the two genes did not completely overlap in their expression. During somitogenesis, many *flh*-positive cells expressed *tbx2b* (Figure 10G). However, some medial cells of the pineal complex anlage expressed *tbx2b* only (Figure 10H). By 24 hpf, the pineal complex anlage expressed both *flh* and *tbx2b* except at its most lateral edges, where only *flh* expression was detected (Figure 10I, J).

Figure 10. *tbx2b* expression in the pineal complex. (A-F, G, I) Dorsal views of embryos or larvae at the indicated stage of development. (H) shows a sagittal section at the level of the arrowhead in G; (J) shows a transverse section at the level of the arrowhead in (I). (A) Expression of *tbx2b* in the future epithalamus began at 6 somites, in two groups of cells at the lateral borders of the neural plate. (B) Following neural tube closure, a single *tbx2b*-expressing domain was detected at 10 somites and (C) 24 hpf. (D) At 4 dpf, expression was maintained in the parapineal (arrowhead) and in the pineal stalk. (E) Expression of *tbx2b* was unchanged in *fby* mutants at 10 somites and (F) 24 hpf. (G) Many *tbx2b* expressing cells (blue) also expressed *flh* (red) in the future epithalamus at 8 somites, although (H) some *tbx2b*+, *flh*- cells were detected medially and dorsally (bracket). (I) By 24 hpf, *tbx2b* and *flh* were co-expressed in much of the pineal complex anlage, although (J) expression of *flh* extended slightly more laterally and ventrally (bracket) than *tbx2b*. Scale bars: 25 μm.

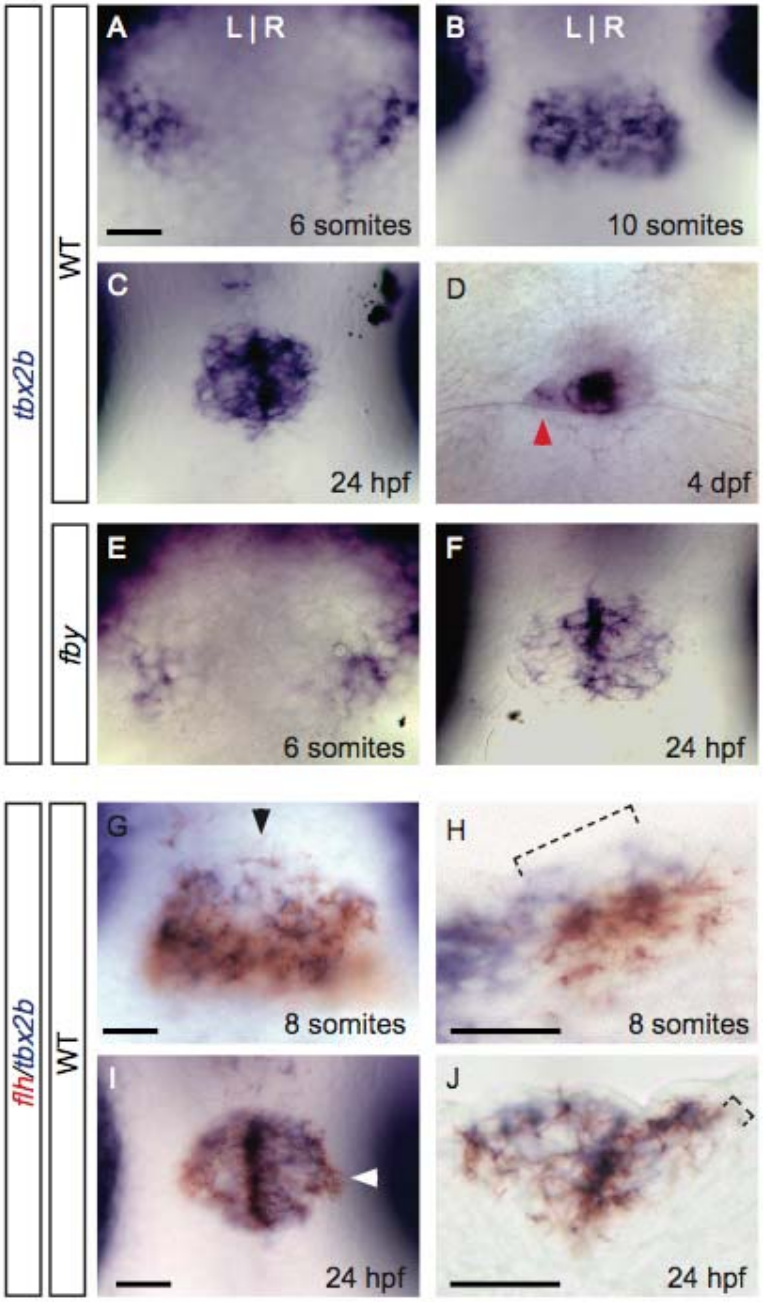
tbx2b
WT
A
L | R
6 somites
B
L | R
10 somites
C
24 hpf
D
4 dpf
fby
E
6 somites
F
24 hpf
flh/tbx2b
WT
G
8 somites
H
8 somites
I
24 hpf
J
24 hpf

Previous reports indicated that during neural plate formation in zebrafish, *tbx2b* expression is regulated by the Wnt receptor *frizzled7a (fz7a)* (Fong et al., 2005), and that in the developing mouse hindbrain, *tbx2b* regulates expression of Wnt planar cell polarity (PCP) genes including *fz7* (Song et al., 2006). However, we find that disrupting the Wnt planar cell polarity signaling pathway, by mutation of the proteoglycan *knypek/glypican* (Topczewski et al., 2001) or the *strabismus* homolog *trilobite/van gogh-like 2* (Jessen et al., 2002), has no effect on *tbx2b* expression, parapineal specification or migration (Figure 11A-I). In addition, neither *fz7a* nor other PCP genes (*wnt11, wnt5, frz7b, trilobite)* are expressed in the epithalamus (Figure 11J-Q and data not shown).

Figure 11. The planar cell polarity pathway is not disrupted in *fby* mutant embryos. (A-I) Dorsal views of the epithalamus in 24 hpf embryos (A-F) or 48-hpf larvae (G-I). Expression of *otx5* (A-C) and *tbx2b* (D-F), and placement of the *gfi-1* positive parapineal cells (G-I), are unaffected in homozygous mutants for the planar cell polarity genes *knypek* (*kny*) or *trilobite* (*tri*). (J-Q) Lateral views of 24-hpf embryos. The Wnt receptor *frz7a* (blue) and the Wnt ligand *wnt11* (blue) are excluded from the *otx5*-positive cells (red, arrowhead) of the pineal complex in WT (J-M) and *fby* mutant (N-Q) embryos. Scale bars: 25 μm in A-I,K,M,O,Q; 100 μm in J,L,N,P.

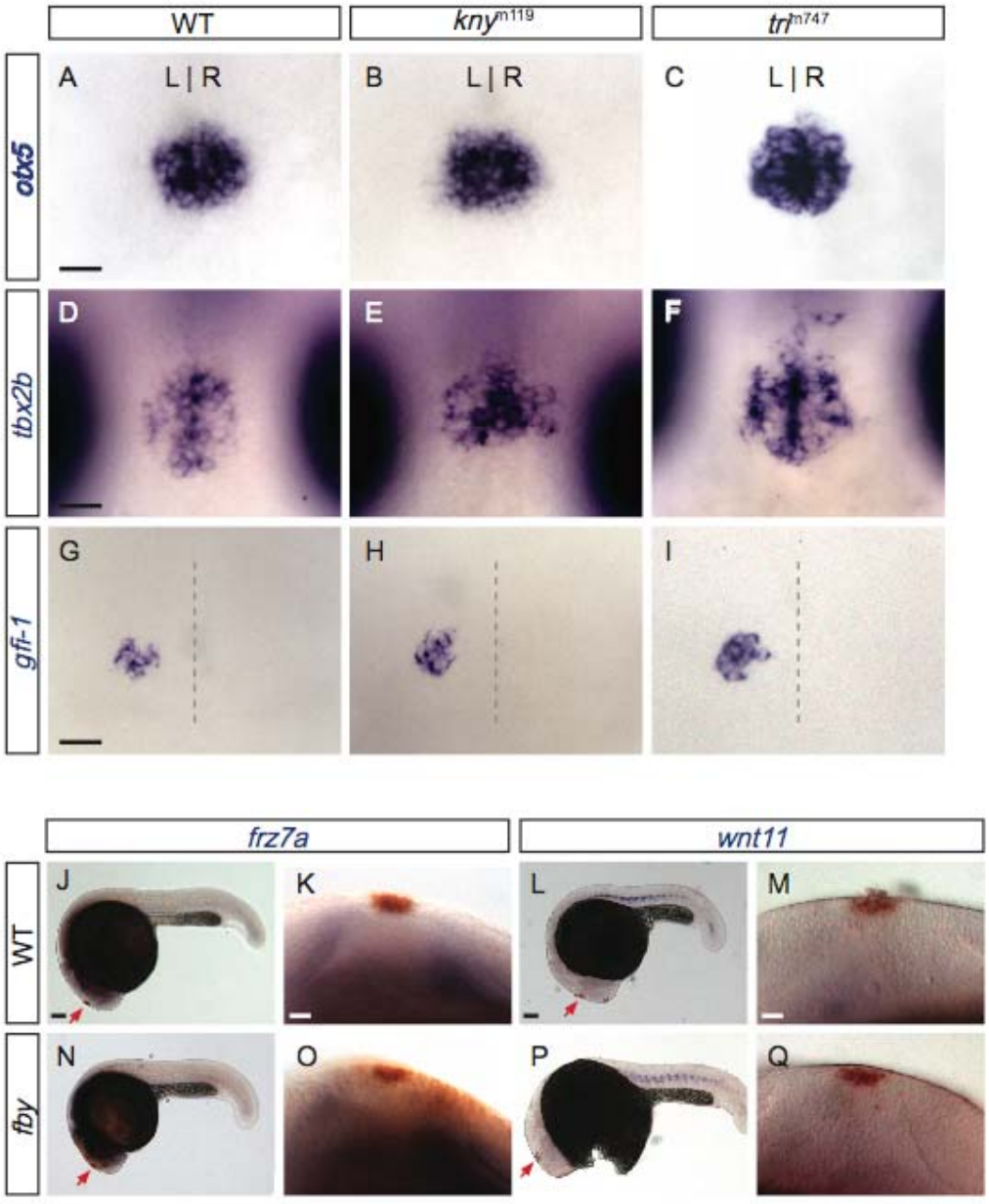
WT
kny m119
tri m747
otx5
tbx2b
gfi-1
A
L | R
B
L | R
C
L | R
D
E
F
G
H
I
frz7a
wnt11
WT
fby
J
K
L
M
N
O
P
Q

Migration of parapineal cells is disrupted in fby mutants

In *fby/tbx2b* mutants, the absence of a distinct left-sided parapineal organ and the development of parapineal cells in an ectopic ventral location suggested that parapineal cells failed to move to the left side of the brain. Although studies have inferred that parapineal precursors migrate out from the anlage to the left side of the brain (Concha et al., 2003; Gamse et al., 2003), these cellular movements have not been directly documented in live embryos. We performed time-lapse analysis using *foxd3:gfp* transgenic embryos, recording cell locations between 24 and 48 hpf (Supplementary Movie 1 located online at: http://dev.biologists.org/content/vol135/issue9/images/data/1693/DC1/016576-movie1.mov). One or two highly protrusive cells extending multiple short and wide filipodia were detected at the anterior left edge of the pineal complex anlage at 31 hpf (Figure 12A). Over the next eight hours, these cells migrated in a leftward and slightly caudal direction (Figure 12D, G). They were very closely followed by more cells that originated from the same anterior left region of the pineal complex anlage (Figure 12J). By 48 hpf, the cells stopped moving, they coalesced into a tightly packed cluster, and extended highly dynamic, thin processes (Figure 12M, P).

In contrast to the robust migration of parapineal cells to the left side of the brain, leftward migrating cells were not observed in *tbx2b* morpholino treated or *fby* homozygous mutant embryos (Supplementary Movie 2 located online at: http://dev.biologists.org/content/vol135/issue9/images/data/1693/DC1/016576-

movie2.mov. Supplementary Movie 3 located online at: http://dev.biologists.org/content/vol135/issue9/images/data/1693/DC1/016576-movie3.mov). At 33 hpf, one or two highly protrusive cells were seen at the anterior end of the pineal complex anlage (Figure 12B, C). They were joined by an additional two or three highly protrusive cells over the next nine hours (Figure 12E, F, H, I, K, L). However, these cells did not migrate to the left of the pineal, but remained close to the midline near the anterior end of the pineal complex anlage. Although in an ectopic location, these cells still extended long, thin processes by 48 hours (Figure 12N, O, Q, R). The time-lapse analyses indicated that *tbx2b* is required for the leftward migration of parapineal cells and their morphogenesis into a coherent cluster.

Figure 12. Parapineal cells do not migrate to the left side of the brain in *fby* mutants. Dorsal views of *foxd3:gfp* expression in live (A, D, G, J, M, P) WT, (B, E, H, K, N, Q) *fby* mutant or (C, F, I, L, O, R) *tbx2b* splice morpholino-treated embryos. The data are snapshots of time-lapse confocal movies imaged from 31 to 48 hpf. (P, Q, R) are magnified and contrast-enhanced regions of the anterior pineal complex from (M, N, O), respectively. In WT embryos, GFP-labeled cells emerged from the anterior left end of the pineal complex as a chain of cells between 31 and 39 hpf. Cells are numbered in the order of their appearance. Cell 1 divided from 39.75 to 40.25, and its daughter is labeled 1'. Note that some parapineal cells (e.g. #3, 4, 7, 8) become hidden by overlying cells. Between 39 and 48 hpf, the parapineal cells compacted together, and extended long thin projections (red arrowhead). In contrast, *fby* mutants and *tbx2b* morpholino-treated embryos had no GFP-labeled cells migrating to the left, but cells at the anterior end of the pineal complex still extended long thin projections. Scale bar: 25 μm.

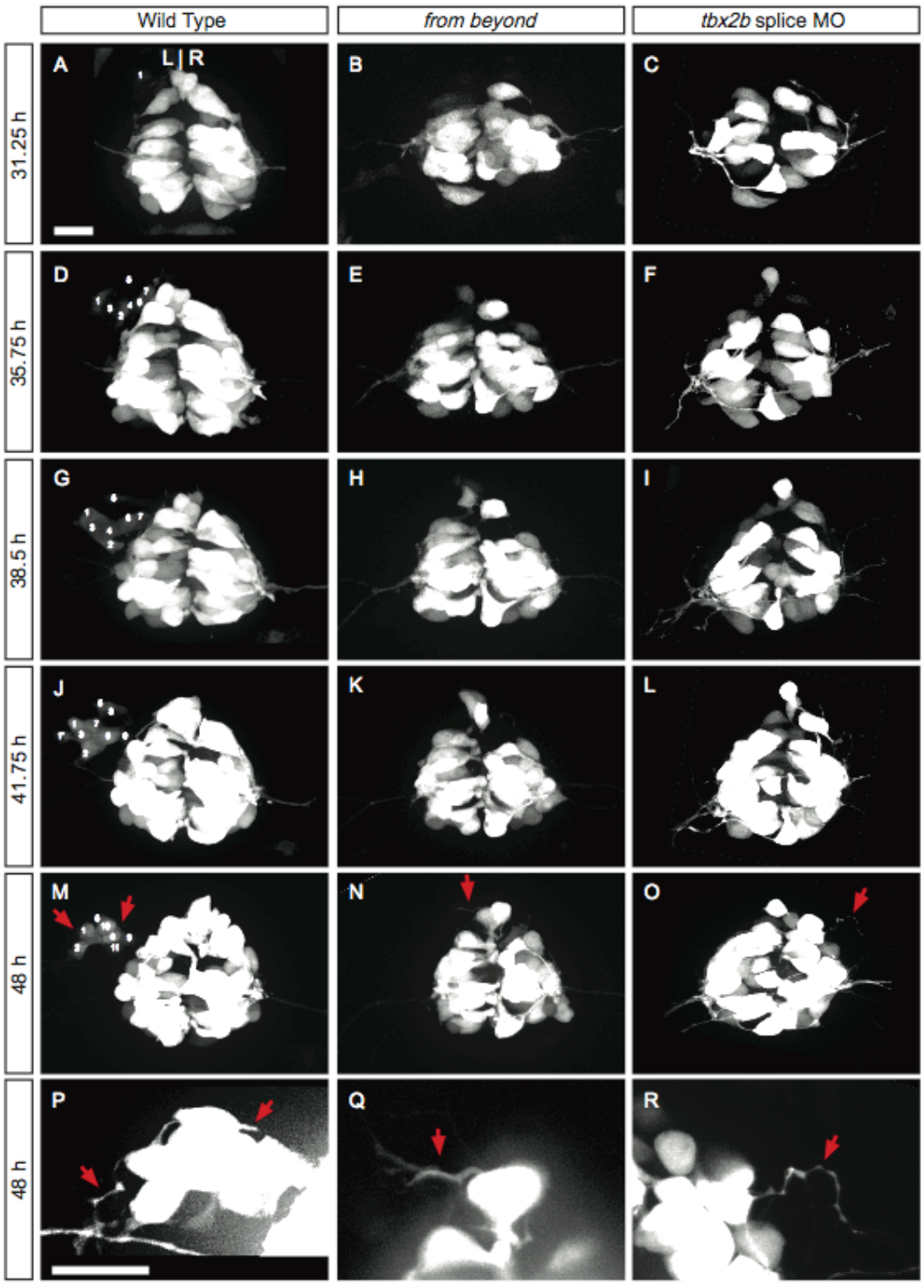
Wild Type
from beyond
tbx2b splice MO
31.25 h
35.75 h
38.5 h
41.75 h
48 h
48 h
A
L | R
B
C
D
E
F
G
H
I
J
K
L
M
N
O
P
Q
R

Discussion

In this study, we examined the specification and migration of cells that form the parapineal organ using the *fby* mutation, which disrupts the *Tbx2b* transcription factor. In *fby* mutants, fewer parapineal cells develop, and these cells fail to migrate to the left side of the brain to coalesce into the parapineal organ. Our findings have identified a genetic regulator of a distinct subpopulation of cells in the pineal complex anlage that is important for their specification and migration.

Expression of tbx2b in the pineal complex specifies parapineal cells

The *tbx2b* gene is expressed in many cells of the pineal complex anlage, but only a dozen cells contribute to the parapineal organ. How does a widely expressed transcription factor play a role in the development of a limited number of parapineal cells? One likely model is that different cell types in the pineal complex anlage are specified by different repertoires of transcription factors that interact with *tbx2b*. Modulation of enhancer binding activity by interaction with other transcription factors (particularly LIM, GATA, and homeodomain proteins) is a common feature of Tbx family members (Naiche et al., 2005; Showell et al., 2004). The *tbx2b* gene is co-expressed with the homeobox gene *flh* in most of the pineal complex anlage at 8 somites. However, a small symmetric domain in the anterior medial region of the anlage expresses *tbx2b* but not *flh*. We propose that cells from this anterior medial domain will be specified as parapineal, while

cells expressing both *flh* and *tbx2b* will generate the pineal organ. This model predicts that the *fby* mutation causes parapineal precursors to be re-specified to a pineal fate. In support of this model, we find that in addition to reduced numbers of *gfi-1* expressing parapineal cells, red-green cone cells typically restricted to the pineal are situated in an ectopic position ventral to the pineal organ.

The absence of a *tbx2b*-exclusive domain in the pineal complex anlage of *fby* mutants affects parapineal specification; however, a few cells still adopt parapineal identity as assessed by *gfi-1* expression. The action of *tbx2b* in combination with additional transcription factors during parapineal and pineal specification will be directly tested by conditional misexpression in the epithalamus using tissue-specific promoters.

A trivial explanation for the formation of a few *gfi-1*-expressing cells in *fby* mutants is that the mutation is hypomorphic; however, the c144 ENU lesion produces a premature stop codon that is predicted to abolish *Tbx2b* binding to DNA. Moreover, depletion of *tbx2b* in WT or *fby* mutant embryos by two highly effective MOs phenocopied all aspects of the *fby* mutation but did not eliminate *gfi-1* expressing cells completely. It is unlikely that a second zebrafish *tbx* gene partially compensates for the loss of *tbx2b*, because the closest relatives of *tbx2b (tbx2a, tbx3, tbx4,* and *tbx5)* do not appear to be expressed in the pineal primordium (Dheen et al., 1999; Ruvinsky et al., 2000).

tbx2b specifies parapineal cells without affecting Nodal signaling

In addition to expression in the pineal complex, *tbx2b* is expressed in the chordoneural hinge (CNH), a structure in the embryonic tailbud (Dheen et al., 1999; Ruvinsky et al., 2000). Expression of the Nodal gene *southpaw* in the chordoneural hinge is required for its subsequent asymmetric expression in the left LPM, where it regulates left-sided expression of another Nodal gene, *cyclops*, in the LPM and epithalamus (Gourronc et al., 2007). Loss of *spaw* activity results in the absence of *cyc* expression in the left epithalamus (Long et al., 2003) and left-right randomization of parapineal location (Gamse et al., 2005). However, *fby* mutant embryos develop with normal left-sided expression of *nodal* genes, indicating that *tbx2b* activity in the chordoneural hinge is not required for initiation of asymmetric *spaw* expression. This suggests that *tbx2b* acts in the pineal complex anlage to regulate specification of the parapineal organ in a pathway that is independent of Nodal signaling.

Parapineal cells require tbx2b activity to migrate away from the pineal complex anlage

In wild-type embryos, migration of parapineal precursor cells from the pineal complex anlage begins with the emergence of a single cell from the anterior left region, followed by other closely apposed cells. This sequence suggests a leader-follower mechanism for directional migration, in which cells at the leading edge coordinate the behavior of the group. Such cellular behavior

has been best described in zebrafish for the migration of the lateral line primordium, where leader cells expressing *cxcr4b* at the anterior end of the primordium organize the migration of the rest of the cells (Haas and Gilmour, 2006). The first cells to emerge from the pineal complex anlage may be leader cells that direct the left-sided movement of the parapineal organ. In *fby* mutants, a reduced number of cells develop with parapineal characteristics, including *gfi-1* expression and anteriorward axonal projections, and they do not migrate to the left side of the epithalamus; rather, at 48 hpf they are found in the midline, at the anterior edge of the pineal complex. The failure of parapineal cells to migrate in *fby* mutants could be due to the reduced number of parapineal precursor cells that are specified, the inability of mutant cells to move, or a loss of leader cell function. We believe that the latter hypothesis is correct. First, reducing the total number of parapineal precursor cells by laser ablation to a number similar to the scattered cells in the *fby* mutant still allows a cohesive organ to form on the left side of the brain. Second, *fby* mutant parapineal cells still move posteriorly and ventrally, and thus are not immobile. Therefore, we speculate that *tbx2b* is required for the specification or maintenance of leader cells. To test this hypothesis will require developing methods to identify the leader cells and specifically destroy them as they emerge from the pineal complex.

One mechanism invoked to mediate *tbx2b* regulation of migration is the Wnt-PCP pathway. While *tbx2b* plays a role in PCP in other contexts (Fong et al., 2005; Song et al., 2006), we find no role for PCP in parapineal migration.

Delayed parapineal migration away from the midline until after 48 hpf has been observed in *masterblind/axin1(mbl)* and RNA-rescued *one-eyed pinhead (*R*oep)* mutants in a significant percentage of larvae (Carl et al., 2007). However, by 96 hpf, the parapineal cells of *mbl* and R*oep* mutants have achieved their correct left-sided position, while the parapineal cells of *fby* mutants remain scattered close to the midline. The data suggest that *mbl* and *oep* regulate the timing or speed of migration, but are not required for leader cell formation.

An evolutionarily conserved role for tbx genes in parapineal formation?

Fish, frog, lizard and bird embryos all develop a pineal and a pineal accessory organ (although in birds the parapineal does not persist in the adult), whereas mammals seem to form only the pineal gland (Borg et al., 1983; Braitenberg and Kemali, 1970; Butler and Hodos, 1996; Hill, 1891). The development of a pineal complex that includes both a pineal and an accessory organ is phylogenetically correlated with the expression of *tbx* homeobox genes in the pineal complex anlage. Such expression is observed for *tbx2b* in zebrafish (Dheen et al., 1999; Ruvinsky et al., 2000)and this study), and for the closely related *tbx3* gene in chick (Gibson-Brown et al., 1998) and Xenopus (Takabatake et al., 2000). However, in the mouse, neither *tbx2* nor *tbx3* is expressed in the developing diencephalon (Chapman et al., 1996). We propose that the pineal accessory organ of non-mammalian vertebrates is specified by Tbx2/3 function.

In lizards and frogs, the pineal accessory organ (known as the parietal eye or frontal organ, respectively) is photoreceptive, expresses certain opsin family

members and is thought to transmit diurnal information (Blackshaw and Snyder, 1997; Eldred et al., 1980; Engbretson et al., 1981; Su et al., 2006). In mammals, which do not receive direct light input to the pineal, the major source of diurnal information is stimulation of the melanopsin-expressing retinal ganglion cells (Hattar et al., 2002). The acquisition of photic input to the pineal via the eyes in mammals rendered a photoreceptive pineal accessory organ unnecessary. Loss of *tbx2/3* expression in the pineal complex anlage may be the mechanism that prevents formation of a pineal accessory organ in mammals, by altered specification and disrupted migration of precursors. How a transcription factor regulates the number and behavior of parapineal cells will be revealed by identification of its downstream target genes.

CHAPTER II

FORMATION OF THE ASYMMETRIC PINEAL COMPLEX IN ZEBRAFISH REQUIRES TWO INDEPENDENTLY ACTING TRANSCRIPTION FACTORS

This paper is published under the same title in *Developmental Dynamics*, December 2008 237(12): 3538-44; (Snelson et al., 2008a)

Abstract

The pineal complex of zebrafish consists of a pineal organ and a left-sided parapineal organ. Mutation of the *floating head (flh)* gene, which encodes a homeodomain protein, causes premature termination of pineal cell division without affecting specification or asymmetric placement of the parapineal. The *from beyond (fby)* mutation, a premature stop codon in the T-domain-containing protein *Tbx2b*, disrupts formation of the parapineal while leaving the pineal largely intact. However, *flh* is reported as being required for *tbx2b* transcription. To resolve the paradox that *flh* and *tbx2b* mutants have opposite phenotypes but have been placed in the same genetic pathway, we have examined transcriptional cross-regulation in single *flh* or *fby* mutants and genetic epistasis in double mutants. Careful analysis shows that *flh* is not required for *tbx2b* transcription and double mutants exhibit an additive phenotype. We conclude that *Flh* and *Tbx2b* regulate separate programs of pineal and parapineal development.

Introduction

The epithalamus, or dorsal diencephalon, of the vertebrate brain includes the left and right habenular nuclei (habenulae) and the melatonin-secreting pineal complex. The habenulae receive afferent input from forebrain regions including the septum, globus pallidus, and lateral hypothalamus, and send efferent axons to the midbrain (Sutherland, 1982). The pineal complex includes the pineal organ, which is placed just to the left of the midline (Liang et al., 2000), and an accessory organ called the parapineal in lampreys and fish (Concha and Wilson, 2001). The parapineal organ is also asymmetrically placed in the brain, a phenomenon first described by Hill (Hill, 1891). In zebrafish, the parapineal lies adjacent to the left habenula and dictates left-right (L-R) differences in size, neuropil and gene expression between the left and right habenulae (Concha et al., 2003; Gamse et al., 2003).

The zebrafish pineal complex anlage gives rise to both the pineal and parapineal organs. Lineage labeling at 22 to 24 hours post fertilization (hpf) reveals that the anterior portion of the pineal complex anlage gives rise to both pineal and parapineal cells, while more posterior regions produce pineal cells only (Concha et al., 2003). Two transcription factors have been identified that regulate pineal or parapineal development: the homeodomain protein Floating head (*Flh*) and the T-box domain protein T-box 2b (*Tbx2b*, previously known as Tbx-c). *Flh* activity promotes the generation of pineal cells; in flh^{n1} mutants,

neurogenesis initiates in the pineal complex but ends prematurely at 18 somites (s) stage (Masai et al., 1997). By contrast, *Tbx2b* is required for the specification and migration of parapineal cells; in *fby*^{c144} mutants (a mutation in *tbx2b)*, few or no parapineal cells develop and those that do fail to migrate to the left side of the brain (Snelson et al., 2008b).

The regulatory relationship between *flh* and *tbx2b* is unclear. In the pineal complex anlage, *flh* expression begins at 80% epiboly (Masai et al., 1997), about 4 hours prior to *tbx2b* expression (Snelson et al., 2008b). Expression of *tbx2b* and *flh* overlaps extensively within the pineal complex anlage at 24 hpf (Snelson et al., 2008b). A previous publication (Cau and Wilson, 2003) suggested that *Flh* is required for expression of *tbx2b*. However, the phenotypes of *flh* and *fby* mutants are very different, arguing against the two genes acting in the same pathway. Asymmetrically placed parapineal cells form in *flh* mutant larvae (Gamse et al., 2002; Gamse et al., 2003), but not *fby* mutant larvae (Snelson et al., 2008b). This observation prompted a re-evaluation of *tbx2b* and *flh* cross-regulation.

Examination of *flh* and *tbx2b* mRNA in *flh* and *fby* mutants reveals that they do not regulate one another's expression, and *flh; fby* double mutants exhibit an additive phenotype. Additionally, in *flh* mutants, specification and asymmetric migration of parapineal cells are indistinguishable from wild-type (WT) embryos. These results indicate that *flh* and *tbx2b* act independently of one another during pineal versus parapineal development.

Materials and Methods

Zebrafish

Zebrafish were raised at 28.5°C on a 14/10 hour light/dark cycle and staged according to hours (h) or days (d) post fertilization (pf). The wild-type AB strain (Walker, 1999); the transgenic lines Tg(*foxd3:gfp*)^{fkg17} and Tg(*foxd3:gfp*)^{fkg3} (Gilmour et al., 2002), and mutants carrying the spontaneous allele *flh*^{n1} (Halpern et al., 1995) and the ethylnitrosourea-induced null allele *fby*^{c144} (Snelson et al., 2008b) were used.

RNA in situ hybridization

Whole-mount RNA in situ hybridization was performed as described previously (Gamse et al., 2003), using reagents from Roche Applied Bioscience. RNA probes were labeled using fluorescein-UTP or digoxygenin UTP. To synthesize antisense RNA probes, *znot* (*flh)* (Talbot et al., 1995) and pBK-CMV-*leftover* (Gamse et al., 2003) were linearized with *Eco*RI and transcribed with T7 RNA polymerase; pCRII-*tbx2b* (Snelson et al., 2008b) with *Bam*HI and T7 RNA polymerase; and pBS-*gfi1* (Dufourcq et al., 2004) with *Sac*II and T3 RNA polymerase. Embryos were incubated at 70°C with probe and hybridization solution containing 50% formamide (or 65% for *cyc*). Hybridized probes were detected using alkaline phosphatase-conjugated antibodies and visualized by 4-nitro blue tetrazolium (NBT) and 5-bromo-4-chloro-3-indolyl-phosphate (BCIP)

staining. All in situ data was collected on a Leica DM6000B microscope with a 20x or 40x objective.

BrdU labeling

For pulse labeling with bromodeoxyuridine (BrdU, Roche), embryos were incubated with ice-cold 10 mM BrdU dissolved in embryo medium plus DMSO at 2% for 10-15 s embryos, 5% for 18 somite stage embryos, or 10% for 24-30 hpf embryos, over a period of 30 minutes. Embryos were then washed extensively with embryo medium and raised to 4 dpf, when they were fixed in 4% paraformaldehyde for 2 hours at room temperature.

Time-lapse imaging

For time-lapse imaging, WT or *flh* mutant embryos carrying the transgene (*foxd3*:*gfp*)^{fkg3} (Gilmour et al., 2002) were mounted in a 0.8% solution of low melt agarose containing 0.003% PTU and anesthetized using 0.04% Tricaine. Images were collected on a Zeiss/Perkin Elmer spinning disk confocal microscope with a 40x oil-immersion objective every 15 minutes from 31 to 46 hpf, and analyzed using Volocity software (Improvision).

Immunofluorescence

For whole-mount immunohistochemistry, 4 dpf larvae were fixed in 4% paraformaldehyde overnight (for anti-Zpr-1/anti-GFP) or 2 hours (for anti-BrdU/anti-GFP). Samples were permeabilized by treatment with 10 µg/ml

Proteinase K (Roche Applied Bioscience) and refixed in 4% paraformaldehyde. For BrdU labeling, samples were additionally washed in deionized water following refixation, and incubated in 2 N HCl for 1 hour. All samples were blocked in PBS with 0.1% Triton X-100, 2% sheep serum, 1% DMSO, and 10% BSA (PBSTrS). For antibody labeling, rabbit anti-GFP (1:1000, Torrey Pines Biolabs), mouse anti-Zpr-1 (1:250, Zebrafish International Resource Center, Eugene, Oregon) and mouse anti-BrdU antibody (1:200, developed by Stephen Kaufman, obtained from the Developmental Studies Hybridoma Bank, University of Iowa) were used. Larvae were incubated overnight in primary antibody diluted in PBSTrS. Primary antibody was detected using goat-anti-rabbit or goat-anti-mouse secondary antibodies conjugated to the Alexa 568 or Alexa 488 fluorophores (1:350, Molecular Probes). Immunofluorescence data were collected on a Zeiss/Perkin Elmer spinning disk confocal microscope or a Zeiss LSM 510 Meta with a 40x oil-immersion objective and analyzed with Volocity software (Improvision).

Results

Parapineal cell division ends prior to pineal cell division

To identify the period of development when pineal and parapineal cells are dividing, we performed BrdU pulse labeling at stages between 10 s and 30 hpf and examined the fate of labeled cells at 4 dpf (days post fertilization). To identify pineal and parapineal cells, embryos carrying the transgene *Tg(foxd3:gfp)*^{fkg3}

were used (Gilmour et al., 2002). Peak labeling of parapineal cells occurred when embryos received a half-hour pulse of BrdU at 15 s stage (Figure 13A, E, F and Table 1); BrdU pulses before (10 s) or after (18 s or later) labeled few or no parapineal cells (Figure 13E, F and Table 1). Pineal cells also have maximal incorporation of BrdU at 15 s; interestingly, a second smaller peak of labeling occurs at 24 hpf (Figure 13 C, E, G and Table 1). In *flh* mutant larvae, pineal and parapineal BrdU labeling at 10 s stage is similar to WT and increases at 15 s; however, almost no BrdU labeling of the pineal or parapineal occurs at or after 18 s (Figure 13B, D, F, G and Table 2). The number of *foxd3:gfp*-positive cells in the pineal organ is reduced (Table 2), consistent with a premature end to pineal neurogenesis in *flh* mutants (Masai et al., 1997).

Figure 13. Cell division of parapineal precursors is largely complete by 18 s. (A-D) are dorsal views of 4 dpf larvae, with BrdU (red) and *foxd3:gfp* (green) labeling in the epithalamus, following a BrdU pulse at (A, B) 15 s or (C, D) 24 hpf stage in (A, C) WT or (B, D) *flh* mutant embryos. Dashed circles in B, D indicate the pineal cells. Scale bar: 25 μM. (E) Line graph of the percentage of WT parapineal (red line) or pineal (blue line) cells that are labeled at 4 dpf, following a BrdU pulse at the indicated developmental stages. (F) Bar graph showing the absolute number of BrdU-positive parapineal or (G) pineal cells in WT or *flh* embryos.

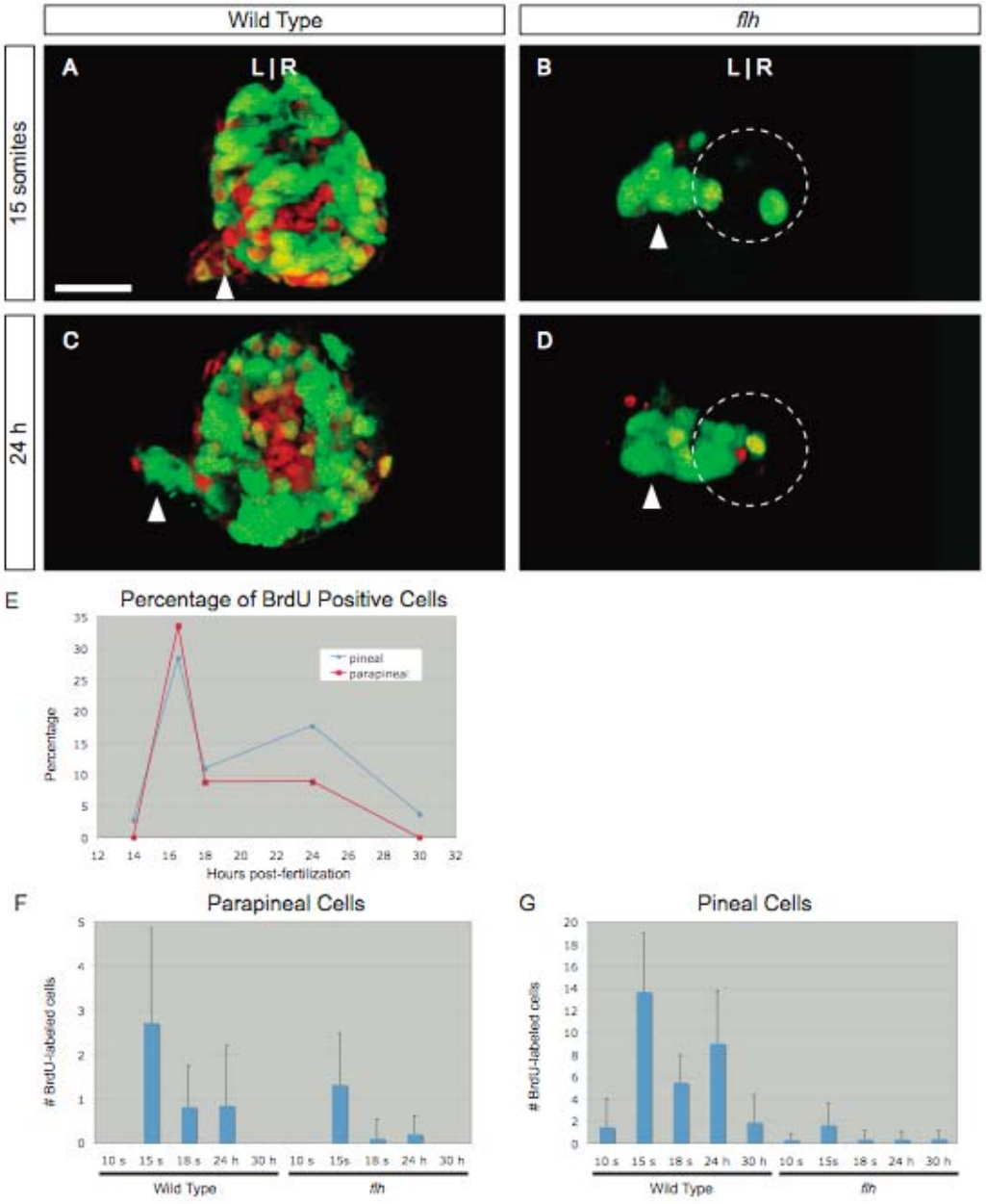
Wild Type
flh
A
L|R
B
L|R
15 somites
C
D
24 h
E
Percentage of BrdU Positive Cells
pineal
parapineal
Percentage
Hours post-fertilization
F
Parapineal Cells
BrdU-labeled cells
10 s
15 s
18 s
24 h
30 h
Wild Type
flh
G
Pineal Cells

Table 2. Fate of pineal complex cells labeled with BrdU between 10 s and 30 hpf

Genotype	Stage[a]	GFP$^+$ pineal cells	BrdU$^+$ pineal cells	GFP$^+$ parapineal cells	BrdU$^+$ parapineal cells	N
WT	10 s	47 +/- 6	1 +/- 3	8 +/- 2	0	11
	15 s	50 +/- 4	14 +/- 5	8 +/- 2	3 +/- 2	25
	18 s	50 +- 4	5 +/- 2 [b]	9 +/- 2	0.8 +/- 0.9 [b]	21
	24 h	51 +/- 5	9 +/- 5 [b, c]	8 +/- 2	1 +/- 1 [b, d]	13
	30 h	48 +/- 7	2 +/- 2	10 +/- 2	0	7
flh$^{-/-}$	10 s	17 +/- 6	0.3 +/- 0.5 [e]	8 +/- 2	0 [b, e]	10
	15 s	16 +/- 5	2 +/- 2 [b]	11 +/- 2	1 +/- 1 [b]	25
	18 s	15 +/- 4	0.3 +/- 0.8 [f]	7 +/- 2	0.1 +/- 0.4 [b, f]	21
	24 hpf	14 +/- 5	0.3 +/- 0.7 [b]	8 +/- 2	0.2 +/- 0.4 [b]	15
	30 hpf	15 +/- 6	0.4 +/- 0.7	10 +/- 3	0	17

a. Developmental stage when BrdU was first applied to embryos during a 0.5 hr pulse; all samples were fixed at 4 dpf for analysis.
b. Significantly different from WT 15 s by 2-tailed T-test, $p < 0.03$
c. Significantly different from WT 18 s by 2-tailed T-test, $p < 0.01$
d. Not significantly different from WT 18 s by 2-tailed T-test, $p > 0.7$
e. Not significantly different from WT 10 s by 2-tailed T-test, $p > 0.17$.
f. Significantly different from WT 18 s by 2-tailed T-test, $p < 0.01$

The parapineal organ in flh mutants develops similarly to WT

In *flh* mutants, a single asymmetrically placed parapineal organ is always observed (Gamse et al., 2002) (although its placement is reversed in half of mutant larvae due to disrupted midline formation (Halpern et al., 1995). To confirm that the timing and migration of parapineal cells in *flh* mutants is similar to WT, time-lapse imaging was used in embryos carrying the transgene *Tg(foxd3:gfp)*^{fkg3} (Figure 14). Similar to WT (Snelson et al., 2008b) and Supplemental Movie 4 located online at: http://www3.interscience.wiley.com/cgi-bin/fulltext/120776016/sm001.mov?PLACEBO=IE.pdf), in *flh* mutants *foxd3:gfp*-positive parapineal cells are first visible at 31 hpf (Figure 14A); cells continue to migrate unilaterally in a cluster between 32 and 46 hpf (Figure 14B-P and Supplemental Movie 5 located online at: http://www3.interscience.wiley.com/cgi-bin/fulltext/120776016/sm002.mov?PLACEBO=IE.pdf).

Figure 14. Parapineal cells migrate asymmetrically in *flh* mutants. All panels are dorsal views of *foxd3:gfp* labeling in the epithalamus of a single embryo at the times indicated. Parapineal cells are circled in yellow, pineal cells in red; a neural crest cell (which also expresses *foxd3:gfp*) in A-C is indicated by a green arrowhead. (A) The first labeled parapineal cells are apparent near the midline at 31 h; (B-E) they migrate leftward and (F-P) are joined by more leftward-migrating parapineal cells during the subsequent 10 hours. Scale bar: 25 μm. (Q) Diagram of a zebrafish larvae, showing the relative position of the pineal (p, red oval) and parapineal (pp, yellow oval) within the head.

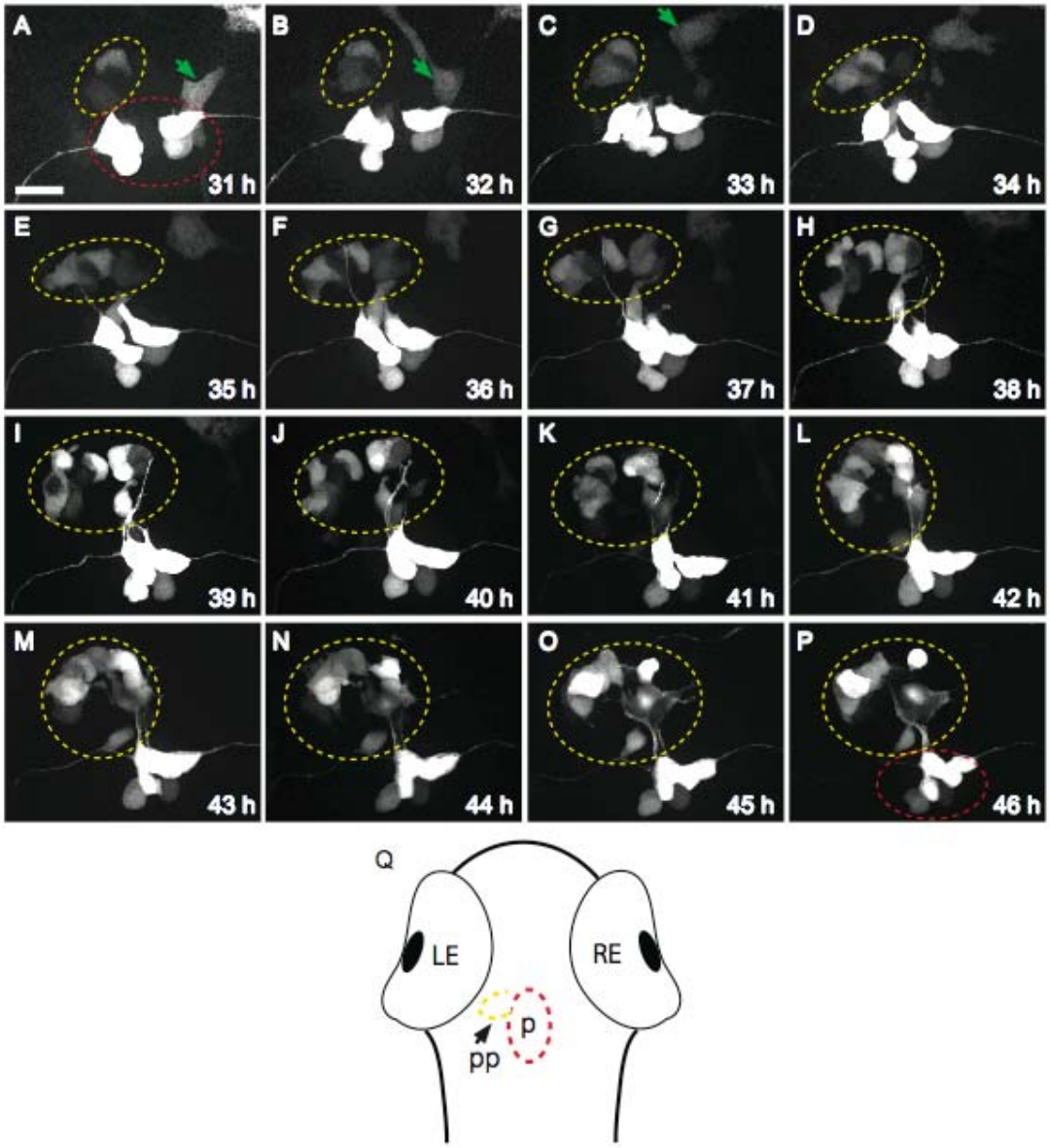
A
31 h
B
32 h
C
33 h
D
34 h
E
35 h
F
36 h
G
37 h
H
38 h
I
39 h
J
40 h
K
41 h
L
42 h
M
43 h
N
44 h
O
45 h
P
46 h
Q
LE
RE
p
pp

To test whether the correct number of parapineal cells are specified in *flh* mutant larvae, we examined the expression of the gene *growth factor independent-1* (*gfi-1)*, which is expressed in parapineal cells from 48 hpf onward; no *gfi-1* expression is seen in pineal cells (Dufourcq et al., 2004). In WT larvae, an average of 10 *gfi-1* expressing cells are found on the left side of the brain in a tight cluster at 4 dpf (Figure 15A and Table 3). Similarly, *flh* mutants form 10 *gfi-1*-expressing cells on average (Figure 15B and Table 3).

To confirm that parapineal cells in *flh* mutant larvae do not express a pineal-specific marker, expression of the Fret43 antigen was examined in the context of the transgene *Tg(foxd3:gfp)*^{fkg3} at 4 dpf. In WT larvae, Fret43 (labeled by the Zpr-1 antibody (Larison and Bremiller, 1990), is expressed on red-green double cone cells found throughout the pineal organ (Masai et al., 1997) but excluded from the parapineal organ (Figure 15C and Table 3). As in WT, none of the parapineal cells in *flh* mutants express Zpr-1 (Figure 15D and Table 3).

To assay the ability of the parapineal in *flh* mutants to dictate L-R differences in the habenulae, expression of the asymmetrically expressed gene *leftover* (*lov*) (Gamse et al., 2003) was examined at 4 dpf. In both WT and *flh* mutant larvae, expression of *lov* was found in more cells of the habenula adjacent to the parapineal than in the contralateral habenula (Figure15E, F).

In sum, all of the characteristics of the parapineal, including number of cells specified, asymmetric migration and ability to direct habenular asymmetry, are comparable between *flh* mutants and WT.

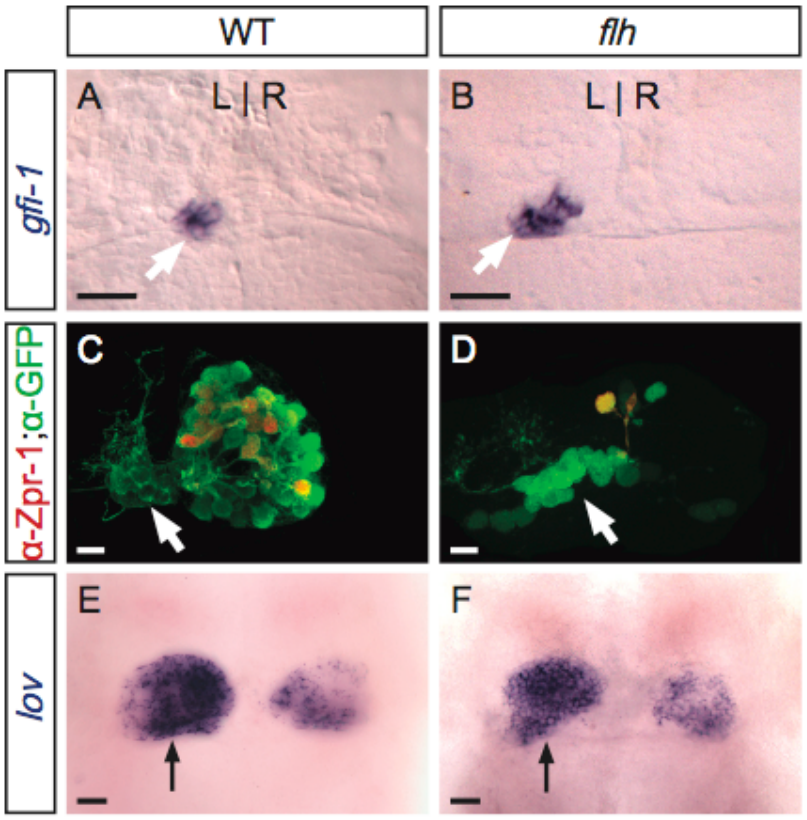

Figure 15. In *flh* mutants, parapineal specification is normal, but the pineal organ is reduced in size. All panels are dorsal views of the epithalamus of 4 dpf larvae. (A) Expression of *gfi-1*(blue), which is restricted to the parapineal organ (arrowhead), reveals ~10 left-sided cells in WT and (B) *flh* larvae. (C) In WT larvae, both the parapineal (arrowhead) and pineal express *foxd3:gfp* (green); many cells of the pineal organ are also labeled by the red-green cone marker Zpr-1 (Fret43) (red), but no parapineal cells are Zpr-1-labeled. (D) In *flh* mutants, the pineal organ is drastically reduced in size, including fewer Zpr-1 labeled cells. As in WT, no Zpr-1-labeled cells are detected in the parapineal. (E) At 4 dpf, lov expression is asymmetric in the habenular nuclei; the habenula adjacent to the parapineal (arrow) expresses *lov* extensively in WT and (F) *flh* mutants. Scale bars: 25 μm.

Table 3. Number of labeled cells present in the pineal complex of single and double mutants

Gene/protein (cell types labeled)	Genotype	Number of cells [a]	N
gfi-1	WT	10 +/- 1	12
(parapineal cells)	*flh*	10 +/- 1	14
	fby; flh	3 +/- 2 [b]	24
GFP in Tg(*foxd3:gfp*)	WT	52 +/- 10	5
(pineal and parapineal cells)	*flh*	28 +/- 7 [c]	5
	fby; flh	24 +/- 10 [c]	7
Zpr-1 antibody	WT	30 +/- 5	5
(red-green double cone cells)	*flh*	5 +/- 5 [c]	4
	fby; flh	7 +/- 1 [c]	4

a. Average number of cells labeled per larvae at 4 dpf, plus or minus one standard deviation.
b. Significantly different from WT and *flh* by 2-tailed T-test, $p < 0.01$
c. Significantly different from WT by 2-tailed T-test, $p < 0.03$

Flh and Tbx2b do not regulate one another's expression

To evaluate cross-regulation of *flh* and *tbx2b*, we examined expression of each gene in the pineal complex of *tbx2b* and *flh* mutants. In WT embryos, expression of *tbx2b* begins at 6 s stage in bilateral groups of cells in the pineal complex anlage, which soon merge to form one medial domain. At 24 hpf, expression is robust (Dheen et al., 1999; Ruvinsky et al., 2000; Snelson et al., 2008b) and Figure 16A, B). *flh* expression begins at 80% epiboly in the pineal complex anlage (Masai et al., 1997), and is found in a single medial domain at 6 s and 24 hpf stages (Figure 16C, D). Double labeling reveals that expression of *tbx2b* overlaps with the *flh* expression domain at 6 s and 24 h; *flh* expression extends further medially that *tbx2b* at 6 s (Figure 16E, F). In *flh* mutants, *tbx2b* expression is still detected at both 6 s and 24 hpf (Figure 16G, H). The total number of *tbx2b*-expressing cells in the pineal complex anlage of *flh* mutants is reduced relative to wild type, consistent with the reduced size of the pineal organ that will develop. In *fby* mutants, the number of *flh*-expressing cells detected at 6 s and 24 hpf is similar to WT (Figure 16I, J). The data demonstrate that *tbx2b* and *flh* expression is maintained in *flh* and *fby* mutants, respectively.

Figure 16. *flh* and *tbx2b* do not regulate one another's expression. All panels are dorsal views of the epithalamus at the stage indicated. (A, B) *tbx2b* and (C, D) *flh* are expressed in the pineal complex anlage at 6 somite and 24 hpf stages. (E,F) Double labeling for *tbx2b* (blue) and *flh* (red) reveals that they overlap in expression at 6 somite and 24 hpf stages; *flh* is expressed further medially than *tbx2b* at 6 somite stage. (G) In *flh* mutants, expression of *tbx2b* initiates on time and (H) is maintained, albeit in a reduced number of cells. (I, J) In *fby* mutants (a lesion in *tbx2b*), expression of *flh* is unaltered relative to WT. Scale bars: 25 μm.

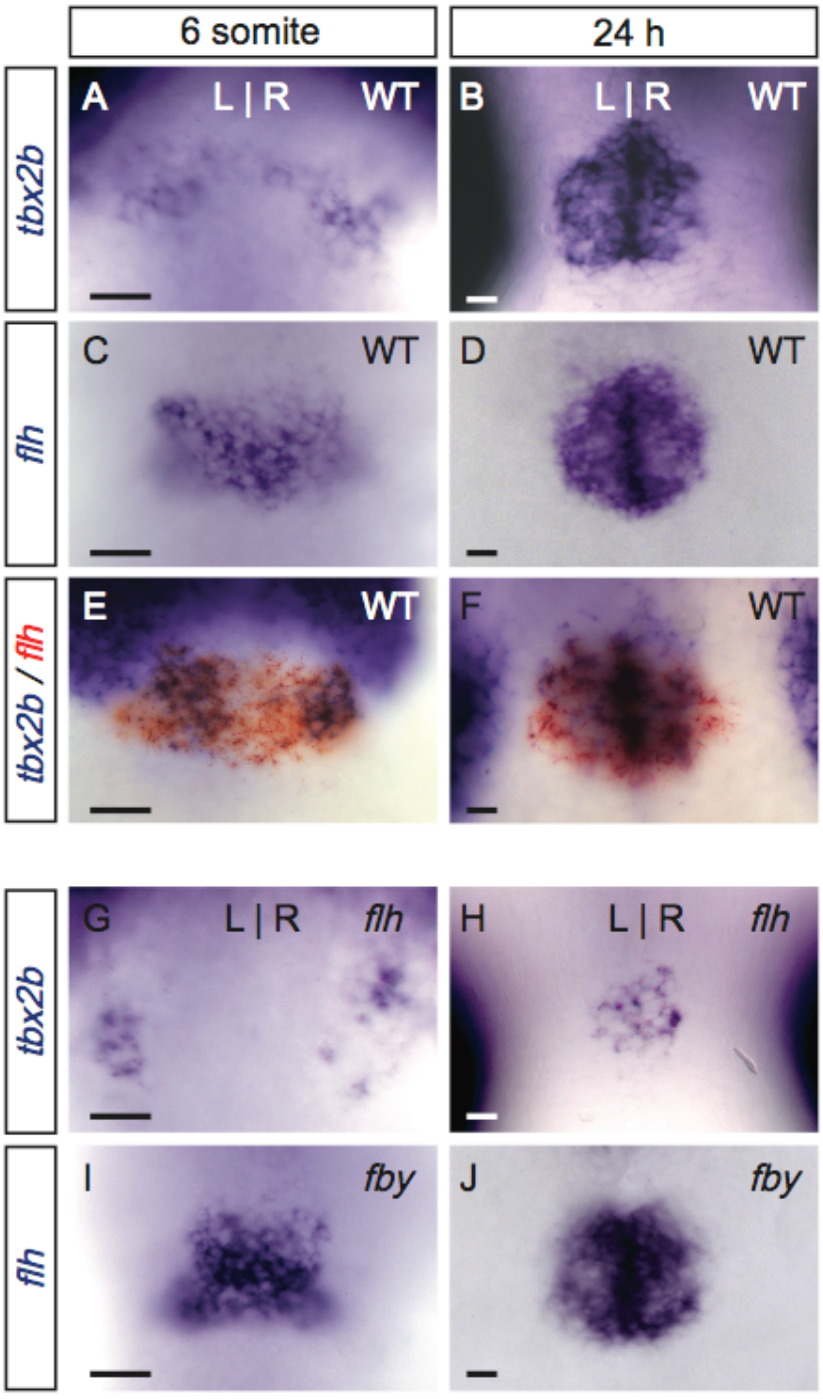
6 somite
24 h
tbx2b
flh
tbx2b / flh
tbx2b
flh
A
L | R
WT
B
L | R
WT
C
WT
D
WT
E
WT
F
WT
G
L | R
flh
H
L | R
flh
I
fby
J
fby

flh; fby double mutants have an additive phenotype

A sensitive test for genetic interaction is examining the phenotype of homozygous *flh;fby* double mutant embryos. In *fby* single mutants at 4 dpf, the pineal organ is similar in size to WT, but the *gfi-1*-expressing parapineal cells are reduced in number, remain near the midline, and fail to upregulate *lov* in the left habenula ((Snelson et al., 2008b), Figure 17A, C, E).

Similar to *fby* single mutants, in *flh;fby* double mutants the *gfi-1*-expressing parapineal cells are fewer in number than WT and do not migrate leftward (Figure 17B). Additionally, *lov* expression in double mutants is not upregulated in the left habenulae, similar to *fby* single mutants (Figure 17F).

The number of GFP-expressing pineal cells in double mutants is reduced to a level similar to the number of pineal cells in *flh* single mutants. In addition, the number of Zpr-1-labeled cells in double mutants is ~5-fold reduced compared to WT and indistinguishable from *flh* single mutants (Figure 17D and Table 3).

These data indicate that *flh;fby* double mutants have an additive phenotype, exhibiting phenotypes in the pineal and parapineal organs characteristic of each single mutant.

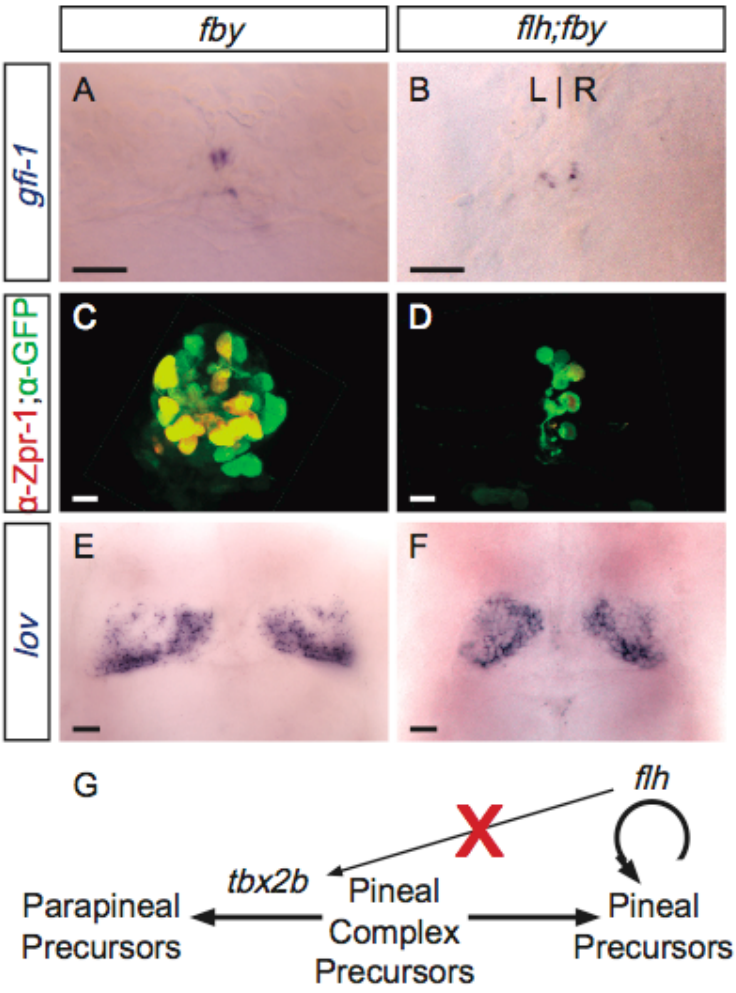

Figure 17. Double homozygous *flh*; *fby* mutants exhibit an additive phenotype. All panels are dorsal views of the epithalamus of 4 dpf larvae. (A) In *fby* single mutants or (B) *flh*; *fby* double mutants, only a few disorganized parapineal cells are specified, and they fail to migrate to the left side of the brain. (C) *fby* single mutants form a pineal organ. (D) *flh*;*fby* double mutant larvae have both a reduced pineal, similar to *flh* single mutants (compare to Figure 3D). (E) In *fby* single mutants and (F) *flh*; *fby* double mutants, reduced lov expression is detected in the left habenula. Scale bars: 25 μm. (G) Summary of *tbx2b* and *flh* activity in pineal complex development. The activity of *tbx2b* gives parapineal precursors their identity, while *flh* is needed for proliferation of pineal precursor cells. Expression of *tbx2b* does not require *flh* activity.

Discussion

Previous work showed that *Flh* is a key regulator of pineal neurogenesis (Cau and Wilson, 2003; Masai et al., 1997) and suggested that *Flh* activates *tbx2b* transcription in pineal complex precursors (Cau and Wilson, 2003). The latter result implies that *flh* mutants should show defects in parapineal formation, which requires *tbx2b* function (Snelson et al., 2008b). However, *flh* mutants develop a parapineal that is indistinguishable from WT larvae with regard to asymmetric migration and number of cells specified. Moreover, disruption of *flh* function does not eliminate the initiation or maintenance of *tbx2b* transcription in the pineal complex. Examination of homozygous double mutants reveals an additive phenotype and supports parallel rather than serial action of *flh* and *tbx2b*. These data argue strongly against *tbx2b* and *flh* acting in the same genetic pathway during the development of the pineal complex (Figure 5G).

On the basis of mutational analyses and BrdU labeling, we propose the following model. Expression of *flh* and *tbx2b* before the 15 s stage defines a field of precursor cells that can divide to produce pineal or parapineal cells. An initial burst of cell division at 15 s stage generates many new pineal complex cells; *tbx2b* activity assigns parapineal fate to some of these cells while the remainder develop with pineal fate. Subsequently, division of parapineal precursor cells drops off sharply, suggesting that *tbx2b* is largely dispensable for parapineal development after the 15 s stage. A method to conditionally inactivate *tbx2b* in the pineal complex will be necessary to test this hypothesis.

Beginning at 18 s, *flh* activity is required for continued production of cells in the pineal anlage (Masai et al., 1997) and this study). Almost all of the cells that divide after 18 s contribute to the pineal lineage. It is not clear why division of cells that give rise to the parapineal organ slows after 15 s stage while division of pineal progenitors continues. One possibility is that separate groups of pineal and parapineal progenitor cells exist, and the latter group largely stops dividing after 15 s. The *tbx2b*-positive and *tbx2b*-negative cells within the *flh*-expressing domain at the 6 s stage (Figure 4E) might represent parapineal and pineal progenitors respectively. A second explanation is that the same progenitor cells can give rise to either pineal or parapineal cells initially, but primarily produce pineal cells after 15 s. Careful lineage labeling of single cells in the pineal complex anlage will distinguish between these two scenarios.

A small number of pineal and parapineal cells still develop in *flh;fby* double mutant embryos. Presumably there are other genes that contribute to proliferation and/or control specification of pineal and parapineal cells; however, these genes have yet to be isolated. Forward genetic screening in a sensitized background such as a *tbx2b* hypomorph should identify these genes.

The independent roles that *tbx2b* and *flh* play in the development of the pineal complex contrasts with the regulation of *tbx2b* expression by *flh* during notochord development. In *flh* mutants, *tbx2b* expression is absent in notochord precursor cells found in the chordoneural hinge (Dheen et al., 1999). In the notochord, *flh* appears to maintain *tbx2b* expression by blocking the action of another T-box transcription factor, *spadetail/tbx16 (spt)* (Dheen et al., 1999). By

contrast, *spt* is not expressed in the pineal anlage (Ruvinsky et al., 1998), which may explain why *flh* and *tbx2b* activity are uncoupled in this tissue. Identification of other genes that are expressed in both the pineal complex anlage and notochord precursors, similar to *flh* and *tbx2b*, will illuminate the genetic networks involved in the patterning of these two tissues, and allow a comparison of evolutionary conservation and divergence between these networks.

CHAPTER IV

PARAPINEAL CELLS ARISE FROM DISTINCT REGIONS WITHIN THE PINEAL COMPLEX ANLAGE

Abstract

The zebrafish embryo rapidly develops from a single fertilized cell into a recognizable organism in only 24 hours (Karlstrom and Kane, 1996). During the course of development, the fertilized cell divides many times, and cells that arise from those divisions will proceed through a process of specification, commitment, and finally determination, resulting in the formation of distinct cell lineages with separate functions. The zebrafish pineal and parapineal organs stem from one such group of cells. These organs develop from a seemingly identical population of cells but undergo different developmental programs that result in separation into two lineages prior to morphogenesis. Using lineage labeling techniques, we show that parapineal cells arise from distinct areas within the pineal complex anlage. Mutations in the gene *tbx2b* result in specification of fewer parapineal cells that are unable to migrate to the left of the pineal organ. We also characterize a second, hypomorphic allele of *tbx2b*, *lots-of-rods* (*lor*), that can be used to determine the transcriptional targets of *tbx2b*. Identification of the molecular targets of *tbx2b* in conjunction with pineal complex fate mapping will

further our understanding of the pathways leading to the establishment of brain asymmetry in the zebrafish.

Introduction

The vertebrate body contains organs that are asymmetrically placed with respect to the left/right (L/R) axis including differences in position/placement, lobation, and rotation within the body cavity (Capdevila and Belmonte, 2000). The vertebrate brain is also grossly asymmetric; the human left planum temporale is larger on the left side than the right (Geschwind and Levitsky, 1968), the right frontal lobe protrudes farther than the left and torques toward the left, while the left occipital lobe protrudes farther than the right and torques toward the right (Toga and Thompson, 2003). Though the molecular steps leading to the specification of asymmetrically placed organs within the body cavity has been well studied, little is known about how asymmetry is established in the vertebrate brain.

The zebrafish, *Danio rerio*, is an ideal model organism in which to study the events that lead to the development of brain asymmetry. In particular, the zebrafish epithalamus is an asymmetric brain structure consisting of the melatonin secreting pineal organ, a left-sided accessory organ called the parapineal organ, and flanking left and right habenular nuclei (habenulae). Placement of the parapineal organ with respect to the L/R axis is dependant on Nodal signaling (Concha et al., 2003), and influences the molecular identity of the

adjacent habenula. The asymmetrically expressed gene *leftover* (*lov*) is more broadly expressed in the left habenula than the right in wild-type animals. When the parapineal organ is ablated at early stages of development, transcription of *lov* in the left habenula is less broadly expressed, similar to that found in the right habenula (Gamse 2003). The *from beyond* (*fby*/*tbx2b*) mutation, in which a reduced number of cells are specified with parapineal fate, results in more symmetric *lov* expression in the habenulae. Furthermore, correct habenular specification is required to properly target efferent axons from the habenulae to their midbrain targets at the interpeduncular nucleus (IPN) (Gamse et al., 2005; Gamse et al., 2003). Though we are starting to understand how L/R asymmetry is established in the brain, and how these asymmetric structures connect to other brain regions, very little is known about the initial development of these epithalamic structures.

Regulated cell division and patterning of an embryo must occur in order for a simple unicellular structure to develop into the adult form with functioning physiological systems. Fate maps constructed from labeling individual cells or groups of cells at an early stage and observation of their development over time has been instrumental in understanding how regulated development occurs. Through a process of specification, cells receive a variety of cues based on their location and lineage that instruct (or restrict) them to become a particular organ or tissue. Once specified, these cells will go through a process of commitment, determination, and finally morphogenesis into the adult form. Fate maps have been instrumental in allowing embryologists to determine how individual cells or

groups of cells are affected during these processes. For instance, cells can be transplanted between individuals at different developmental stages, or different positions within the same embryo, to demonstrate cell specification and determination. Most famously, fate mapping generated by transplantation and radioactive dye labeling has been used to demonstrate that chick neural crest cells that arise from the trunk region can give rise to wing epidermis and feathers (Weston, 1963).

In model organisms with an indeterminate cell lineage, early fate maps focused on whole organ system development, and were relatively low resolution. With the development of more sophisticated tools, embryologists can now construct higher resolution fate maps that in conjunction with molecular techniques such as microarray studies, will help to determine the exact developmental events that cause cells to adopt certain fates. Previously, fate mapping of individual structures within the diencephalon was limited to expression patterns of specific genes (Staudt and Houart, 2007). The pineal and parapineal organs develop from a seemingly uniform population of cells, are morphologically indistinguishable until approximately 28 hpf (Gamse et al., 2003), and express all the same early developmental markers (*otx5*, (Gamse et al., 2003); *flh*, (Concha et al., 2003; Gamse et al., 2003); *tbx2b*, (Snelson et al., 2008b). Because the two developmental programs are currently molecularly indistinguishable, fate mapping of these lineages at the single cell resolution has been technically challenging. Previously published fate mapping experiments have shown that parapineal cells are located in the anterior third of the pineal

complex anlage at 24 hpf (Concha et al., 2003). In order to understand the specification defect in *fby* mutants, high resolution fate mapping, taking advantage of newly developed molecular tools, was performed in wild-type embryos to identify the location of parapineal cells prior to initiation of their asymmetric morphogenesis. The construction of these fate maps, along with live cell imaging, aid our understanding of the developmental processes that occur in the pineal complex anlage that lead to the eventual separation of the pineal and parapineal organs into two distinct lineages.

Furthermore, the identities of many of the genes required for development of the pineal and parapineal organs into separate lineages are unknown. A second allele of *tbx2b*, called *lots-of-rods* (*lor*) was identified in a genetic screen for ENU induced mutations resulting in altered rod cell patterning in the zebrafish retina (Alvarez-Delfin et al., 2009). The *lor* mutation is a hypomorphic mutation of *tbx2b* that reduces the total number of *tbx2b* transcripts in the embryo, but allows the mutation to be maintained in fertile, homozygous adult zebrafish, which has so far been impossible for *fby* homozygous fish. Initial characterization of the *lor* mutation shows a very similar eye and pineal phenotype to *fby* mutants, and is likely an excellent source of RNA that can be used to hybridize to a microarray or used to perform RNA-seq. The combination of fate mapping with the discovery of *tbx2b* transcriptional targets will help us to understand the molecular events that lead to the establishment of brain laterality as well as pineal and parapineal development.

Materials and Methods

Zebrafish

Zebrafish were raised at 28.5°C on a 14/10 hour light/dark cycle and staged according to hours (h) or days (d) post fertilization (pf). The wild-type AB strain (Walker, 1999), the transgenic lines Tg(*GAL4VP16:cfos*)^{s1445t}; Tg(*UAS:kaede*)^{s1999t} (Scott et al., 2007) and Tg(*foxd3:gfp*)^{fkg3} (Gilmour et al., 2002), the N-ethyl-N-nitrosourea- induced mutations *lor*^{p25bbtl}(Alvarez-Delfin et al., 2009) and *fby*^{c144} (Snelson et al., 2008b) were used.

Photoconversion

Zebrafish embryos were raised to 24 hpf in 0.003% PTU, anesthetized with 0.04% Tricaine and embedded in 0.8% agar in a glass bottomed petri dish (Warner Instruments). They were then placed on an Olympus FluoView FV1000 inverted confocal microscope, and Kaede fluorescence was converted from green to red with 20 sequential pulses from a directed ultraviolet laser through a 40X oil immersion objective. Embryos were then incubated until 56 hpf in the same media and re-photographed. Images were collected using FV10-ASW 1.6 software and analyzed using Volocity software (Improvision).

Time-lapse imaging

For time-lapse imaging, embryos selected for exceptional photoconversion were mounted in a 0.8% solution of low melt agarose containing 0.003% PTU

and anesthetized using 0.04% Tricaine. Images were collected on a Zeiss/Perkin Elmer spinning disk confocal microscope with a 40x oil-immersion objective every 15 minutes from 24 hpf to 48 hpf, and analyzed using Volocity software (Improvision).

RNA in situ hybridization

Whole mount RNA in situ hybridization was performed as described previously (Gamse et al., 2003), using reagents from Roche Applied Bioscience. RNA probes were labeled using fluorescein-UTP or digoxygenin-UTP. To synthesize antisense RNA probes, pCRII-*tbx2b* was linearized with *Bam*HI and transcribed with T7 RNA polymerase. Embryos were incubated at 70ºC with probe and hybridization solution containing 50% formamide. Hybridized probes were detected using alkaline phosphatase-conjugated antibodies and visualized by 4-nitro-blue tetrazolium (NBT) and 5-bromo-4-ch*lor*o-3-indolyl-phosphatase (BCIP) staining for single labeling. All in situ data were collected on a Leica DM6000B microscope with a 10X or 20X objective.

Results

Parapineal cells express the transgene (GAL4VP16)^{s1145t} at the appropriate time and place

A GAL4 enhancer trap screen performed by the Baier lab identified previously unknown neuronal enhancers, including several that were expressed in pineal tissue at very early stages of development. We obtained a line of fish carrying a pineal specific driver, *GAL4VP16^{s1145t}*, generated by this screen and a second transgene containing *UAS:Kaede^{s1999t}* (Scott et al., 2007), a photoconvertable protein that can be changed from green fluorescence to red by exposure to ultraviolet light (Ando et al., 2002). In order to assure that parapineal cells express these transgenes at 24 hpf, the entire pineal complex was photoconverted by exposure to UV light (Figure 18). Subsequently we found that parapineal cells were still red at 48 hpf, indicating that the transgene was expressed in pre-migratory parapineal cells at 24hpf. This proves that the *GAL4VP16* line can drive Kaede expression at the right time and in the correct tissue to facilitate fate-mapping studies.

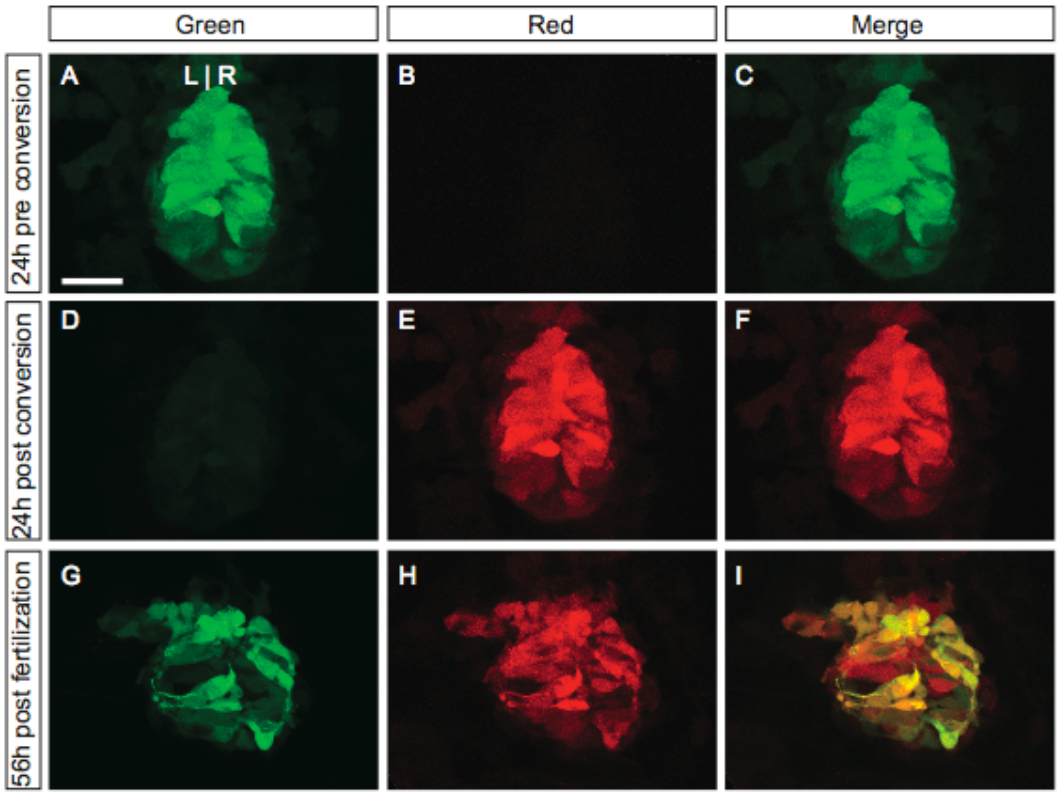

Figure 18. Parapineal cells express Kaede at 24 hpf in Tg(*cfos:GAL4VP16*)^{s1145t}. Embryos carrying the transgenes Tg(*cfos:GAL4VP16*)^{s1145t} and Tg(*UAS:Kaede*)^{s1999t} were grown to 24 hpf and exposed to UV light. (A-C) Dorsal views of the pineal organ of an embryo that had not been photoconverted (A) green channel (B) red channel (C) merged image. (D-F) The same embryo immediately following photoconversion. (D) green channel (E) red channel, and (F) merged image (G-I) this embryo was allowed to grow until 56 hpf, and was rephotographed after the parapineal organ had emerged. (G) Green Kaede protein has been newly synthesized after photoconversion. (H) Kaede protein that had been photoconverted at 24 hpf is still present at 56 hpf in both the pineal and parapineal organs. (I) Merge of the red and green channels at 56 hpf showing the pineal and parapineal cells contain both converted and unconverted Kaede protein (Scale bar: 25μm)

Parapineal cells migrate from the left and right sides of the pineal complex anlage

We performed one to two cell photoconversion experiments in order to establish a high-resolution fate map of the pineal complex at 24hpf. Examples of these experiments are shown in Figure 19. Prior to photoconversion, the pineal complex expresses the Kaede protein uniformly throughout the pineal complex (Figure 19A and A'). Immediately following exposure to UV light, one cell in the anterior left corner of the pineal complex anlage has photoconverted from green to red (Figure 19B). In transverse section (Figure 19B') the area that has been photoconverted extends from the dorsal to ventral aspects of the pineal complex. At 56 hpf photoconverted cells of the anterior left region have migrated to occupy a position within the pineal complex anlage as viewed dorsally (Figure 19C), and in transverse section (Figure 19C'). Figure 19D-F is a similar example in which photoconverted cells of the right side of the pineal complex anlage have become parapineal cells.

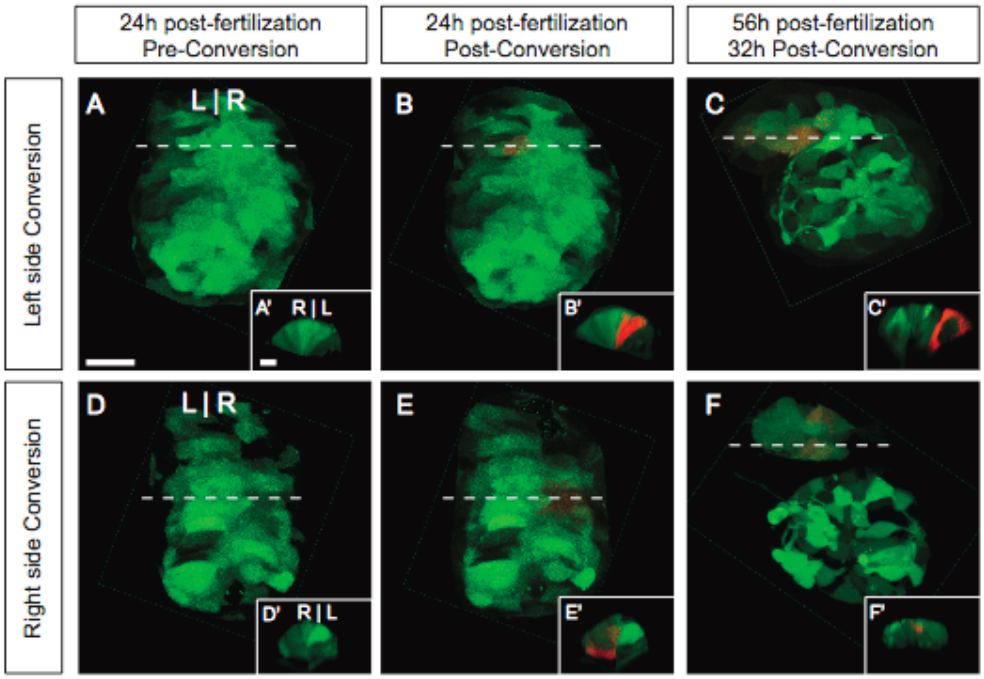

Figure 19. Photoconversion of the anterior region of the pineal complex anlage at 24 hpf highlights parapineal cells. (A-F) Dorsal views of the pineal complex (A'-F' (insets)) transverse sections through the photoconverted cell(s). Dashed white lines in A-F indicate where location of transverse section. Non-photoconverted cells are in green, photoconverted cells are in red. (A) A pineal complex at 24hpf that has not yet been photoconverted (green). (A') transverse section through the anterior region that has been photoconverted in (B') (B) Same view as (A) immediately following photoconversion of left-sided cell in the anterior pineal complex anlage (red). (C). Same embryo as (A,B) at 56 hpf, after the parapineal organ has migrated away from the pineal organ. Photoconverted cells (white arrowheads) have migrated into the parapineal nucleus. (D-F) Similar photoconversion experiment as (A-C) except cells of the right side of anterior region pineal complex anlage are photoconverted. (D) Immediately prior to photoconversion (E) immediately following photoconversion (F) 56 hpf after the parapineal organ has migrated away from the pineal organ. Scale bars: 25µm

In order to understand the dynamic processes that parapineal cells undergo before, during, and after migration, we performed high-resolution time-lapse confocal microscopy on embryos in which several cells had been photoconverted (Supplementary Movie 6). Photoconverted parapineal cells (in red) are initially indistinguishable from pineal complex cells in morphology, however, by 32 hpf, right sided parapineal cells change shape considerably; they contract along the anterior/posterior axis, align perpendicularly to the anterior/posterior axis, and show highly protrusive activity towards the left side of the embryo. Still images taking from this time-lapse movie highlight these activities (Figure 20). Following these shape changes, parapineal cells rapidly traverse the midline of the pineal complex and take a position within the migrating parapineal nucleus. Often, parapineal cells that originate on the right side of the pineal complex anlage will move to a position on the leading edge of the parapineal nucleus during migration. Preliminary experiments suggest that parapineal cells that arise from the left side of the pineal complex anlage migrate to a position in the caudal portion of the parapineal nucleus (works in progress, and data not shown).

Figure 20. Parapineal cells exhibit dynamic movement through migration from right side of the pineal complex anlage to the leading edge of the parapineal nucleus. Photoconverted cells are in red, non-photoconverted cells are in white. Photoconverted cells were photographed at 15 minute intervals from 26hpf over the following 22 hours to show that parapineal cells can arise from the right side of the pineal complex anlage, traverse the midline, and occupy a position within the parapineal organ on the left side of the pineal organ. (A) Immediately following photconverstion, 2 cells have been photoconverted (B) Cell 2 divides into 2 and 2'. (C) Cell 1 either dies or intercalates into the middle of the pineal organ (white arrow). Cell 2' rounds up and aligns next to the midline while cell 2 lengthens (yellow bracket) and contracts along the A/P axis (white bracket) (D) Cell 2 lengthens even further (yellow bracket), contracts further along the A/P axis (white bracket) and aligns the left side against the midline, while cell 2' has quickly traversed the midline and is barely visible within the developing parapineal tissue. (E) Cell 2 contracts (yellow bracket) and lies against the midline, while cell 2' becomes visible within the parapineal tissue and is assuming a position close to the leading edge of the parapineal nucleus (F) Within one hour cell 2 traverses the midline and begins to lengthen once again. Cell 2' becomes visible in the dorsal aspect of the parapineal nucleus (G) Cell 2' is barely visible once again, and cell 2 lengthens. (H) Cell 2' is at the leading edge of the parapineal nucleus, while cell 2 is barely visible having migrated into the middle of the parapineal nucleus (I) Cell 2' appears to be contracting back toward the pineal organ, however cell 2 is clearly visible at the dorsal aspect of the parapineal nucleus, migrating towards the leading edge.

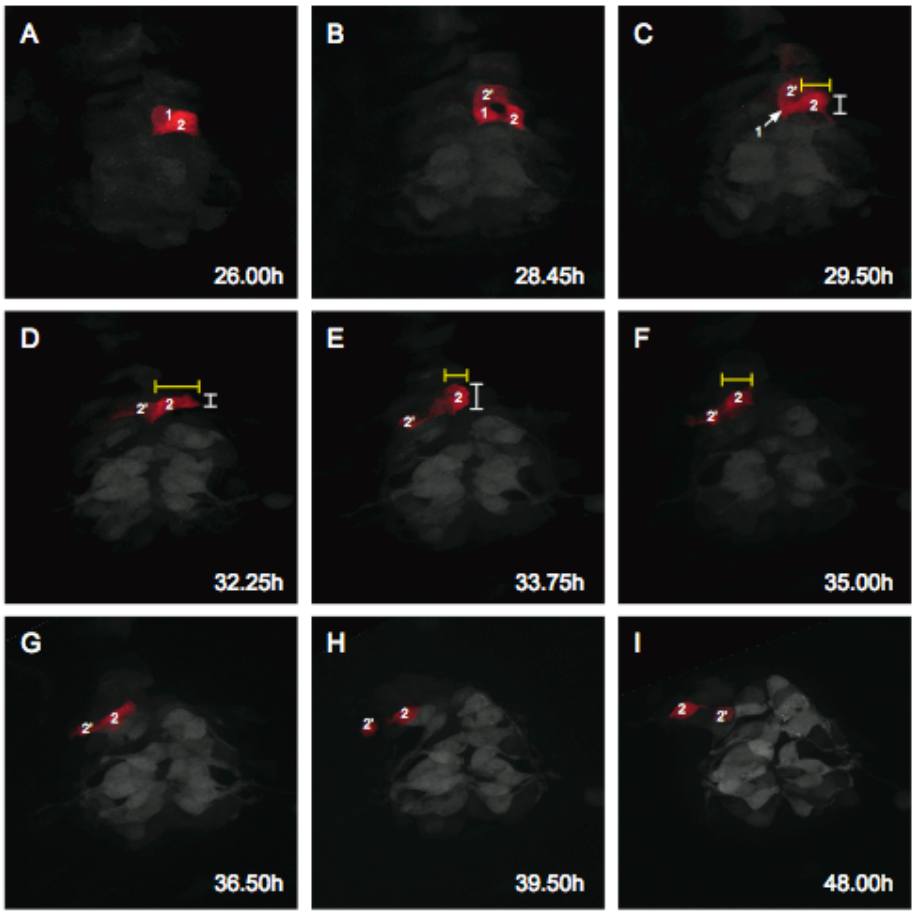
A
26.00h
B
28.45h
C
29.50h
D
32.25h
E
33.75h
F
35.00h
G
36.50h
H
39.50h
I
48.00h

Parapineal cells arise from discrete locations within the pineal complex anlage

Previously published data suggested that at 24 hpf parapineal cells arise on either side of the midline in the anterior third of the pineal complex anlage, while posterior aspects of the pineal complex anlage never gave rise to parapineal cells (Concha et al., 2003). These studies were informative, however they were performed prior to the development of more advanced mapping tools, which now make fate mapping at the cellular level possible. Based on the published fate mapping data (Concha et al., 2003), we concentrated our efforts at defining specific areas within the anterior third of the pineal complex anlage that gave rise to parapineal cells exclusively. Using the previously described transgenic lines (Figure 18), we performed one to two cell photoconversions throughout the pineal complex anlage at 24 hpf. Compiling data from individual embryos, we generated a heat map of the pineal complex anlage at 24 hpf highlighting discrete areas from which parapineal cells arise (Figure 21A). Interestingly, parapineal cells appear to arise at greater frequency within areas close to the left and right margins of the pineal complex. The photoconversion experiments highlighting cells that gave rise only to parapineal cells were further studied on an individual basis in order to investigate whether the cells from one particular area within the pineal complex anlage migrate to a specific position within the parapineal nucleus (Figure 21B,C). It is interesting to note that those cells from the anterior-most section of the pineal complex anlage appear to eventually reside within the posterior-most aspect of the parapineal nucleus, though more trials are necessary to confirm this observation.

Figure 21
Parapineal cells arise from discrete locations within the pineal complex anlage. For each individual embryo, a 10 X10 grid divides the pineal complex into 100 evenly spaced squares. The grid was then overlaid onto dorsal views of each photoconverted pineal complex and aligned with the anterior, posterior, left, and right borders of the pineal complex. Photoconverted cells were assigned a location based on the location within the grid that contained the highest amount of photoconverted (red) area. To compensate for differing sizes of pineal organs, the grids were each fit onto the pineal complex, and then each was stretched to 50mm square to normalize each sample. Circles that are ovoid in shape indicate the direction the box was stretched to compensate for overall size of the pineal organ. (i.e. a circle that is taller and thinner indicates that the pineal organ that was used to map that cell is actually shorter and wider.) (A) A heat map was generated by the compilation of data from these fate mapping experiments. Areas that more often give rise to parapineal cells are darker blue, while areas that never give rise to parapineal cells are white. Gray areas have currently not been tested. (B) Raw data for each of the 100 squares used to divide the pineal complex anlage. Each individual box is bisected by a diagonal line. The number in the top right of each box represents the number of trials that resulted in a photoconverted cell becoming a parapineal cell. The lower number is the total number of trials for that area. (C) Individual experiments in which photoconversions gave rise only to parapineal cells are shown at 24 hours, immediately following photoconversion. Each color represents a different embryo. (D) The same individuals as outlined in (C) but at 56 hpf, after the parapineal nucleus has moved away from the pineal organ. Some photoconverted cells are pineal cells, shown to the right in (D).

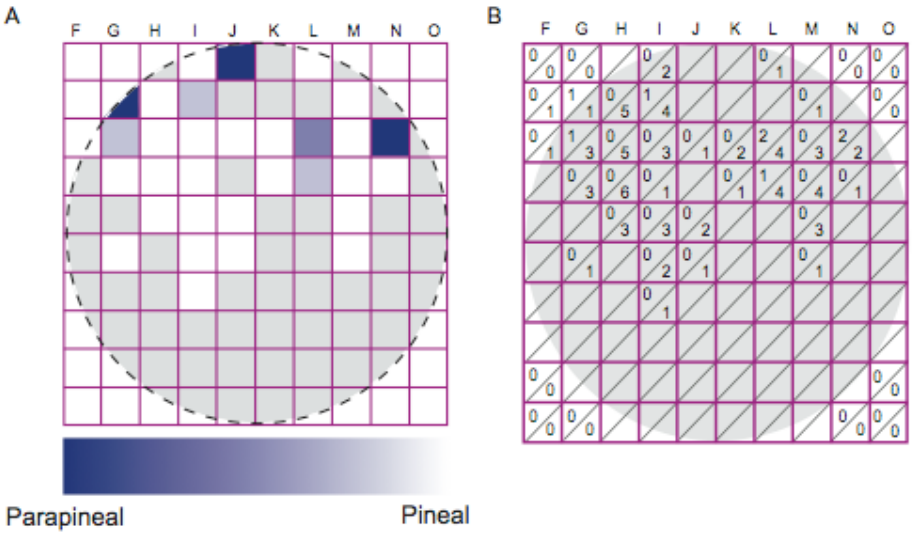
A
F G H I J K L M N O
Parapineal
Pineal
B
F G H I J K L M N O
C
24 hours post fertilization
A B C D E
F G H I J K L M N O
1 2 3 4 5 6 7 8 9 10
D
56 hours post fertilization
A B C D E
F G H I J K L M N O
1 2 3 4 5 6 7 8 9 10

tbx2b transcripts exhibit the same pattern in both fby and lor^{p25bbtl} mutant embryos

In addition to fate mapping, mutational analysis can also be used to study parapineal development. In the case of the pineal and parapineal organs, a lack of *tbx2b* activity prevents proper specification and migration of parapineal cells, and renders them indistinguishable from pineal cells until 48 hpf when they begin to express the parapineal specific marker *growth factor independent-1* (*gfi-1*) (Snelson, et al. 2008b). In order to identify the genes important for separating the pineal and parapineal lineages at an early stage, a homozygous population of *tbx2b* mutants must be generated. These embryos may be used to hybridize RNA to a microarray to look for transcriptional targets of *tbx2b*. To date, maintaining a fertile, adult homozygous population of *fby* mutants has been impossible, complicating efforts to generate such a population.

A second mutant in *tbx2b*, called *lots-of-rods* (*lor*) that can be maintained as a fertile adult homozygous line, was discovered in a forward genetic screen designed to identify mutations that result in rod cell patterning defects (Alvarez-Delfin et al., 2009). The *lor* mutation results in a decrease in the total number of *tbx2b* transcripts in the zebrafish embryo as shown by RT-PCR. Compared to wild type (Figure 22A) in situ hybridization of *tbx2b* in the retina of homozygous *lor* mutant larvae, homozygous *fby* mutant larvae and *fby*/*lor* heteroallelic larvae show a decrease in the total amount of *tbx2b* staining (Alvarez-Delfin, et al., 2009; Figure 22 A,C,E,G). The photosensitive pineal organ shares some types of cells with the retina, and also expresses *tbx2b* (Dheen et al., 1999; Robinson

et al., 1995; Ruvinsky et al., 2000). We wanted to check specifically whether there was a visible reduction in *tbx2b* transcripts in the pineal organ as compared to wild-type in *lor*$^{-/-}$, *fby*$^{-/-}$, and *lor*/*fby* heteroallelic embryos. In wild-type embryos there is a distinct stripe of *tbx2b* expression at the midline of the pineal complex at 24hpf that is notably missing in *lor*-/-, *fby*-/-, and *lor*/*fby* heteroallelic embryos (Figure 22B,D,F,H). Additionally, regions flanking the stripe of *tbx2b* expression in the wild-type pineal organ are conspicuously missing in our mutants (red arrowheads in Figure 22 B,D,F,H).

Figure 22. Expression of *tbx2b* is reduced in *fby*$^{-/-}$; *lor*$^{-/-}$; and *fby*; *lor* transheterozygotes at 24 hpf as compared to wild type. Expression of *tbx2b* in the eyes is shown in A,C,E,G, and in the pineal organ in B,D,F,H. In (A,B) wild type embryos, *tbx2b* expression is strongest in a the anterior region of the (A) eyes (red brackets, and (B) in a stripe along the dorsal midline of the pineal organ (red arrowheads). The levels of *tbx2b* transcription in (C,D) *fby* mutants is comparable to that of the *tbx2b* hypomorphic mutation (E,F) *lots-of-rods* (*lor*) and in (G,H) *fby*/*lor* transheterozygotes. Reduced transcription in the eyes (C,E,G) of mutant lines is highlighted with green brackets. Notably, the stripe of *tbx2b* expression in (B) wild type is not as sharp in the (D,F,H) mutants, and expression in the overall area of *tbx2b* expression is reduced laterally to the midline (green arrowheads). Scale bars: 25µm

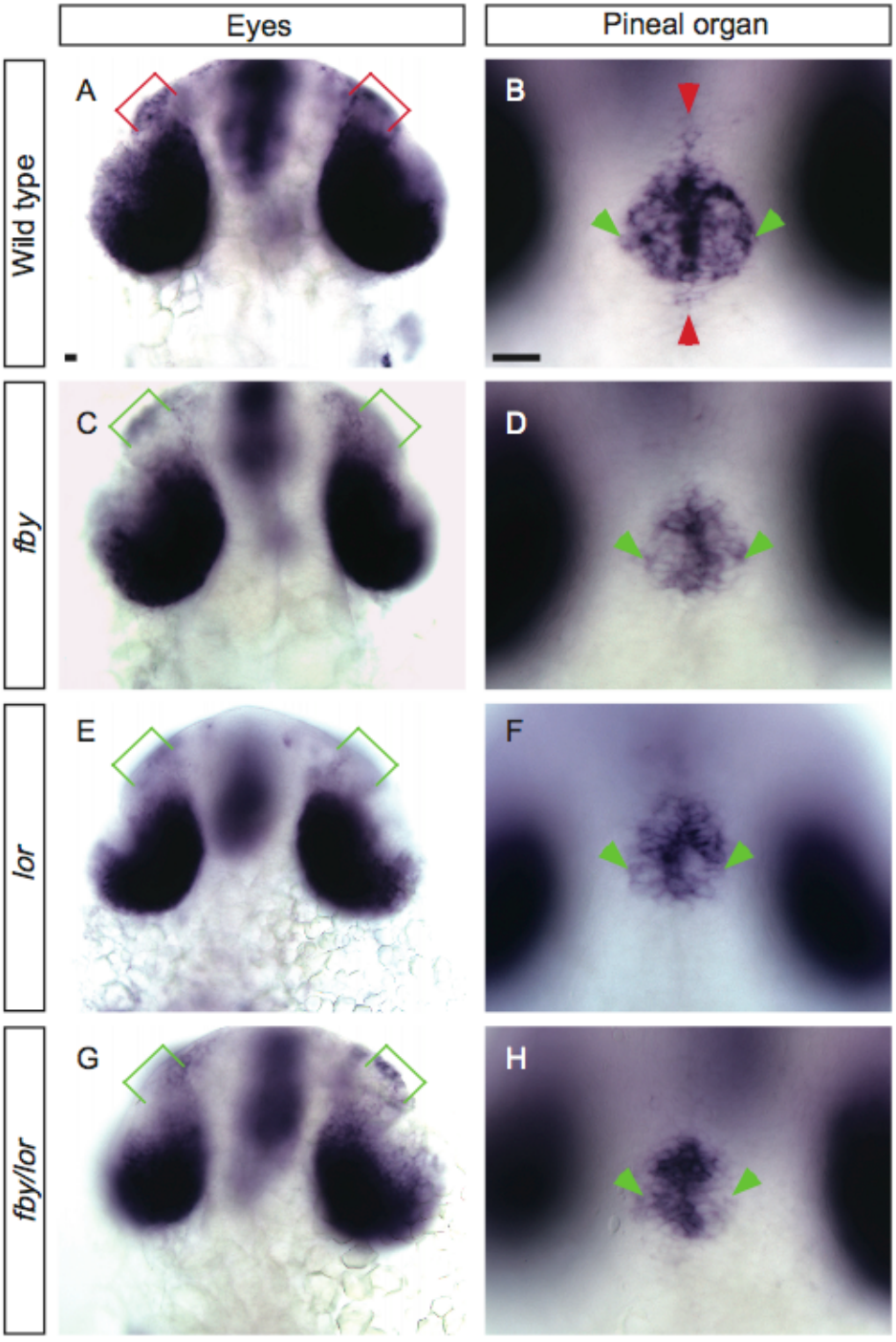
Eyes
Pineal organ
Wild type
fby
lor
fby/lor
A
B
C
D
E
F
G
H

The pineal complex phenotype of lor^{p25bbtl} is morphologically similar but not identical to fby^{c144}

The pineal complex of wild-type embryos contains 60±10 cells expressing the *foxd3:gfp* (Gilmour et al., 2002) transgene at 4 dpf (Snelson et al., 2008b). Interestingly, the same number of GFP+ cells is found in the pineal complex of the *fby* mutant, though in ectopic locations (Snelson et al., 2008b). Remarkably, a similar phenotype is found in both *lor* homozygous embryos and *fby*/*lor* transheterozygotes (Figure 23). Because *lor* mutants have reduced but not completely abrogated *tbx2b* transcription at 20 hpf (Alvarez-Delfin et al., 2009), when we suspect activity of *tbx2b* is crucial for specifying parapineal cells, a secondary phenotype occurs in approximately 49.5% (n= 368) of all *lor* homozygotes; a reduced parapineal organ can be identified, along with ectopic GFP+ cells similar to that which is seen in *fby* mutants (Snelson et al., 2008b). Additionally, axons of the parapineal organ that coalesce into the parapineal tract in wild type larvae are present on the left side of the pineal organ in *lor* homozygous mutant larvae, however, no discernable parapineal nucleus is present (50.5%, n= 368). The exact lesion in *tbx2b* that causes the *lor* phenotype has not been identified in either the coding region or within 1kb upstream of the start site of transcription (J.T.G and J.M.F, personal communication), suggesting that the lesion is within an enhancer of *tbx2b*. These results in conjunction with reduced expression of *tbx2b* in the eyes and the pineal complex anlage confirm that *lor* is a second, hypomorphic, allele that does not complement the *fby* mutation.

Figure 23. The *lots-of-rods* (*lor*) hypomorphic mutation in *tbx2b* phenocopies the *fby* mutation (A,C,E,G) dorsal and (B,D,F,H) frontal views of *foxd3:gfp* expression in the pineal complex of 4 dpf larvae. (A,B) In wild type embryos, the parapineal organ is found as a discrete group of cells located to the left of the pineal organ (white arrowheads). In (C,D) *fby* $^{-/-}$; (E,F) lor$^{-/-}$; and (G,H) *fby*/*lor* transheterozygotes, the pineal organ is single mass of cells with two ventral expansions of *foxd3:gfp* positive cells (yellow arrowheads), but does not have a discrete parapineal organ.

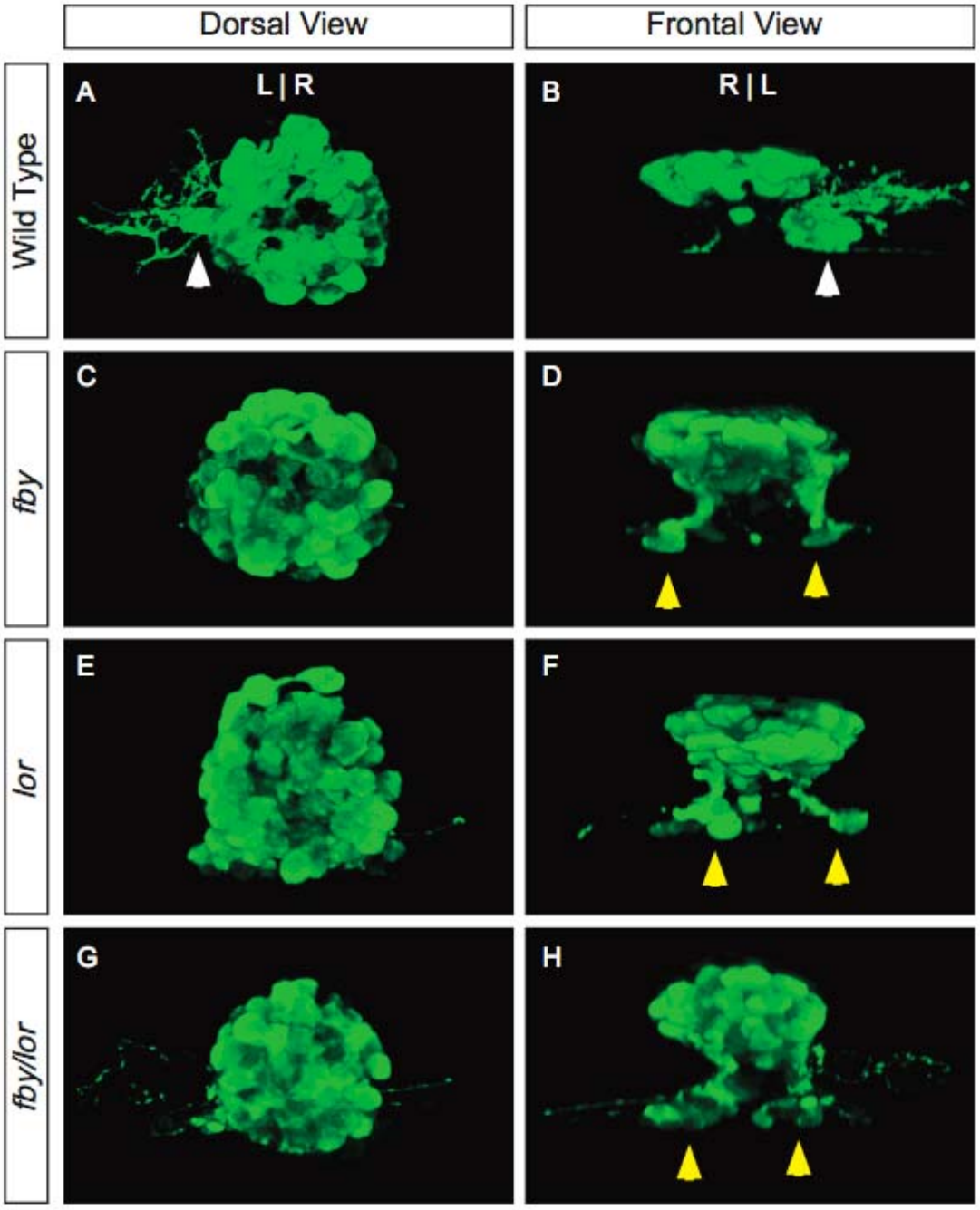
Dorsal View
Frontal View
Wild Type
fby
lor
fby/lor
A
L | R
B
R | L
C
D
E
F
G
H

Discussion

Fate mapping has been instrumental in our understanding of how an embryo develops from a fertilized cell to developing three germ layers that give rise to all of the tissues and organ systems of the body. In this study, we have initiated fate mapping experiments of an asymmetric region of the brain, the zebrafish epithalamus. Furthermore, we have begun characterizing a second allele of *tbx2b*, the lots-of-rods (*lor*) mutant, which shows a reduction in the total number of *tbx2b* transcripts in both the eyes and in the pineal complex anlage.

Early fate mapping may distinguish between two models of parapineal cell development

Previously documented fate mapping experiments have determined that parapineal cells arise from the anterior third of the pineal complex anlage (Concha et al., 2003), however discrete locations from which those cells arise could not be determined. The fate mapping experiments outlined in this study have confirmed and extended these results, highlighting discrete areas from which parapineal cells arise with greater frequency. Interestingly, parapineal cells appear to be highly proliferative around 16 hpf and have largely completed proliferation by 18 hpf (Snelson et al., 2008a). This, along with our whole pineal organ photoconversion data (Figure 18) suggests that by 24 hpf, when these experiments are taking place, the total number of parapineal cells that will develop within the pineal complex anlage are already present, albeit indistinguishable from pineal cells.

Currently, it is unknown how parapineal cells differ from pineal cells prior to initiation of migration. One possibility is that a single parapineal cell of determinant lineage is specified such that it can only give rise to parapineal cells while proliferating. A second hypothesis suggests that the lineage of pineal complex anlage cells is indeterminate at the time of proliferation, and can be influenced by an external cue to develop into either lineage. The results obtained from these studies will be used to identify parapineal cells within the time frame that they are proliferative, 16 to18 hpf. By determining the location of proliferative pineal complex anlage cells at early developmental stages, we may be able to distinguish between these two models.

In *fby* mutant embryos, fewer parapineal cells are specified, and they are unable to migrate to the left of the pineal organ. Intriguingly, in wild-type embryos there is a stripe of *tbx2b* expression in the ventral midline of the pineal complex at 24 hpf and in areas lateral to the ventral midline, though to a lesser extent. Both the stripe of *tbx2b* expression in the ventral midline as well as in a portion of the flanking area lateral to the midline are conspicuously reduced and/or missing in *fby* mutant embryos. Previously, it has been postulated that parapineal cells arise from the midline in wild-type embryos (Concha et al., 2000). The absence of the stripe of *tbx2b* in *fby* mutant embryos along with the fact that there are fewer parapineal cells present that remain scattered within the pineal complex leads us to hypothesize that expression of *tbx2b* in this stripe is required to specify the proper number of parapineal cells. The fate mapping

experiments outlined above will be performed in *fby* mutant embryos in an attempt to determine whether localized expression of *tbx2b* is required to specify the proper number of parapineal cells.

How does Nodal signaling affect the behavior of parapineal cells?

Placement of the parapineal organ with respect to the L/R axis is dependent on Nodal signaling. In embryos in which Nodal signaling has been disrupted, such as in rescued *one-eyed-pinhead* (*oep*) mutants, the parapineal organ migrates to either the left or the right side of the pineal organ with equal frequency (Gamse et al., 2002). We have noted in this work that the parapineal cells that arise from the right side of the pineal complex anlage appear to behave slightly differently from those that arise from the left. Just prior to initiation of migration, right-sided parapineal cells retract in length and align themselves more perpendicularly to the A/P axis. Often, these cells traverse the midline quickly to occupy the most distal position within the parapineal nucleus, while cells derived from the left side will remain more proximal to the pineal organ. Cells to the left of the pineal complex anlage do not have to traverse the same distance, and therefore behave slightly differently. Further information gathered from time-lapse imaging of wild-type embryos may be used to address differing cell behaviors in the left versus right side of pineal complex of Nodal signaling mutants.

Characterization of the lor mutant identifies a second hypomorphic allele of tbx2b

The *lots-of-rods* (*lor*) mutation was identified in a screen aimed to identify genes that are responsible for rod cell patterning within the eye. Characterization of the *lor* mutant embryos indicates that it shares the same very early gene expression patterns as age matched *fby* embryos within the pineal complex. At 4 dpf, however, half of all *lor* mutants have a phenotype identical to the *fby* mutation. Intriguingly, the other half of *lor* mutants have a parapineal phenotype that varies from being nearly identical to wild type embryos to being indistinguishable from wild type. The parapineal cells of wild type embryos extend processes that coalesce into the parapineal tract. In *fby* mutants, putative parapineal cells still extend processes, however they do not appear to coalesce into a parapineal tract. Interestingly, although parapineal cells do not migrate in the majority of *lor* embryos, a parapineal tract of efferent axons can still be observed suggesting that perhaps the specification defect and the migration defect observed in *fby* mutant embryos may be separable events dependent of the amount of *tbx2b* present in the cells. Careful characterization of the parapineal cells in *lor* mutants is required to determine the exact nature of this mutation.

Though the exact lesion in the *tbx2b* gene has not been identified in *lor* mutants, it appears not to be within the coding region of the gene. Based on RT-PCR results and expression data in these mutants, the number of *tbx2b* transcripts is severely abrogated (Alvarez-Delfin et al., 2009). Because *lor*

mutants can be maintained as a viable homozygous line, while *fby* mutants cannot, we are fully characterizing this line with the hopes that we will be able to obtain RNA from the pineal complexes of *lor* mutants that can be used to hybridize to a microarray. We suspect that this approach will highlight a number of categories of genes, however we will prioritize potential transcriptional targets of *tbx2b* based on expression pattern within the pineal organ, and whether available mutants and morpholinos are available. RNA from genes that are likely to be transcriptionally regulated by *tbx2b* will be injected into *fby* or *lor* mutants in an attempt to rescue the mutation (s). With luck, we hope to be able to identify the molecular and cellular pathways affected by the *tbx2b* mutation.

CHAPTER V

CONCLUSIONS AND FUTURE DIRECTIONS

The visceral organs are asymmetrically placed within the vertebrate body cavity, and many of the molecular cues that establish their asymmetry have been determined (Palmer, 2004). Similarly, observations of the gross anatomy of vertebrate brains have established that the two hemispheres are also morphologically asymmetric, but the molecular basis of this asymmetry is just starting to be established (Geschwind and Levitsky, 1968; Toga and Thompson, 2003). The zebrafish epithalamus, consisting of the pineal complex and paired habenular nuclei, exhibits asymmetries that are easily studied; much of what is currently known about the processes that lead to the development of brain asymmetry stems from studies of the zebrafish epithalamus.

The establishment of the epithalamic asymmetry with respect to placement of the parapineal along the L/R axis has been an intense focus of study over the last decade; however, the epithalamus also lends itself to the study of basic developmental processes involved in parapineal organogenesis. For instance, the pineal and parapineal organs originate from a seemingly uniform population of cells to become morphologically distinct during later stages of development. This uniform population must undergo specification and determination of precursor cells into two distinct lineages before initiating the migration program that is unique to parapineal cells. Zebrafish harboring

mutations in which these fundamental developmental processes have been disrupted in the epithalamus have allowed us to begin to identify the genes required for the formation of these organs.

A role for the parapineal organ in establishing left-right laterality in the zebrafish epithalamus had been previously established (Gamse et al., 2003). Laser ablation of the parapineal organ at early stages results in the development of symmetric habenulae demonstrating that in the absence of the parapineal organ, the left habenula will adopt a right-sided state, including gene expression, neurogenesis, and neuropil density. Further, proper molecular identity of the habenular nuclei is important to accurately establish correct midbrain targeting to the interpeduncular nucleus (Kuan et al., 2007). When both habenular nuclei resemble the right habenular nucleus in gene expression (ie. the KCTD genes *leftover* (*lov), righton* (*ron)*, and *dexter* (*dex*), reflecting the default state of habenular identity, axons from both habenulae are targeted toward the ventral IPN (Gamse et al., 2003; Snelson et al., 2008b). This work demonstrates the absolute requirement of the parapineal organ for establishing epithalamic asymmetry, but until recently none of the genes required for development of the parapineal organ were known.

To begin to understand how the parapineal organ is formed, a forward genetic screen was performed by the members of the Halpern lab, and is described in Snelson et al., 2008b (Chapter 2 of this work). Several mutations disrupting asymmetric gene expression in the habenular nuclei were discovered. The *from beyond* (*fby*) mutation was generated in this screen and has been the

basis of my work in the Gamse laboratory. This mutation ultimately causes a reduction in the number of parapineal cells, and those cells that are specified are unable to migrate to the left of the pineal organ. Subsequently, this mutation also affects the identity of the adjacent habenular nuclei. The absence of a left-sided parapineal organ results in fewer *lov* transcripts in the left habenula, similar to laser ablation of parapineal tissue at early stages. Positional cloning identified the *fby* mutation as a lesion in the transcription factor Tbx2b, and thus identified the first gene required for parapineal organ development (Snelson et al., 2008b), Chapter 2).

This work stimulated further questions, such as what other genes may be responsible for formation of the parapineal organ? Previous reports had implicated the homeobox transcription factor Floating Head (Flh) as the upstream activator of *tbx2b* transcription (Cau and Wilson, 2003). A mutation in *flh* causes a severe reduction in pineal neurogenesis, which ceases abruptly at 14 hpf (Masai et al., 1997), but does not affect the formation of the parapineal nucleus (Gamse et al., 2003; Snelson et al., 2008a). Our previous work had demonstrated that a mutation in *fby* causes a reduction in the total number of parapineal cells, but leaves the pineal organ largely intact (Snelson et al., 2008b). We used *flh*; *fby* double mutant embryos to specifically address the hypothesis that *flh* was required for transcriptional activation of *tbx2b* in the pineal complex anlage. We observed that mutations in both transcription factors causes an additive phenotype: a reduction in pineal neurogenesis due to a lack of *flh* activity, and a reduction in the number of parapineal cells due to a mutation

in *tbx2b*. This work conclusively demonstrates that *flh* does not regulate transcription of *tbx2b* (Snelson et al., 2008a), Chapter 3 of this work).

Both the pineal and parapineal organs originate from a precursor population of cells termed the pineal complex anlage, but the process by which particular cells decide to adopt one or the other fate is poorly understood. To further our understanding of how parapineal cells develop and differentiate from pineal complex cells, fate-mapping was performed in wild-type embryos. Low-resolution fate-mapping experiments have demonstrated that parapineal cells have a bilateral, anterior origin within the pineal complex anlage (Concha et al., 2003), and those presumptive parapineal cells that are initially located on the right side traverse the midline to occupy a position within the mature parapineal organ (Concha et al., 2003). Data from Chapter 4 of this work confirms and extends these results, indicating distinct areas from which parapineal cells arise within the greater population of centrally located, bilaterally symmetric pineal complex cells. Following photoconversion, parapineal development in some embryos was also analyzed via time-lapse confocal microscopy, allowing us to describe the morphogenetic movements of parapineal cells prior to and during migration. As described in Snelson et al, 2008a (Snelson et al., 2008a), parapineal cells undergo rapid proliferation around 16 hpf. Information gathered from fate-mapping wild type embryos at 24 hpf will be used as a foundation for fate-mapping at earlier stages, which should aid in our understanding of where parapineal cells emerge during their rapid proliferation. Given that the parapineal organ arises quite normally in *flh* mutants, we suspect that there may be a

progenitor cell that can give rise to both pineal and parapineal cells. Presumably the influence of the *flh* homeobox transcription factor on only pineal cells occurs after the initial division of the progenitor cells. With information gathered from early fate-mapping, we may be able to identify this potential progenitor cell. Studies of the progenitor cell will allow us to determine whether it is transcriptionally different from it's pineal organ counterparts, whether it is the leader of the chain of parapineal cells as discussed in Snelson, et al. 2008b, and whether is capable of responding to a directional cue, perhaps left-sided Nodal signaling within the epithalamus, or left lateral plate mesoderm (LLPM) as in the case of *spaw*, which is only expressed in the LLPM, but still influences placement of the parapineal organ with respect to the L/R axis.

Future directions

The work outlined in this thesis and preliminary work from other labs is just the beginning of what is currently known of how the pineal and parapineal organs develop from a uniform population of precursor cells. We are beginning to understand this process through the characterization of induced mutations in the genes required to establish these separate lineages, such as the *fby* mutation, however several questions currently remain unanswered.

What genes are responsible for parapineal cell migration?

Analysis of the *fby* mutation identified the first gene (*tbx2b*) required at an early stage of parapineal organ formation. The other genes involved in this

process are currently unknown. In order to identify other genes important for the formation of the parapineal organ, a microarray performed with *tbx2b* mutant embryo RNA can be compared to one performed with RNA from wild-type siblings. Generating homozygous populations of *fby* larvae has not been possible because adult homozygous *fby* fish cannot be maintained as a viable stock. A second allele of *tbx2b*, *lot-of-rods* (*lor*^{p25bbtl}) was identified in a screen performed by the Fadool laboratory that can be maintained as a viable homozygous adult stock (Alvarez-Delfin et al., 2009). Work in Chapter 4 (Figure 23) shows that the parapineal phenotype of *fby* and *lor* is similar, and complementation testing of *fby* and *lor* transheterozygous embryos defines *lor* as a second allele of *tbx2b* that affects parapineal organ development.

In order to obtain RNA to hybridize to a microarray, we will surgically remove the pineal tissue from approximately 50 wild type and *lor* homozygous embryos expressing the *GAL4VP16*^{s1145t} transgene at 24 hpf, prior to the onset of parapineal cell migration. By specifically selecting pineal complex tissue, we will avoid potentially confounding results from other tissues that also express the transgene.

It is possible that RNA obtained from the pineal organs of wild-type or *lor* mutant embryos may not show any appreciable difference in transcription levels. In order to specifically enrich for parapineal cells in future microarrays, we could follow two different approaches. A recently described insertion line, Tg(*ET11:GFP*), (Regan et al., 2009), appears to be parapineal specific, enabling us to select for solely for GFP+ parapineal cells in both the wild-type and *lor*

mutant backgrounds. Another way to enrich for parapineal cells specifically is to cross the *lor* mutant background in the *flh*^{n1} mutant line. The mutation in *flh* causes a reduction or abrogation of pineal neurogenesis without affecting parapineal organogenesis (Gamse, et al., 2003; Masai, et al., 1997). By removing the parapineal organs from *flh* mutant fish, and *flh;lor* double homozygous fish, we can enrich for parapineal cells specifically.

Three commercially available microarray platforms exist for hybridization of zebrafish RNA. The first is produced by Affymetrix, and is based on 2003 genome sequence data. It is spotted with 25-mer oligonucleotides representing approximately 15,000 genes, and costs nearly twice the other two options. The second platform is produced by Nimblegen. These arrays are spotted with 60-mer oligonucleotides representing over 37,000 genes, with 12-fold coverage per gene. The final platform is produced by Agilent, and is nearly identical to the Nimblegen platform in the types of genes represented, their fold-coverage, reference genome sequences, and the cost. Because the Affymetrix chip is more expensive, represents fewer genes, and hasn't been updated in six years, we are excluding this platform as a possibility for our microarray studies. Though the Nimblegen and Agilent platforms do not differ significantly in the types of sequences spotted on the arrays, the software that accompanies the Agilent chip (Gene Spring GX) has been tested by the Vanderbilt Microarray Core Facility, and is likely to give the cleanest, most reliable results.

A newer alternative to microarrays, RNA-Seq, has recently become available at Vanderbilt through the Genome Technology Core. In this method, mRNA is extracted from whole tissue, transcribed into cDNA, and massively sequenced by the Sanger method. These samples are then mapped to the reference genome sequence, and then the total number of hybridizations of each sequence are tallied to give an accurate number and density of transcripts found for each gene in a given tissue. This method avoids some of the major pitfalls of microarray hybridizations, including false positives obtained from low transcript numbers, and has the added benefit of being able to identify potential splice variants (Mortazavi et al., 2008) without being significantly more expensive than traditional microarray hybridizations. Comparison of the new RNA-seq procedure with standard Affymetrix microarray analysis has shown that the RNA-seq method can identify the same differentially expressed genes from an Affymetrix microarray for approximately 80% of all expressed genes in the samples tested (human kidney and liver). Q-PCR was used to test transcript level discrepancies of several genes that were differentially expressed between RNA-Seq and the Affymetrix microarray. These results demonstrated that the RNA-Seq method for identifying differentially expressed genes is more accurate than the Affymetrix array (Marioni et al., 2008), and likely represents a method by which we can obtain far greater accuracy when comparing the transcript levels of certain genes between wild-type embryos and *tbx2b* mutants.

If we successfully find genes with appreciably different levels of transcription between wild-type and *lor* homozygous mutants, we will further

characterize their expression patterns by in situ hybridization in wild-type embryos and *fby* or *lor* mutants. Those genes that show a difference in transcription in the pineal tissue of wild-type and mutant embryos, have an appreciably different in situ hybridization pattern, and are involved in neuronal migration will be selected for further study. RNA from potential candidates will be injected into *fby* or *lor* homozygous mutant embryos in an attempt to rescue the phenotype caused by the lack of *tbx2b* activity. Over-expression of candidate RNA will also be performed in wild-type embryos.

We expect that these microarray or RNA-seq experiments will reveal many potential candidates, and several types of genes could be identified in this manner. Based on the migration defect in *fby* mutant parapineal cells, it is possible that we may not only identify genes required for proper neuronal migration, but also components of the extracellular matrix (ECM) or ECM receptor such as an integrin, cell adhesion molecule(s), chemokines, or genes involved in cytoskeletal rearrangement. Additionally, it is possible that the polarity of parapineal cells has been disrupted such that they are no longer capable of initiating or maintaining neuronal migration. However, expression of several planar cell polarity genes is not disrupted in *fby* mutants, and the parapineal organ of *odysseus/cxcr4b* migrates to the left in all cases (data not shown). Based on characterization of the *fby* mutant, *tbx2b* is responsible not only for proper migration of parapineal cells, but also specification of the correct number of parapineal cells.

How does tbx2b affect specification of the parapineal organ?

It has been established that *tbx2b* is required for the formation of the parapineal organ (Snelson et al., 2008b), but the exact role of *tbx2b* in this specification process has not been determined. Previously published experiments have demonstrated a fate change in notochord tissue in wild-type embryos injected with *tbx2b* mRNA (Dheen et al., 1999). In this instance, *tbx2b* seems to play an instructive role by expanding axial mesoderm at the expense of paraxial mesoderm. Similarly, it is possible that *tbx2b* could instruct pineal complex cells to adopt a parapineal fate at the expense of a pineal fate. If this hypothesis is correct, we would expect to see a greater number of *gfi-1* positive parapineal cells and fewer pineal cells in a larval fish when *tbx2b* is over-expressed in pineal tissue. Alternatively, *tbx2b* could be a permissive cue for parapineal organ formation. If this is the case, we would not see a change in the fate of wild-type cells following *tbx2b* over-expression. As a test of the hypothesis that *tbx2b* may be a permissive cue, over-expression of *tbx2b* in *fby* mutants should restore the wild-type number of parapineal cells, without changing the number of *gfi-1* positive parapineal cells in wild-type larvae. In order to definitively answer these questions, conditional expression of *tbx2b* specifically in pineal tissue using the *GAL4/UAS* reporter system during the phase of parapineal cell specification is required.

One additional problem that has repeatedly occurred during the course of my work in the Gamse Lab is that there are no known markers of parapineal cells that differentiate them from pineal cells prior to the initiation of left-sided

migration. An additional possible result from this set of microarray or RNA-Seq experiments is that other genes that are specifically expressed in parapineal cells as they are being specified may be discovered. Currently, the only identified parapineal specific marker is the gene *growth factor independent-1* (*gfi-1*) (Dufourcq et al., 2004), which is expressed late during development after the parapineal organ has migrated to the left of the pineal organ, and has begun to extend neuronal processes. Determining the identity of other genes that are only expressed in parapineal tissue prior to the initiation of parapineal cell migration will further our understanding of how and when the two precursor populations differ from one another, and will be a great boon to other students working on these problems.

How has the fate of the parapineal cells in fby been changed?

The zebrafish pineal complex is composed of photoreceptor cells and projection neurons. The parapineal organ primarily contains projection neurons, and in rare instances may also contain a photoreceptive cell (Concha et al., 2000). In wild-type embryos there are only about 10 *gfi-1* positive cells present within the parapineal organ. In *fby* mutant larvae, there are fewer *gfi-1* positive parapineal cells, but the total number of pineal complex cells remains unchanged from wild type. Initial counts from antibody labeling against a rod-specific opsin (Adamus et al., 1991), and the red-green cone-specific antigen Zpr-1 (ZIRC, Eugene, OR) have shown that the same number of photoreceptors are present in the pineal organs of *fby* larvae and wild-type embryos, although in *fby* mutants

they are ectopically placed (Snelson et al., 2008b). The question remains, however, what fate(s) have the missing parapineal cells adopted? Is there a default state of the pineal complex anlage cells? Since the overall red-green cone or rod cell number has not changed in *fby* mutants from their wild-type siblings, it is possible that the missing parapineal cells in *fby* have become another type of cone cell (UV or blue) or pineal projection neurons within the pineal organ. Further testing using a more comprehensive panel of antibodies specific to different types of photoreceptors and pineal projection neurons is required to determine the fate of the mis-specified parapineal cells.

Do parapineal cells follow a leader cell during migration?

Time-lapse microscopy has been instrumental in understanding the morphological processes that parapineal cells undergo to achieve their precise location at the appropriate time during development (Snelson et al., 2008b). From our time-lapse movies we have hypothesized that individual parapineal cells play different roles during migration. For instance, one cell seems to lead the remaining cells towards the left side of the pineal complex (Snelson, et al. 2008b). In the lateral line system, in which cells migrate from a region just posterior to the otic placode to occupy positions along the body axis, a few cells are specified from a group of common cells as “leaders” of this migratory pathway (Ghysen and Dambly-Chaudiere, 2007). We propose that a similar phenomenon may be occurring in parapineal tissue. This hypothesis was initially addressed by ablating the earliest emergent parapineal cells at 31 hpf. By this

stage, when a few cells are ablated, the remaining cells are still capable of migrating, suggesting that the activity of a “leader” cell is either no longer required or can be fulfilled by another parapineal cell. In order to address the hypothesis that a leader is indeed required to initiate migration from within the pineal complex anlage, ablation of cells at earlier stages, before parapineal cells begin their migration program, is necessary. The recently acquired transgenic line *GAL4VP16*^{s1145t} that allows all pineal complex precursor cells to be distinguished as early as the 12 s stage through 4 dpf will facilitate these experiments, and by completing the microarray studies, we may also discover other genes that are likely to serve as earlier markers of parapineal cells. Information gathered from multiple time-lapse movies in conjunction with our fate mapping efforts, and microarray studies should allow us to determine when parapineal cells initiate migration.

How does the mutation in tbx2b affect pineal organ development?

In zebrafish, the photoreceptive pineal organ produces the hormone melatonin rhythmically in a circadian manner (Cahill, 2002). In wild-type embryos between 4 and 14 dpf, the pineal complex undergoes rapid changes that result in the extension of the pineal organ from a stalk, while the parapineal organ remains at the base of the stalk, adjacent to the left habenula (Gamse et al., 2003). Observation of 4 dpf *fby* mutant larvae carrying the *foxd3*:*gfp* transgene revealed that not only do parapineal cells fail to migrate laterally, there are also subtle changes in the overall morphology of the pineal organ. In wild-type

embryos, the pineal organ is disc-shaped, densely packed, and only 2-3 cell layers deep, while in *fby* mutant larvae, the pineal organ is 5 to 7 cell layers deep and no longer disc shaped or densely packed (Figure 6).

It is possible that the morphological changes caused by a mutation in *tbx2b* may subtly affect the circadian rhythm of *fby* mutants by increasing the number of pineal cells relative to wild type larvae, or because parapineal input to the habenular nucleus has been disrupted. Since *fby* mutant larvae generally survive until 14 dpf, it is possible to monitor larval locomotor activity or expression of genes that are rhythmically expressed (*aanat2*, *reverb-alpha*, and *interphotoreceptor binding protein*, *irbp*) to determine whether a subtle change in the composition in the pineal complex affects circadian timing. The overall pineal complex phenotype of *fby* mutant larvae is distinguishable as early as 3 dpf. A small percentage (4%) of *fby* homozygous mutant larvae are capable of surviving to adulthood (Snelson et al., 2008b). Dissection of these adult brains has demonstrated that the pineal complex phenotype observed in larval *fby* mutant fish persists into adulthood (data not shown), allowing for circadian experiments to be performed on adult *fby* or *lor* homozygous fish.

Models of Parapineal Specification and Migration

Previously published fate mapping studies have shown that at 24 hpf parapineal cells are located in the anterior region of the pineal complex anlage (Concha et al., 2003). Experiments described in Chapter 4 of this work have

confirmed and extended these findings. Shortly after 24 hpf, parapineal cells located in the right anterior region traverse the midline to join parapineal cells that arise on the left side of the pineal complex anlage to occupy a position within the migrating parapineal nucleus. Based on expression of *tbx2b* and the *fby* and *lor* mutant phenotypes, we have generated three potential models regarding parapineal formation.

The first model suggests that the dosage of *tbx2b* expression in the pineal complex anlage is crucial for proper parapineal cell specification and migration. At 24 hpf, prior to the emergence of parapineal cells, expression of *tbx2b* is strongest along the midline of the pineal complex anlage (Snelson et al., 2008b). Intriguingly, it has been postulated that parapineal cells originate in this area (Concha et al., 2000), and then undergo a migration event that locates them in the anterior region prior to initiating leftward migration. The presence of a strong band of *tbx2b* expression at the midline of the pineal complex anlage, and the observation that fewer parapineal cells are specified in *fby* mutant larvae, suggests a model in which high levels of *tbx2b* acts instructively to assign parapineal fate to cells located near the midline (Figure 24A). The reduced number of parapineal cells found in *fby* mutant larvae corresponds to a decrease in the amount of *tbx2b* expressed in the midline of the pineal complex at 24 hpf. The *lor* mutation, which is a suspected hypomorph of *tbx2b* has more parapineal cells that do not migrate, but appear to coalesce together within the pineal complex region, and extend processes to the left side (data not shown). This suggests that the dosage of *tbx2b* is crucial for both proper migration and proper

specification; *lor* mutants, which have reduced *tbx2b* expression in midline of the pineal complex anlage appear only to have a defect in parapineal cell migration, while *tbx2b* expression is even further reduced in the same region of *fby* mutants, which have a defect in both specification and migration of parapineal cells (Figure 22). Fate maps at earlier time points, early pineal-ablation experiments, and over-expression of *tbx2b* in the pineal complex of wild-type and mutant larvae during the time at which parapineal cells are specified will test the validity of this hypothesis.

Based on the phenotype of the *fby* mutation, isolated parapineal cells dispersed throughout the pineal complex, we propose a second model of how parapineal cells may develop. In this model, parapineal cells may arise through a process of lateral inhibition (Figure 24B). Though this phenomenon has not been previously described for pineal complex development, there is precedent for it in neural precursor development within the nervous system. In the Drosophila eye (reviewed in Corbin et al, 2008), as well as the zebrafish spinal cord (Appel and Eisen, 1998) the Delta/Notch interaction is crucial for the maturation of neurons; without this interaction, neurons do not differentiate appropriately, but remain in their precursor state and continue to proliferate. *Mindbomb* (*mib*) mutants are defective in the E3 ubiquitin ligase required for proper Delta/Notch signaling, resulting in excessive neurogenesis (Itoh et al., 2003), and are a logical first mutant to test to determine whether a lack of Delta/Notch causes a similar pineal complex phenotype to *fby*. Previously published experiments looking specifically at the pineal organ phenotype of *mib*

mutants shows that a reduction in Notch signaling causes an increase in the number of projection neurons at the expensive of photoreceptors within the pineal organ (Cau et al., 2008). This study did not specifically address parapineal cell development in these Notch mutants, however preliminary results from our laboratory show that in the pineal tissue of *mib* mutants there is a reduction of *otx5* positive pineal cells, while parapineal organ development appears to be largely unaffected (Caleb Doll, unpublished observation). These observations decrease the likelihood of Notch-dependent lateral inhibition as a model for the proper specification of parapineal cells.

One final model describing a possible method by which the parapineal organ develops posits that there is an external signaling cue that dictates its proper specification and placement. In this scenario, putative parapineal cells, expressing *fgfr4* are responding *fgf8a* secreted from the habenular precursors (Regan, et al., 2009 and Figure 24C). This model is supported by studies of the *acerebellar* (*ace*^{ti282}/*fgf8a*) hypomorphic allele, and *ace*^{x15}/*fgf8a* null allele in which fewer parapineal cells are specified and are able to coalesce in the anterior region of the pineal complex anlage, but are unable to complete leftward migration (Regan, et. al., 2009 and Joshua Clanton, unpublished data). Studies *of fby/ace*^{x15} double homozygous mutants reveal an additive phenotype, such that even fewer parapineal cell are specified, though the migration phenotype of these double mutants remains to be tested (Joshua Clanton, personal communication). In this scenario, the role of *tbx2b* would be to assure that parapineal cells have migrated to the anterior region of the pineal complex

anlage such that they are able to receive a signal from the surrounding tissue. Once located in the anterior region, parapineal cells may migrate as a result of both the activity of the Fgf8a/Fgfr4, and a directional cue provided by Nodal signaling.

Currently, we favor a model in which parapineal specification and migration can be explained by a combination of the first and third models (Figure 24D). Expression of *fgf8a* in the tissues surrounding the pineal complex, and its receptor, *fgfr4*, in the anterior pineal tissue, along with studies of *fgf8a* mutants highlights the necessity of this signaling system for parapineal migration (Regan et al., 2009), and Joshua Clanton, unpublished observations). Studies of the *fby* mutant show that *tbx2b* is required for parapineal specification, and without it these cells are incapable of migration. The first and third models in combination would suggest that the areas in which *fgfr4* expression in the anterior region of the pineal complex that also overlaps with *tbx2b* expression in the anterior midline outline a region in which anterior pineal complex cells are instructed to become parapineal cells whose leftward migration is made possible by *fgf8a/fgfr4* signaling and perhaps a directional cue provided by Nodal signaling (Figure 24D). A fate map of *ace* or *fby* mutant embryos will be instrumental in determining the validity of this hypothesis.

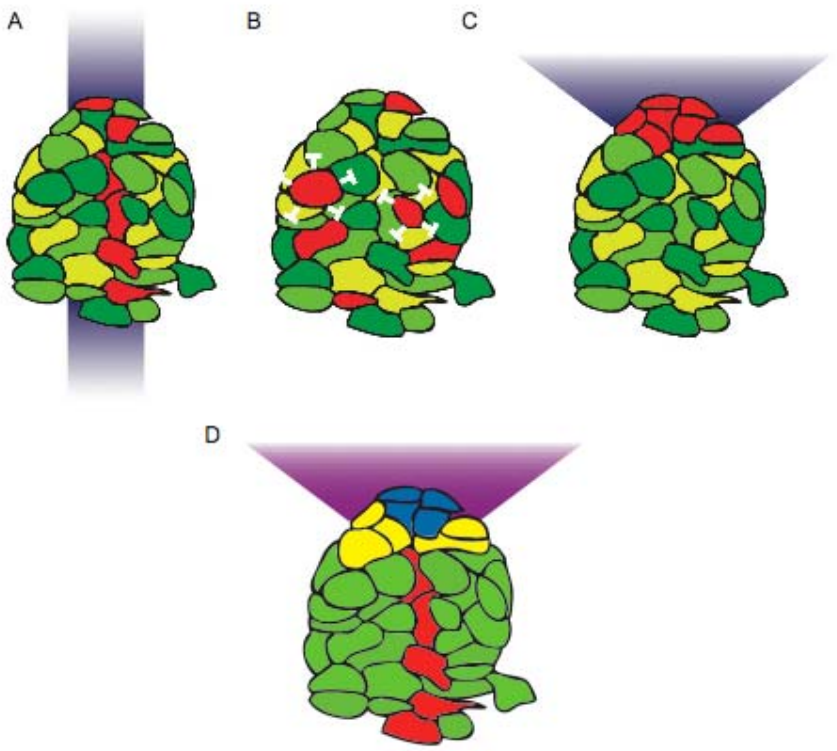

Figure 24.
Models of parapineal cell formation. Putative parapineal cells are in red, pineal cells are in green. (A) *tbx2b* is expressed in a ventral stripe along the midline of the pineal complex anlage that is missing in *fby* mutants. Parapineal cells may arise from this stripe. Tbx2b plays an instructive role in this scenario. (B) Parapineal cells in *fby* mutants are not located in a cohesive group, but are scattered throughout the pineal complex at 4 dpf. In this scenario, parapineal cells arise through a process of lateral inhibition. Tbx2b plays a permissive role in this scenario. (C) The parapineal organ emerges from the pineal complex anlage as a result of an external signaling cue. Tbx2b plays a permissive role in this scenario. (D) Merge of models A and C. The green cells are pineal complex cells that do not express *tbx2b*, *fgf8a* or *fgfr4*. The yellow cells express *fgfr4*, the red cells express *tbx2b*, the purple area expresses *fgf8a*, and the blue cells that are located in the anterior, midline region, express both *tbx2b* and *fgfr4* are adjacent to the surrounding pineal tissue that expresses *fgf8a*. In this model, these cells will develop as parapineal cells.

Concluding Remarks

This work identifies a new mutation in the transcription factor *tbx2b* that is required for the proper specification and migration of the parapineal organ. We know from previous work (Masai et al., 1997) that the homeobox transcription factor *flh* is required for pineal neurogenesis, but does not influence formation of the parapineal organ (Gamse et al., 2003; Snelson et al., 2008a). Currently, we suggest a hypothesis in which parapineal formation occurs in a two-step process. The first step requires *tbx2b* to properly specify parapineal cells and allow them to coalesce in a "staging area" in the anterior region of the pineal complex anlage by 24 hpf. A second step, requiring the concerted efforts of *fgf8a* and its receptor *fgfr4*, which is expressed in both pineal and parapineal tissue, allows for the continued migration of the parapineal organ to its proper left-sided location within the epithalamus between 24 and 48 hpf (Figure 25). This simplistic model describes what is currently known about development of the parapineal organ, and we suspect that what is happening is far more complex. By completing the fate map of the developing pineal complex, performing a microarray on *tbx2b* mutant embryos, and continual study of genes expressed in this tissue, we hope to be able to determine the exact mechanism of parapineal organ formation.

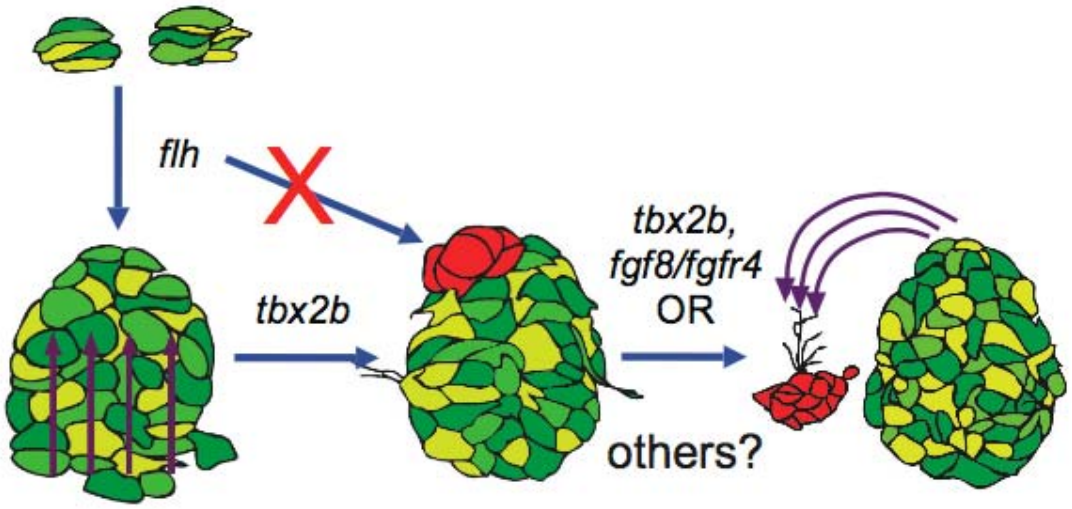

Figure 25.
Current model of pineal complex development. *Flh* is required to assure that pineal neurogenesis occurs properly, however is not required for neurogenesis of parapineal cells (blue arrow, red X). After pineal neurogenesis occurs, *tbx2b* may be required to locate parapineal cells to the anterior region of the pineal complex anlage. After parapineal cells are properly located, *tbx2b*, *fgf8/fgfr4* or another factor is required to complete the migration of those cells to the left side of the pineal organ.

REFERENCES

Adamus, G., Zam, Z. S., Arendt, A., Palczewski, K., McDowell, J. H. and Hargrave, P. A. (1991). Anti-rhodopsin monoclonal antibodies of defined specificity: characterization and application. *Vision Res* **31**, 17-31.

Aizawa, H., Bianco, I. H., Hamaoka, T., Miyashita, T., Uemura, O., Concha, M. L., Russell, C., Wilson, S. W. and Okamoto, H. (2005). Laterotopic representation of left-right information onto the dorso-ventral axis of a zebrafish midbrain target nucleus. *Curr Biol* **15**, 238-43.

Aizawa, H., Goto, M., Sato, T. and Okamoto, H. (2007). Temporally regulated asymmetric neurogenesis causes left-right difference in the zebrafish habenular structures. *Dev Cell* **12**, 87-98.

Alvarez-Delfin, K., Morris, A. C., Snelson, C. D., Gamse, J. T., Gupta, T., Marlow, F. L., Mullins, M. C., Burgess, H. A., Granato, M. and Fadool, J. M. (2009). Tbx2b is required for ultraviolet photoreceptor cell specification during zebrafish retinal development. *Proc Natl Acad Sci U S A*.

Amack, J. D., Wang, X. and Yost, H. J. (2007). Two T-box genes play independent and cooperative roles to regulate morphogenesis of ciliated Kupffer's vesicle in zebrafish. *Dev Biol* **310**, 196-210.

Ando, R., Hama, H., Yamamoto-Hino, M., Mizuno, H. and Miyawaki, A. (2002). An optical marker based on the UV-induced green-to-red photoconversion of a fluorescent protein. *Proc Natl Acad Sci U S A* **99**, 12651-6.

Appel, B. and Eisen, J. S. (1998). Regulation of neuronal specification in the zebrafish spinal cord by Delta function. *Development* **125**, 371-80.

Bahary, N., Davidson, A., Ransom, D., Shepard, J., Stern, H., Trede, N., Zhou, Y., Barut, B. and Zon, L. I. (2004). The Zon laboratory guide to positional cloning in zebrafish. *Methods Cell Biol* **77**, 305-29.

Barth, K. A., Miklosi, A., Watkins, J., Bianco, I. H., Wilson, S. W. and Andrew, R. J. (2005). fsi zebrafish show concordant reversal of laterality of viscera, neuroanatomy, and a subset of behavioral responses. *Curr Biol* **15**, 844-50.

Bisgrove, B. W., Essner, J. J. and Yost, H. J. (2000). Multiple pathways in the midline regulate concordant brain, heart and gut left-right asymmetry. *Development* **127**, 3567-79.

Blackshaw, S. and Snyder, S. H. (1997). Parapinopsin, a novel catfish opsin localized to the parapineal organ, defines a new gene family. *J Neurosci* **17**, 8083-92.

Borg, B., Ekstrom, P. and Van Veen, T. (1983). The parapineal organ of teleosts. *Acta Zoolog* **64**, 211-218.

Braitenberg, V. and Kemali, M. (1970). Exceptions to bilateral symmetry in the epithalamus of lower vertebrates. *J Comp Neurol* **138**, 137-46.

Butler, A. B. and Hodos, W. (1996). Comparative Vertebrate Neuroanatomy: Evolution and Adaptation. New York: Wiley-Liss.

Cahill, G. M. (2002). Clock mechanisms in zebrafish. *Cell Tissue Res* **309**, 27-34.

Cantalupo, C. and Hopkins, W. D. (2001). Asymmetric Broca's area in great apes. *Nature* **414**, 505.

Capdevila, I. and Belmonte, J. C. (2000). Knowing left from right: the molecular basis of laterality defects. *Mol Med Today* **6**, 112-8.

Carl, M., Bianco, I. H., Bajoghli, B., Aghaallaei, N., Czerny, T. and Wilson, S. W. (2007). Wnt/Axin1/beta-catenin signaling regulates asymmetric nodal activation, elaboration, and concordance of CNS asymmetries. *Neuron* **55**, 393-405.

Cau, E., Quillien, A. and Blader, P. (2008). Notch resolves mixed neural identities in the zebrafish epiphysis. *Development* **135**, 2391-401.

Cau, E. and Wilson, S. W. (2003). Ash1a and Neurogenin1 function downstream of Floating head to regulate epiphysial neurogenesis. *Development* **130**, 2455-66.

Chapman, D. L., Garvey, N., Hancock, S., Alexiou, M., Agulnik, S. I., Gibson-Brown, J. J., Cebra-Thomas, J., Bollag, R. J., Silver, L. M. and Papaioannou, V. E. (1996). Expression of the T-box family genes, Tbx1-Tbx5, during early mouse development. *Dev Dyn* **206**, 379-90.

Christoph, G. R., Leonzio, R. J. and Wilcox, K. S. (1986). Stimulation of the Lateral Habenula Inhibits Dopamine-Containing Neurons in the Substantia Nigra and Ventral Tegmental Area of the Rat. *The Journal of Neuroscience* **6**, 613-619.

Concha, M. L., Burdine, R. D., Russell, C., Schier, A. F. and Wilson, S. W. (2000). A nodal signaling pathway regulates the laterality of neuroanatomical asymmetries in the zebrafish forebrain. *Neuron* **28**, 399-409.

Concha, M. L., Russell, C., Regan, J. C., Tawk, M., Sidi, S., Gilmour, D. T., Kapsimali, M., Sumoy, L., Goldstone, K., Amaya, E. et al. (2003). Local tissue interactions across the dorsal midline of the forebrain establish CNS laterality. *Neuron* **39**, 423-38.

Concha, M. L. and Wilson, S. W. (2001). Asymmetry in the epithalamus of vertebrates. *J Anat* **199**, 63-84.

Cooke, J. (2004). Developmental mechanism and evolutionary origin of vertebrate left/right asymmetries. *Biol Rev Camb Philos Soc* **79**, 377-407.

Cooper, M. S. and D'Amico, L. A. (1996). A cluster of noninvoluting endocytic cells at the margin of the zebrafish blastoderm marks the site of embryonic shield formation. *Dev Biol* **180**, 184-98.

Corballis, M. C. (2003). From mouth to hand: gesture, speech, and the evolution of right-handedness. *Behav Brain Sci* **26**, 199-208; discussion 208-60.

Deng, C. and Rogers, L. J. (2002). Prehatching visual experience and lateralization in the visual Wulst of the chick. *Behav Brain Res* **134**, 375-85.

Dheen, T., Sleptsova-Friedrich, I., Xu, Y., Clark, M., Lehrach, H., Gong, Z. and Korzh, V. (1999). Zebrafish tbx-c functions during formation of midline structures. *Development* **126**, 2703-13.

Driever, W., Stemple, D., Schier, A. and Solnica-Krezel, L. (1994). Zebrafish: genetic tools for studying vertebrate development. *Trends Genet* **10**, 152-9.

Dufourcq, P., Rastegar, S., Strahle, U. and Blader, P. (2004). Parapineal specific expression of gfi1 in the zebrafish epithalamus. *Gene Expr Patterns* **4**, 53-7.

Eckert, M. A. and Leonard, C. M. (2004). Developmental Disorders: Dyslexia. In *The Asymmetrical Brain*, (ed. K. Hugdahl and R. J. Davidson), pp. 651-680. Cambridge: The MIT Press.

El-Messaoudi, S. and Renucci, A. (2001). Expression pattern of the frizzled 7 gene during zebrafish embryonic development. *Mech Dev* **102**, 231-4.

Eldred, W. D., Finger, T. E. and Nolte, J. (1980). Central projections of the frontal organ of Rana pipiens, as demonstrated by the anterograde transport of horseradish peroxidase. *Cell Tissue Res* **211**, 215-22.

Engbretson, G. A., Reiner, A. and Brecha, N. (1981). Habenular asymmetry and the central connections of the parietal eye of the lizard. *J Comp Neurol* **198**, 155-65.

Essner, J. J., Amack, J. D., Nyholm, M. K., Harris, E. B. and Yost, H. J. (2005). Kupffer's vesicle is a ciliated organ of asymmetry in the zebrafish embryo that initiates left-right development of the brain, heart and gut. *Development* **132**, 1247-60.

Facchin, L., Burgess, H. A., Siddiqi, M., Granato, M. and Halpern, M. E. (2008). Determining the function of zebrafish epithalamic asymmetry. *Philos Trans R Soc Lond B Biol Sci*.

Fong, S. H., Emelyanov, A., Teh, C. and Korzh, V. (2005). Wnt signalling mediated by Tbx2b regulates cell migration during formation of the neural plate. *Development* **132**, 3587-96.

Gamse, J. T., Kuan, Y. S., Macurak, M., Brosamle, C., Thisse, B., Thisse, C. and Halpern, M. E. (2005). Directional asymmetry of the zebrafish epithalamus guides dorsoventral innervation of the midbrain target. *Development* **132**, 4869-81.

Gamse, J. T., Shen, Y. C., Thisse, C., Thisse, B., Raymond, P. A., Halpern, M. E. and Liang, J. O. (2002). Otx5 regulates genes that show circadian expression in the zebrafish pineal complex. *Nat Genet* **30**, 117-21.

Gamse, J. T., Thisse, C., Thisse, B. and Halpern, M. E. (2003). The parapineal mediates left-right asymmetry in the zebrafish diencephalon. *Development* **130**, 1059-68.

Geschwind, N. and Levitsky, W. (1968). Human brain: left-right asymmetries in temporal speech region. *Science* **161**, 186-7.

Ghysen, A. and Dambly-Chaudiere, C. (2007). The lateral line microcosmos. *Genes Dev* **21**, 2118-30.

Gibson-Brown, J. J., S, I. A., Silver, L. M. and Papaioannou, V. E. (1998). Expression of T-box genes Tbx2-Tbx5 during chick organogenesis. *Mech Dev* **74**, 165-9.

Gilbert, S. F. (2006). The Emergence of the Ectoderm: Central Nervous System and Epidermis. In *Dev Biol*, pp. 373-406. Sunderland, MA: Sinauer Associates Inc.

Gilmour, D. T., Maischein, H. M. and Nusslein-Volhard, C. (2002). Migration and function of a glial subtype in the vertebrate peripheral nervous system. *Neuron* **34**, 577-88.

Gothilf, Y., Coon, S. L., Toyama, R., Chitnis, A., Namboodiri, M. A. and Klein, D. C. (1999). Zebrafish serotonin N-acetyltransferase-2: marker for

development of pineal photoreceptors and circadian clock function. *Endocrinology* **140**, 4895-903.

Gourronc, F., Ahmad, N., Nedza, N., Eggleston, T. and Rebagliati, M. (2007). Nodal activity around Kupffer's vesicle depends on the T-box transcription factors Notail and Spadetail and on Notch signaling. *Dev Dyn* **236**, 2131-46.

Green, M. F., Sergi, M. J. and Kern, R. S. (2004). The Laterality of Schizophrenia. In *The Asymmetrical Brain*, (ed. K. Hugdahl and R. J. Davidson), pp. 743-772. Cambridge: The MIT Press.

Gross, J. M. and Dowling, J. E. (2005). Tbx2b is essential for neuronal differentiation along the dorsal/ventral axis of the zebrafish retina. *Proc Natl Acad Sci U S A* **102**, 4371-6.

Gurusinghe, C. J. and Ehrlich, D. (1985). Sex-dependent structural asymmetry of the medial habenular nucleus of the chicken brain. *Cell Tissue Res* **240**, 149-52.

Haas, P. and Gilmour, D. (2006). Chemokine signaling mediates self-organizing tissue migration in the zebrafish lateral line. *Dev Cell* **10**, 673-80.

Habib, M. and Robichon, F. (2004). Structural Correlates of Brain Asymmetry: Studies in Left-Handed and Dyslexic Individuals. In *The Asymmetrical Brain*, (ed. K. Hugdahl and R. J. Davidson), pp. 681-716. Cambridge: The MIT Press.

Hafeez, M. A. and Merhige, M. E. (1977). Light and electron microscopic study on the pineal complex of the coelacanth, Latimeria chalumnae Smith. *Cell Tissue Res* **178**, 249-65.

Halpern, M. E., Gunturkun, O., Hopkins, W. D. and Rogers, L. J. (2005). Lateralization of the vertebrate brain: taking the side of model systems. *J Neurosci* **25**, 10351-7.

Halpern, M. E., Liang, J. O. and Gamse, J. T. (2003). Leaning to the left: laterality in the zebrafish forebrain. *Trends Neurosci* **26**, 308-13.

Halpern, M. E., Thisse, C., Ho, R. K., Thisse, B., Riggleman, B., Trevarrow, B., Weinberg, E. S., Postlethwait, J. H. and Kimmel, C. B. (1995). Cell-autonomous shift from axial to paraxial mesodermal development in zebrafish floating head mutants. *Development* **121**, 4257-64.

Hamada, H., Meno, C., Saijoh, Y., Adachi, H., Yashiro, K., Sakuma, R. and Shiratori, H. (2001). Role of asymmetric signals in left-right patterning in the mouse. *Am J Med Genet* **101**, 324-7.

Hamada, H., Meno, C., Watanabe, D. and Saijoh, Y. (2002). Establishment of vertebrate left-right asymmetry. *Nat Rev Genet* **3**, 103-13.

Hattar, S., Liao, H. W., Takao, M., Berson, D. M. and Yau, K. W. (2002). Melanopsin-containing retinal ganglion cells: architecture, projections, and intrinsic photosensitivity. *Science* **295**, 1065-70.

Heisenberg, C. P., Houart, C., Take-Uchi, M., Rauch, G. J., Young, N., Coutinho, P., Masai, I., Caneparo, L., Concha, M. L., Geisler, R. et al. (2001). A mutation in the Gsk3-binding domain of zebrafish Masterblind/Axin1 leads to a fate transformation of telencephalon and eyes to diencephalon. *Genes Dev* **15**, 1427-34.

Herkenham, M. and Nauta, W. J. (1977). Afferent connections of the habenular nuclei in the rat. A horseradish peroxidase study, with a note on the fiber-of-passage problem. *J Comp Neurol* **173**, 123-46.

Hill, C. (1891). Development of the epiphysis in Coregonus albus. *Journal of Morphology* **5**, 503-510.

Hobert, O., Johnston, R. J., Jr. and Chang, S. (2002). Left-right asymmetry in the nervous system: the Caenorhabditis elegans model. *Nat Rev Neurosci* **3**, 629-40.

Hubbard, T. J., Aken, B. L., Beal, K., Ballester, B., Caccamo, M., Chen, Y., Clarke, L., Coates, G., Cunningham, F., Cutts, T. et al. (2006). Ensembl 2007. *Nucleic Acids Res*.

Inbal, A., Kim, S. H., Shin, J. and Solnica-Krezel, L. (2007). Six3 represses nodal activity to establish early brain asymmetry in zebrafish. *Neuron* **55**, 407-15.

Itoh, M., Kim, C. H., Palardy, G., Oda, T., Jiang, Y. J., Maust, D., Yeo, S. Y., Lorick, K., Wright, G. J., Ariza-McNaughton, L. et al. (2003). Mind bomb is a ubiquitin ligase that is essential for efficient activation of Notch signaling by Delta. *Dev Cell* **4**, 67-82.

Jessen, J. R., Topczewski, J., Bingham, S., Sepich, D. S., Marlow, F., Chandrasekhar, A. and Solnica-Krezel, L. (2002). Zebrafish trilobite identifies new roles for Strabismus in gastrulation and neuronal movements. *Nat Cell Biol* **4**, 610-5.

Karlstrom, R. O. and Kane, D. A. (1996). A flipbook of zebrafish embryogenesis. *Development* **123**, 461.

Kemali, M., Guglielmotti, V. and Fiorino, L. (1990). The asymmetry of the habenular nuclei of female and male frogs in spring and in winter. *Brain Res* **517**, 251-5.

Kimmel, C. B., Warga, R. M. and Schilling, T. F. (1990). Origin and organization of the zebrafish fate map. *Development* **108**, 581-94.

Kozlowski, D. J., Murakami, T., Ho, R. K. and Weinberg, E. S. (1997). Regional cell movement and tissue patterning in the zebrafish embryo revealed by fate mapping with caged fluorescein. *Biochem Cell Biol* **75**, 551-62.

Kramer-Zucker, A. G., Olale, F., Haycraft, C. J., Yoder, B. K., Schier, A. F. and Drummond, I. A. (2005). Cilia-driven fluid flow in the zebrafish pronephros, brain and Kupffer's vesicle is required for normal organogenesis. *Development* **132**, 1907-21.

Kuan, Y. S., Gamse, J. T., Schreiber, A. M. and Halpern, M. E. (2007). Selective asymmetry in a conserved forebrain to midbrain projection. *J Exp Zoolog B Mol Dev Evol* **308**, 669-78.

Larison, K. D. and Bremiller, R. (1990). Early onset of phenotype and cell patterning in the embryonic zebrafish retina. *Development* **109**, 567-76.

Lennox, B. R., Park, S. B., Jones, P. B. and Morris, P. G. (1999). Spatial and temporal mapping of neural activity associated with auditory hallucinations. *Lancet* **353**, 644.

Liang, J. O., Etheridge, A., Hantsoo, L., Rubinstein, A. L., Nowak, S. J., Izpisua Belmonte, J. C. and Halpern, M. E. (2000). Asymmetric nodal signaling in the zebrafish diencephalon positions the pineal organ. *Development* **127**, 5101-12.

Liu, Y. and Halloran, M. C. (2005). Central and peripheral axon branches from one neuron are guided differentially by Semaphorin3D and transient axonal glycoprotein-1. *J Neurosci* **25**, 10556-63.

Long, S., Ahmad, N. and Rebagliati, M. (2003). The zebrafish nodal-related gene southpaw is required for visceral and diencephalic left-right asymmetry. *Development* **130**, 2303-16.

Makita, R., Mizuno, T., Koshida, S., Kuroiwa, A. and Takeda, H. (1998). Zebrafish wnt11: pattern and regulation of the expression by the yolk cell and No tail activity. *Mech Dev* **71**, 165-76.

Marioni, J. C., Mason, C. E., Mane, S. M., Stephens, M. and Gilad, Y. (2008). RNA-seq: an assessment of technical reproducibility and comparison with gene expression arrays. *Genome Res* **18**, 1509-17.

Masai, I., Heisenberg, C. P., Barth, K. A., Macdonald, R., Adamek, S. and Wilson, S. W. (1997). floating head and masterblind regulate neuronal patterning in the roof of the forebrain. *Neuron* **18**, 43-57.

McManus, C. (2002). Right Hand, Left Hand. London: Weidenfeld and Nicolson.
Meiniel, A. and Collin, J. P. (1971). [The pineal complex of the ammocoete (Lampetra planeri). Connections of the pineal and parapineal organs with the epithalamic roof]. *Z Zellforsch Mikrosk Anat* **117**, 354-80.

Mortazavi, A., Williams, B. A., McCue, K., Schaeffer, L. and Wold, B. (2008). Mapping and quantifying mammalian transcriptomes by RNA-Seq. *Nat Methods* **5**, 621-8.

Naiche, L. A., Harrelson, Z., Kelly, R. G. and Papaioannou, V. E. (2005). T-box genes in vertebrate development. *Annu Rev Genet* **39**, 219-39.

Palmer, A. R. (2004). Symmetry breaking and the evolution of development. *Science* **306**, 828-33.

Park, M. R. (1987). Monosynaptic inhibitory postsynaptic potentials from lateral habenula recorded in dorsal raphe neurons. *Brain Res Bull* **19**, 581-6.

Purves, D., Augustine, G. J., Fitzpatrick, D., Katz, L. C., LaMantia, A.-S., McNamara, J. O. and Williams, S. M. (2001). Early Brain Development. In *Neuroscience*, vol. 2nd (ed. D. Purves G. J. Augustine D. Fitzpatrick L. C. Katz A.-S. LaMantia J. O. McNamara and S. M. Williams). Sunderland, MA: Sinauer Associates, Inc.

Rauch, G.-J., Granato, M. and Haffter, P. (1997). A polymorphic zebrafish line for genetic mapping using SSLPs on high-percentage agarose gels. *Technical Tips Online* **T01208**.

Raya, A. and Belmonte, J. C. (2006). Left-right asymmetry in the vertebrate embryo: from early information to higher-level integration. *Nat Rev Genet* **7**, 283-93.

Rebagliati, M. R., Toyama, R., Fricke, C., Haffter, P. and Dawid, I. B. (1998a). Zebrafish nodal-related genes are implicated in axial patterning and establishing left-right asymmetry. *Dev Biol* **199**, 261-72.

Rebagliati, M. R., Toyama, R., Haffter, P. and Dawid, I. B. (1998b). cyclops encodes a nodal-related factor involved in midline signaling. *Proc Natl Acad Sci U S A* **95**, 9932-7.

Regan, J. C., Concha, M. L., Roussigne, M., Russell, C. and Wilson, S. W. (2009). An Fgf8-dependent bistable cell migratory event establishes CNS asymmetry. *Neuron* **61**, 27-34.

Robinson, J., Schmitt, E. A. and Dowling, J. E. (1995). Temporal and spatial patterns of opsin gene expression in zebrafish (Danio rerio). *Vis Neurosci* **12**, 895-906.

Ruvinsky, I., Oates, A. C., Silver, L. M. and Ho, R. K. (2000). The evolution of paired appendages in vertebrates: T-box genes in the zebrafish. *Dev Genes Evol* **210**, 82-91.

Ruvinsky, I., Silver, L. M. and Ho, R. K. (1998). Characterization of the zebrafish tbx16 gene and evolution of the vertebrate T-box family. *Dev Genes Evol* **208**, 94-9.

Sampath, K., Rubinstein, A. L., Cheng, A. M., Liang, J. O., Fekany, K., Solnica-Krezel, L., Korzh, V., Halpern, M. E. and Wright, C. V. (1998). Induction of the zebrafish ventral brain and floorplate requires cyclops/nodal signalling. *Nature* **395**, 185-9.

Sarmah, B., Winfrey, V. P., Olson, G. E., Appel, B. and Wente, S. R. (2007). A role for the inositol kinase Ipk1 in ciliary beating and length maintenance. *Proc Natl Acad Sci U S A* **104**, 19843-8.

Sarmah, B., Latimer, A.J., Appel, B. Wente, S.R. (2005). Inositol polyphosphates regulate zebrafish left-right asymmetry. *Dev. Cell.* **1**, 133-45

Scott, E. K., Mason, L., Arrenberg, A. B., Ziv, L., Gosse, N. J., Xiao, T., Chi, N. C., Asakawa, K., Kawakami, K. and Baier, H. (2007). Targeting neural circuitry in zebrafish using GAL4 enhancer trapping. *Nat Methods* **4**, 323-6.

Shen, M. M. (2007). Nodal signaling: developmental roles and regulation. *Development* **134**, 1023-34.

Sherman, S. M. and Spear, P. D. (1982). Organization of visual pathways in normal and visually deprived cats. *Physiol Rev* **62**, 738-855.

Showell, C., Binder, O. and Conlon, F. L. (2004). T-box genes in early embryogenesis. *Dev Dyn* **229**, 201-18.

Sinha, S., Abraham, S., Gronostajski, R. M. and Campbell, C. E. (2000). Differential DNA binding and transcription modulation by three T-box proteins, T, TBX1 and TBX2. *Gene* **258**, 15-29.

Snelson, C. D., Burkart, J. T. and Gamse, J. T. (2008a). Formation of the asymmetric pineal complex in zebrafish requires two independently acting transcription factors. *Dev Dyn*.

Snelson, C. D. and Gamse, J. T. (2008). Building an asymmetric brain: Development of the zebrafish epithalamus. *Semin Cell Dev Biol*.

Snelson, C. D., Santhakumar, K., Halpern, M. E. and Gamse, J. T. (2008b). Tbx2b is required for the development of the parapineal organ. *Development* **135**, 1693-702.

Solessio, E. and Engbretson, G. A. (1993). Antagonistic chromatic mechanisms in photoreceptors of the parietal eye of lizards. *Nature* **364**, 442-5.

Solessio, E. and Engbretson, G. A. (1999). Electroretinogram of the parietal eye of lizards: photoreceptor, glial, and lens cell contributions. *Vis Neurosci* **16**, 895-907.

Solnica-Krezel, L., Stemple, D. L., Mountcastle-Shah, E., Rangini, Z., Neuhauss, S. C., Malicki, J., Schier, A. F., Stainier, D. Y., Zwartkruis, F., Abdelilah, S. et al. (1996). Mutations affecting cell fates and cellular rearrangements during gastrulation in zebrafish. *Development* **123**, 67-80.

Song, M. R., Shirasaki, R., Cai, C. L., Ruiz, E. C., Evans, S. M., Lee, S. K. and Pfaff, S. L. (2006). T-Box transcription factor Tbx20 regulates a genetic program for cranial motor neuron cell body migration. *Development* **133**, 4945-55.

Staudt, N. and Houart, C. (2007). The prethalamus is established during gastrulation and influences diencephalic regionalization. *PLoS Biol* **5**, e69.

Su, C. Y., Luo, D. G., Terakita, A., Shichida, Y., Liao, H. W., Kazmi, M. A., Sakmar, T. P. and Yau, K. W. (2006). Parietal-eye phototransduction components and their potential evolutionary implications. *Science* **311**, 1617-21.

Sutherland, R. J. (1982). The dorsal diencephalic conduction system: a review of the anatomy and functions of the habenular complex. *Neurosci Biobehav Rev* **6**, 1-13.

Takabatake, Y., Takabatake, T. and Takeshima, K. (2000). Conserved and divergent expression of T-box genes Tbx2-Tbx5 in Xenopus. *Mech Dev* **91**, 433-7.

Talbot, W. S., Trevarrow, B., Halpern, M. E., Melby, A. E., Farr, G., Postlethwait, J. H., Jowett, T., Kimmel, C. B. and Kimelman, D. (1995). A homeobox gene essential for zebrafish notochord development. *Nature* **378**, 150-7.

Thisse, C. and Thisse, B. (1999). Antivin, a novel and divergent member of the TGFbeta superfamily, negatively regulates mesoderm induction. *Development* **126**, 229-40.

Toga, A. W. and Thompson, P. M. (2003). Mapping brain asymmetry. *Nat Rev Neurosci* **4**, 37-48.

Topczewski, J., Sepich, D. S., Myers, D. C., Walker, C., Amores, A., Lele, Z., Hammerschmidt, M., Postlethwait, J. and Solnica-Krezel, L. (2001). The zebrafish glypican knypek controls cell polarity during gastrulation movements of convergent extension. *Dev Cell* **1**, 251-64.

Vallortigara, G., Rogers, L. J. and Bisazza, A. (1999). Possible evolutionary origins of cognitive brain lateralization. *Brain Res Brain Res Rev* **30**, 164-75.

Walker, C. (1999). Haploid screens and gamma-ray mutagenesis. In *Methods in Cell Biology*, vol. 60, pp. 43-70. London: Elsevier.

Weston, J. A. (1963). A radioautographic analysis of the migration and localization of trunk neural crest cells in the chick. *Dev Biol* **6**, 279-310.

Woo, K. and Fraser, S. E. (1995). Order and coherence in the fate map of the zebrafish nervous system. *Development* **121**, 2595-609.

Woo, K., Shih, J. and Fraser, S. E. (1995). Fate maps of the zebrafish embryo. *Curr Opin Genet Dev* **5**, 439-43.

Wree, A., Zilles, K. and Schleicher, A. (1981). Growth of fresh volumes and spontaneous cell death in the nuclei habenulae of albino rats during ontogenesis. *Anat Embryol (Berl)* **161**, 419-31.

Wright, C. V. and Halpern, M. E. (2002). Specification of left-right asymmetry. *Results Probl Cell Differ* **40**, 96-116.

Yan, Y. T., Gritsman, K., Ding, J., Burdine, R. D., Corrales, J. D., Price, S. M., Talbot, W. S., Schier, A. F. and Shen, M. M. (1999). Conserved requirement for EGF-CFC genes in vertebrate left-right axis formation. *Genes Dev* **13**, 2527-37.

Yanez, J. and Anadon, R. (1996). Afferent and efferent connections of the habenula in the rainbow trout (Oncorhynchus mykiss): an indocarbocyanine dye (DiI) study. *J Comp Neurol* **372**, 529-43.

Yanez, J., Pombal, M. A. and Anadon, R. (1999). Afferent and efferent connections of the parapineal organ in lampreys: a tract tracing and immunocytochemical study. *J Comp Neurol* **403**, 171-89.

Zhang, J., Talbot, W. S. and Schier, A. F. (1998). Positional cloning identifies zebrafish one-eyed pinhead as a permissive EGF-related ligand required during gastrulation. *Cell* **92**, 241-51.

Zhu, L., Marvin, M. J., Gardiner, A., Lassar, A. B., Mercola, M., Stern, C. D. and Levin, M. (1999). Cerberus regulates left-right asymmetry of the embryonic head and heart. *Curr Biol* **9**, 931-8.

Zilles, K., Schleicher, A. and Wingert, F. (1976). [Quantitative growth analysis of limbic nuclei areas fresh volume in diencephalon and mesencephalon of an albino mouse ontogenic series. III. Nucleus interpe-uncularis]. *J Hirnforsch* **17**, 21-9.